CZECH TECHNICAL UNIVERSITY IN PRAGUE

FACULTY OF CIVIL ENGINEERING

DEPARTMENT OF STEEL AND TIMBER STRUCTURES

MASTER'S THESIS

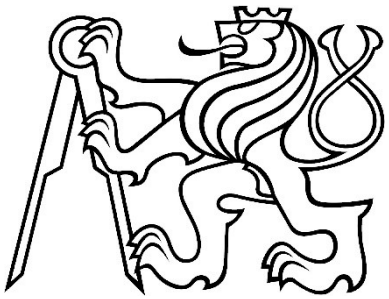

THE INFLUENCE OF DAMAGED ZONES IN WOOD COLUMN ON ITS LOAD BEARING CAPACITY

JANUARY 2017

Author:

Bc. Jakub Mareš

Supervisors:

Prof. Dipl.-Ing. Dr.techn. Martin Schneider

Ing. Karel Mikeš, Ph.D.

Study programme:

Civil Engineering

Branch of study:

Building Structures

ČESKÉ VYSOKÉ UČENÍ TECHNICKÉ V PRAZE
Fakulta stavební
Thákurova 7, 166 29 Praha 6

ZADÁNÍ DIPLOMOVÉ PRÁCE

I. OSOBNÍ A STUDIJNÍ ÚDAJE

Příjmení: Mareš Jméno: Jakub Osobní číslo: 380876

Zadávající katedra: K134

Studijní program: Civil Engineering

Studijní obor: Building Structures

II. ÚDAJE K DIPLOMOVÉ PRÁCI

Název diplomové práce: The influence of damaged zones in wood column on its load bearing capacity.

Název diplomové práce anglicky: The influence of damaged zones in wood column on its load bearing capacity.

Pokyny pro vypracování: Vypracujte odborou práci na téma „Vliv poškození dřeva na únosnost tlakového sloupku".

Seznam doporučené literatury: Timber Engineering; Larsen, Thelandersson Structural Timber Design · Porteous, Kermani

Jméno vedoucího diplomové práce: Ing. Karel Mareš, Ph. D.

Datum zadání diplomové práce: 4.10.2016 Termín odevzdání diplomové práce: 9.1.2017

Údaj uveďte v souladu s datem v časovém plánu příslušného ak. roku

[redacted]

Podpis vedoucího práce

[redacted]

Podpis vedoucího katedry

III. PŘEVZETÍ ZADÁNÍ

Beru na vědomí, že jsem povinen vypracovat diplomovou práci samostatně, bez cizí pomoci, s výjimkou poskytnutých konzultací. Seznam použité literatury, jiných pramenů a jmen konzultantů je nutné uvést v diplomové práci a při citování postupovat v souladu s metodickou příručkou ČVUT „Jak psát vysokoškolské závěrečné práce" a metodickým pokynem ČVUT „O dodržování etických principů při přípravě vysokoškolských závěrečných prací".

4.10.2016

Datum převzetí zadání

[redacted]

Podpis studenta(ky)

AFFIDAVIT

I hereby declare that all information in this document has been obtained and presented in accordance with academic rules and ethical conduct and that I stated all the references in accordance with the Guidelines for the ethical training of university theses.

8th January 2017

Jakub Mareš

Mareš

Abstract

This master's thesis has been founded as a theoretical support for the project led by Prof. Dipl.-Ing. Dr.techn. Martin Schneider. This project is focused on the inspection of historical timber roof structures. My task in this project was to analyse the influence of damaged zones on the load bearing capacity in timber columns.

The Idea was to simulate damage by drilling holes into the wood. An exponential function for calculation of the modulus of elasticity of damaged wood was derived from direct measurements on specimens with certain artificial porosity. Based on results of static load tests it was proven that compressive strength depends linearly on the remaining cross section area. Following this, two sets of columns (in scale of approximately 1:3 to columns typically used in structures) containing artificially damaged zone in the middle of the length were subjected to the static load test. Determined load bearing capacity was compared with results obtained by calculation using the composite cross section method and material properties determined from previously derived formulas. The average difference between calculated and measured values was 11%.

The micro-resistance drilling was used for localization and rating of the damaged zones in a partially rotted piece of timber. For the purpose of this thesis it was used as a column. Based on the developed procedure the load bearing capacity of this column was predicted with precision of 1%. Validated procedure was used for examining a theoretical real-sized column and a significant influence of the damaged zone was detected.

Further, I have performed a practical inspection of historic roof members condition. Micro-resistance drilling was used again for localization and rating of the damaged parts of the roof. Based on the results, recommendations for future reconstruction of the building were stated.

Keywords

timber column, damaged wood, damaged column, static load test, compressive strength, modulus of elasticity, simulation of damaged wood, micro-resistance drilling

Abstrakt

Tato diplomová práce vznikla jako teoretická podpora pro projekt vedený Prof. Dipl.-Ing. Dr.techn. Martinem Schneiderem. Tento projekt je zaměřen na inspekci historických krovů. Cílem mé páce v tomto projektu je analyzovat vliv poškozených částí dřevěného sloupu na jeho únosnost.

Myšlenka byla simulovat poškození vrtáním děr do dřeva. Exponenciální funkce pro určení modulu pružnosti byla odvozena z přímého měření vzorků s určitou umělou porozitou. Na základě výsledků zátěžových zkoušek byla prokázána lineární závislost pevnosti v tlaku na zbývající průřezové ploše. Následně byly dva soubory sloupků v měřítku přibližně 1:3 obsahující uměle poškozenou část uprostřed své délky podrobeny zátěžovým zkouškám. Určená únosnost byla porovnána s výsledky výpočtů provedených metodou spřaženého průřezu s použitím materiálových vlastností určených z dříve odvozených vztahů. Průměrný rozdíl vypočítaných a změřených únosností byl 11%.

Odporová mikrovrtačka byla použita pro lokalizaci a hodnocení poškození v nahnilém kusu dřeva. Pro účely této práce byl použit jako sloupek. Na základě vyvinutého postupu byla spočítána únosnost tohoto sloupku s přesností 1%. Ověřený postup byl použit pro zkoumání teoretického sloupu reálných rozměrů, u kterého byl zjištěn významný vliv poškozené oblasti.

Dále jsem provedl praktickou inspekci stavu historických střešních prvků. Odporové vrtání bylo znovu použito pro lokalizaci a hodnocení poškozených částí. Na základě výsledků jsou uvedeny doporučení pro budoucí rekonstrukci budovy.

Klíčová slova

dřevěný sloup, poškozené dřevo, poškozený sloup, statická zkouška únosnosti, pevnost v tlaku, modul pružnosti, simulace poškozeného dřeva, odporová mikrovrtačka

ACKNOWLEDGEMENT

I would like to express my gratitude to the Carinthia University of Applied Sciences which hosted me during the creation of this thesis and provided the necessary laboratory equipment. Furthermore, I would like to thank both my supervisors Prof. Dipl.-Ing. Dr.techn. Martin Schneider (CUAS) and Ing. Karel Mikeš, Ph.D. (CTU) for useful comments and advice. I would like to highlight the program Erasmus+ which provided me with the financial and legal support. Also, I thank my colleague BSc Sebastian Gigli who spend a lot of time with me and helped me with preparation of the samples for experiments and thought me how to use the Resistograph® device. Least but not last, I would like to thank my loved ones, who have supported me throughout entire study.

Jakub Mareš

Preface

Wood was the ancient construction material but it's still widely used. Indeed, the word "material" itself comes from the Latin *materies, materia*: the trunk of a tree. [1] It is easily available and easily workable. Nevertheless, it was not the case all the time in the past. During the sixteenth century, the demand for wood for shipbuilding was so huge that all suitable forests of England were deplaned. By the seventeenth century, timber for ships had to be imported into The Old Continent from The New World. Further, during the nineteenth century much of Europe's forests had been cut down because of an exponential increase of the consumption of wood. [1] Nowadays, we witness a great deforestation in tropical jungles powered by an inconsolable hunger of western society for cheap agricultural products, especially the palm oil.

Today the world production of wood is roughly 10^9 tonnes per year, which is roughly the same as the production of steel. [1] Most of the total production is used in the building industry. There are various species of wood with different properties and use. The subject of this thesis are structures so it is focused on wood spices used for structures such as spruce or fir.

CONTENTS

List of formulas

List of Figures

List of tables

List of charts

List of photos

INITIAL ANALYSIS

1.1 INTRODUCTION

I have written this thesis during an internship at the Carinthia University of Applied Sciences in Austria. Prof. Dipl.-Ing. Dr.techn. Martin Schneider accepted me in his project and as a true professor of university of applied sciences he let me use various measuring devices, e.g. Resistograph®. I also had the possibility to make static load tests in the laboratory of CUAS in Villach. Whit this option, it was possible to compare my calculations with the real behavior of wood structures.

Naturally, to work efficiently on site, the measurements were done with the help of my colleague BSc Sebastian Gigli. He is responsible for the inspection of roof structures in this project.

1.2 ASSIGNMENT

1.2.1 DAMAGED WOOD MEMBER

The main goal of the thesis was to find a procedure for estimating the load bearing capacity of damaged wood columns, find out how big is the influence of damaged zones and how to estimate the degree of the damage of timber.

At the beginning, the basic problem was to decide if it is worth to take the damaged zone in to account during assessment of a wood member. After closer analysing of the topic, all attention was paid to the columns and associated stability problems. The simple Figure 1-1 was sketched on a paper and a lot of questions were raised.

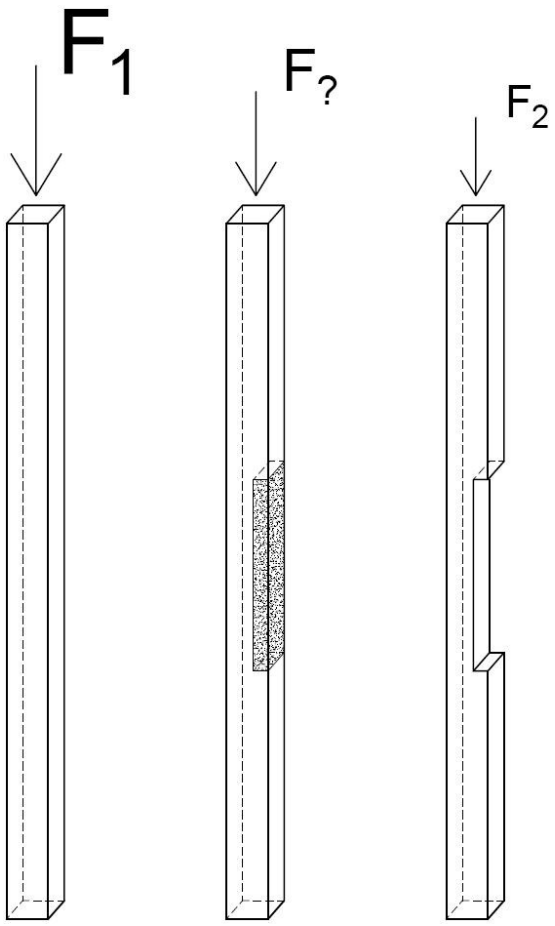

Figure 1-1 Elementary problem

1.2.2 INSPECTION OF THE ROOF STRUCTURE

Another task was to help with the technical inspection of the roof structure of the public elementary school Khevenhüller in Villach, Austria.

THEORETICAL PART

2.1 MATERIAL PROPERTIES OF TIMBER STRUCTURES IN TERMS OF THE REMEDIATION

2.1.1 DURABILITY OF WOOD IN EXISTING BUILDINGS

In terms of the durability of wood, particular structure of the material must be taken into account as well as the conditions, which it is exposed to. Natural durability of wood is the resistance against attack of wood destroying organisms. Durability has to be assessed for each wood-destroying organism separately. Natural durability is determined in a laboratory by measuring the weight loss of the sample before and after the exposure. Durability is divided into five classes: very durable, durable, medium durable, little durable and non-durable. When designing the remediation of timber elements, natural durability has to be investigated. If the natural durability is not sufficient, it is necessary to improve it. [2]

Generally, influences acting on timber can be divided into biotic and abiotic. The main negative influences can include: microorganisms (bacteria), decaying mushrooms and other fungi, animals (wood-destroying insects), thermal agents (flame), atmospheric factors (water, corrosive gases, dust, solar radiation etc.) and chemical agents. Types of degradation of timber are shown in the Table 2-1[2]

Type of degradation of timber	Degradation agent
1) Destruction of polymers - chemical reactions	
The hydrolysis, dehydration, oxidative and other reactions, decrystallization	**Aggressive chemicals:** (SO2, NOx), acids and bases, inorganic additives
The hydrolysis, dehydration and thermal-oxidative reactions	**Thermal effects:** fire, increased temperature, UV radiation
Photo-oxidation reactions mainly in lignin (depth of .05 to 2.5 mm)	**Wood-decaying fungi:** white and brown rot
Biochemical reactions catalyzed fungal enzymes	**Insect**
Mechano-biochemical decomposition	
2) Without the initial destruction of polymers	
Mechanical cracks	Humidity and temperature gradients
Macroscopic holes	Insect
Change of color	Microfungi
Damage by thinning	Bacteria, fungi

Table 2-1 Type of degradation of timber [2]

Wooden elements are divided into five classes of risk due to their exposure to the environment. The timber roof elements are usually included in the second class of threats which is characterized by the following possible occurrence of biotic factors:

Class of threat	The incidence of biotic factors				
	Wood-decaying fungi		Wood color changing fungi		Insect
	Basidiomycetes	Mushrooms causing soft rot	Mushrooms causing blueing	Mold	Beetles
2	Yes	No	Yes	Yes	Yes

Table 2-2 The incidence of biotic factors [2]

2.1.2 PROCEDURE OF THE DETERMINATION OF THE QUALITY OF WOOD

During the investigation of wood elements, material characteristics must be determined by tests carried out in-situ or by taking specimens into a laboratory for further evaluation or comparison with the reference samples. Material properties can be obtained from a construction technical exploration. Usually a number of methods is applied sequentially to identify the degree of wood degradation. [2]

The methods can be divided into direct methods that instantly analyze the structure of wood and indirect methods with additional validation. The direct methods include macroscopic analysis, microscopic analysis, physico-chemical analysis and physico - mechanical analysis. Indirect methods mostly use electro, acoustic, radiometric, or thermo-physical principles. [2]

Macroscopic analysis:

The easiest method is to perform a regular visual check of wooden structural elements and their connections. One of the first steps is to check if there is moisture on the surface of elements. If it is found, it is necessary to find the cause of it. Defects and structural failures caused by mechanical violation (cracks, knots, twists, release) and biotic violation (rot, discolouration, surface mycelia, presence grub holes) or abiotic violation are monitored. In terms of finding indicative of the mechanical condition of the element, percussion or scratch tests can be performed during the macroscopic analysis. The type of timber damage must be properly recorded. Most commonly seen type of degradation in historic buildings is biotic damage of wood, where the range of damage can be characterized as follows: [2]

Infestation by wood decaying fungi: [3]

> **Superficial** – To determine the type of a fungus the discoloration of wood, change in shape, surface mycelium, incidence rhizomorph and fruiting bodies are primarily evaluated.
>
> **Complete** – Recognizable by scratch test for designation of the loss of strength.

Infestation by wood decaying insects: [4]

Superficial – Interferes are maximally 5 mm deep. Damage does not affect the physical and mechanical properties of wood.

Shallow - Extends to the depth of 5-50 mm. Damage is already affecting the mechanical properties of wood.

Complete - Reaches the depth more then 50 mm. In buildings the damage is usually caused by woodworm and old-house borer.

In case of wood-destroying fungi, the kind of attack is assessed by typical characteristics of each fungus. In case of wood-destroying insects, range of damage is determined by the shape of exit holes, larvae found in corridors, hallways shape and their filling, eventually dead adult beetles. [2]

Microscopic analysis:

Microscopic analysis is performed as a complementary objective assessment of the condition of wood - to determine the shape, size and arrangement of cells, presence of hyphae in the wood element or stage of wood rot when exposed to fungal decay. Primarily optical microscopes, electron microscopes and fluorescence microscopes are used.

Physico-chemical analysis:

Changes in the degree of wood structure degradation can be accurately quantified. Chemical methods are used primarily to determine the proportion of structural polymers and polysaccharides in degraded wood. The classic and effortless method of distinguishing the brown and white rot is the indication of the oxidase reaction. The pH value of wood can be determined to verify the extent of degradation of wood.

Physico-mechanical analysis:

It may by necessary to determine selected material characteristics of an embedded timber element from the static point of view. During local investigation the values of the temperature and the moisture content of wood elements are usually detected. Micro resistance drilling can by used for localization of the damage and estimation of the degree of damage. Furthermore, samples for determination of selected physical characteristics (humidity, density) and mechanical properties (compressive strength, bending strength, modulus of elasticity) are taken to a laboratory for further examination. The dimensions of samples should correspond with appropriate norms. [2]

2.1.3 CONCLUSION

In conclusion, degradation of structural elements changes the behavior of a structure. The spatial behavior of the structure is significant. Damaged members do not transfer all the load which they were supposed to transfer and it can cause big deformations or even a failure of the structure. Based on the type and extent of the disruption it is necessary to decide whether the structure can be rehabilitated or has to be replaced.

2.2 MICRO-RESISTANCE DRILLING FOR TIMBER INSPECTION

2.2.1 INTRODUCTION

This method uses thin needles to inspect trees and wood structures. It is used since 1987. First versions of micro-resistance drilling machines were able to discover cavity and severe damage of the material. New electronic high-resolution devices also provide the information about cracks, delaminations and the layout of annual rings. However, the user has to be educated in wood anatomy to be able to interpret resulting profiles correctly. [5]

2.2.2 HISTORIC DEVELOPMENT

In the 1984 W. Kamm and S. Voss (German engineers) developed a device which was able to record penetration resistance of a thin needle in wood. This drill was equipped with a spring mechanism which was responsible for recording the resistance. Nevertheless, the resonance of the spring caused unneglectable errors. This problem was partially solved by adding compensating spring for damping. Unfortunately, after all attempts for improvements, errors were still nonlinear, non-reproducible and thus uncorrectable. So overall, measurements led to wrong evaluations. Improvement came with the usage of electrically recording mechanisms. [5]

The resistance drilling method was then further developed within a project of The Hohenheim University and The Environmental Physics Institute of Heidelberg University. The intra-annual density variations of annual rings were measured. The use of electronic regulation and recording of motor power consumption has brought reproducible profiles and reliable results that can be linearly correlated to the wood density. [5]

There are two motors driving the drill. One responsible for the penetration of the needle and second one for the rotation. After many tests it was found that recording of the power consumption of booth motors is not necessary because all information is carried by profile coming form motor responsible for rotation of the needle. [5]

Since that time only the electrical power consumption of the rotation motor is measured and recorded. This value is proportional to the mechanical torque of the needle (if the engine operates linearly), and depends primarily on the density of wood. [5]

2.2.3 NEEDLE GEOMETRY

For both scientific and practical applications, the resistance drilling must meet several different requirements. It took years of testing of different materials and shapes of needles until a solution was found. The aim was to determine the radial density profile at the highest possible resolution. At the end a flat tip was considered to be the best solution. Given that the annual ring boundaries are not linear, but more or less concentric or even curly, the width of the needle tip determines the resolution of tangential averaging and should be minimized. Naturally the damage to the examined specimen (tree or construction element) should be minimized as well, the needle should be as thin as possible. Thin needles (<1 mm) were often diverted by knots or other wooden anatomical inhomogeneities and did not drill sufficiently straight. Finally, a good compromise was found: the shaft diameter of 1.5 mm and 3.0 mm flat tip. [5]

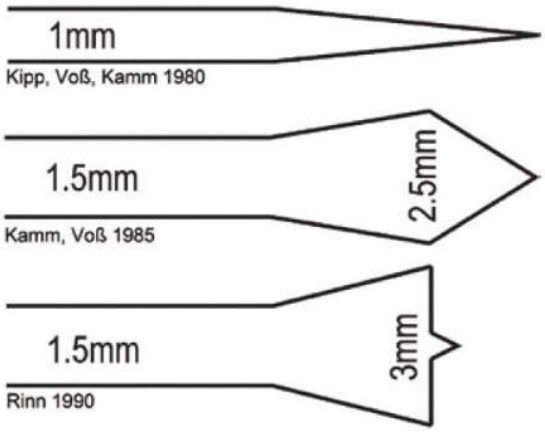

Figure 2-1 Tested geometry of the needle [6]

2.2.4 BASIS OF THE PROFILE INTERPRETATION

If the geometry of the needle follows the instructions described above, the local density of the timber at the position of the needle tip is the main factor that affects the mechanical penetration resistance. Because density

of latewood and earlywood is different, the angle and position of drilling dramatically influences the shape of the resulting curves. [5] Practically, the results of drilling made in radial direction (perpendicular to the annual rings) are most valuable. In this case the loss of amplitude mostly discovers a problem in the wood member. Nevertheless, this loss of amplitude can be coursed by tangential direction of drilling. Therefore, the knowledge of basic anatomical characteristics of wood is a prerequisite for proper interpretation of the resulting profiles. The interpreter always has to know where the drilling was made and how did the surface of the object look like.

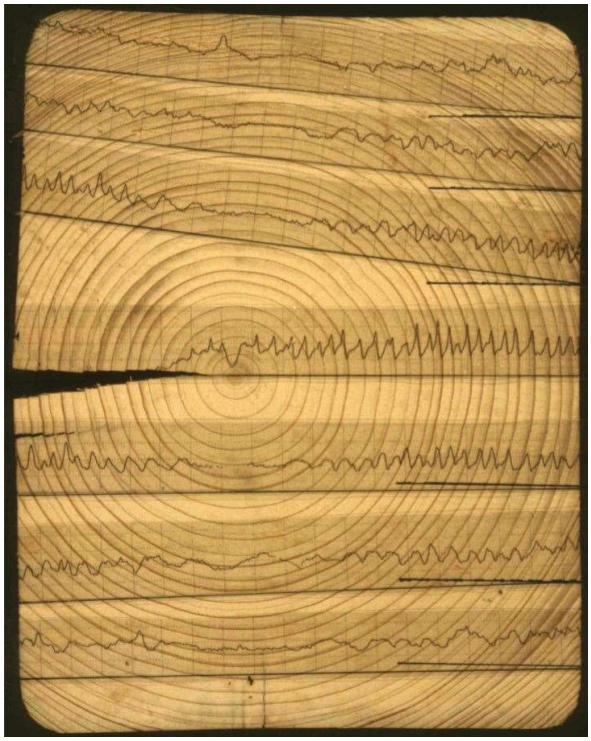

Figure 2-2 The difference in the profiles drilled in the tangential and radial direction [2]

For the inspection of timber members, it is sometimes possible to drill in the direction longitudinal to the fibers. In such case, the profile should be more or less linear until the needle enters damaged wood and the resistance drops.

2.2.5 Conclusion

This method is suitable for the localization of damaged zones in wood members. The precision is about 1 cm. Furthermore, the degree of damage can by determined from a decrease of the average drilling resistance. (Chapter 3.4.2.2)

EXPERIMENTAL PART

THE INFLUENCE OF DAMAGED ZONES IN WOOD COLUMN ON ITS LOAD BEARING CAPACITY.

3.1 USED SYMBOLS

$\square_c$	*Lower index „c" means, that it deals with calculated value*
$\square_D$	*Lower index „D" means, that it deals with damaged material*
$\square_m$	*Lower index „m" means, that it deals with measured value*
$\square_N$	*Lower index „N" means, that it deals with undamaged material*
A'	*Area under a curve in a resistance drilling diagram [graphically m2]*
A_m	*Missing area of a cross section [m2]*
A_o	*Original area of a cross section [m2]*
b	*Width [m]*
c	*Error of calculation [-]*
d	*Degree of damage [-]*
E	*Modulus of elasticity [Pa]*
E_{mean}	*Mean value of modulus of elasticity [Pa]*
$E_{mean,fin}$	*Final mean value of modulus of elasticity [Pa]*
f_c	*Compressive strength [Pa]*
$f_{c,d}$	*Design compressive strength [Pa]*
$f_{c,k}$	*Characteristic compressive strength [Pa]*
F	*Compressive force [N]*
F_1	*Force which causes stress of $0,1f_c$ in a specimen [N]*
F_2	*Force which causes stress of $0,33f_c$ in a specimen [N]*
h	*Depth [m]*
k_{def}	*Deformation factor [-]*
k_{mod}	*Modification factor for duration of stresses in an apex zone [-]*
l	*Length [m]*
p	*Porosity [-]*
R	*Average relative resistance of a part of a cross section [graphically m]*
s	*Speed of loading [m/s]*
S_m	*Missing area [m2]*
S_o	*Original area [m2]*
t	*Time [s]*
V_m	*Missing volume of a sample [m3]*
V_o	*Original volume of a sample [m3]*
w_1	*Deformation caused by F_1 in a specimen [m]*
w_2	*Deformation caused by F_2 in a specimen [m]*
γ_M	*Partial factor for material properties [-]*
γ	*Efficiency of connection of parts of composite cross section [-]*
ε	*Strain [-]*
σ	*Normal stress [Pa]*
Ψ_2	*Factor for quasi-permanent value of a variable action [-]*

3.2 MATERIAL PROPERTIES OF DAMAGED WOOD

3.2.1 INTRODUCTION

The aim of this chapter is to provide a procedure for calculation of the load bearing capacity of a partially damaged timber column.

Both localization of the damaged zones and determination of material properties are crucial. For estimation of the modulus of elasticity and the compressive strength of an old wood an indirect method based on the density of selected material was used. For the determination of these two properties of damaged wood, formulas which generate reduced values based on original values and quantity which is named degree of damage d were developed. The formulas were developed from results of series of static load tests of new wood members influenced by artificial porosity. Degree of damage d of naturally damaged wood can by determined from outputs of a resistance drilling as well as location of damage zones.

To use this method, it is necessary to have:

a) An access to the member at least from one side in its full length
b) Dimensions and boundary conditions of the member
c) Resistance drilling device
d) Modulus of elasticity and compressive strength of undamaged material or its density

3.2.2 SIMULATION OF DAMAGE BY POROSITY

The following theory is based on measuring modulus of elasticity parallel to grain of wood E and compressive strength of wood f_c in static load test provided by laboratory of the Carinthia University of Applied Sciences in Villach, Austria.

3.2.2.1 Procedure

Damage in wood was simulated by drilling holes through samples. As a smallest unit of area, 1 cm^2 was chosen. One hole of a varying diameter was drilled into each unit. Two elementary properties which characterise the damage of wood were set up:

For the artificial damaged wood, the degree of damage d is the ratio between missing cross section area A_m and original cross section area A_o (Figure 3-1). It can be expressed by Formula 3–1:

$$d = \frac{A_m}{A_o} \; [-]$$

Formula 3–1 Degree of damage

For the artificial damaged wood, the porosity p is the ratio between missing volume V_m and original volume V_o (Figure 3-1). It can be expressed by Formula 3–2:

$$p = \frac{V_m}{V_o} \; [-]$$

Formula 3–2 Porosity

The relation between porosity and degree of damage is given by geometry of distribution of holes and fact that holes are circular. For homogeneous and rectangular system used in samples B_N; $B4_0$; $B5_0$; $B6_0$ and $B7_0$ the porosity is defined by Formula 3–3:

$$p = \frac{\pi}{4} \cdot d^2 \; [-]$$

Formula 3–3 Porosity from geometry

Samples $B34_0$a and $B34_0$b are out of this trend. The reason for it is to get more information from tests. $B34_0$a and $B34_0$b had the same degree of damage but a different porosity (Photo 3–1).

All samples had an undamaged strip of 10 mm at the top and the bottom end. This material served for transferring load into the sample. Influence of this strip on the compressive strength f_c was neglected because samples always collapsed in the damaged region. Modulus of elasticity was measured in the damaged part only so the strips had practically no influence on results.

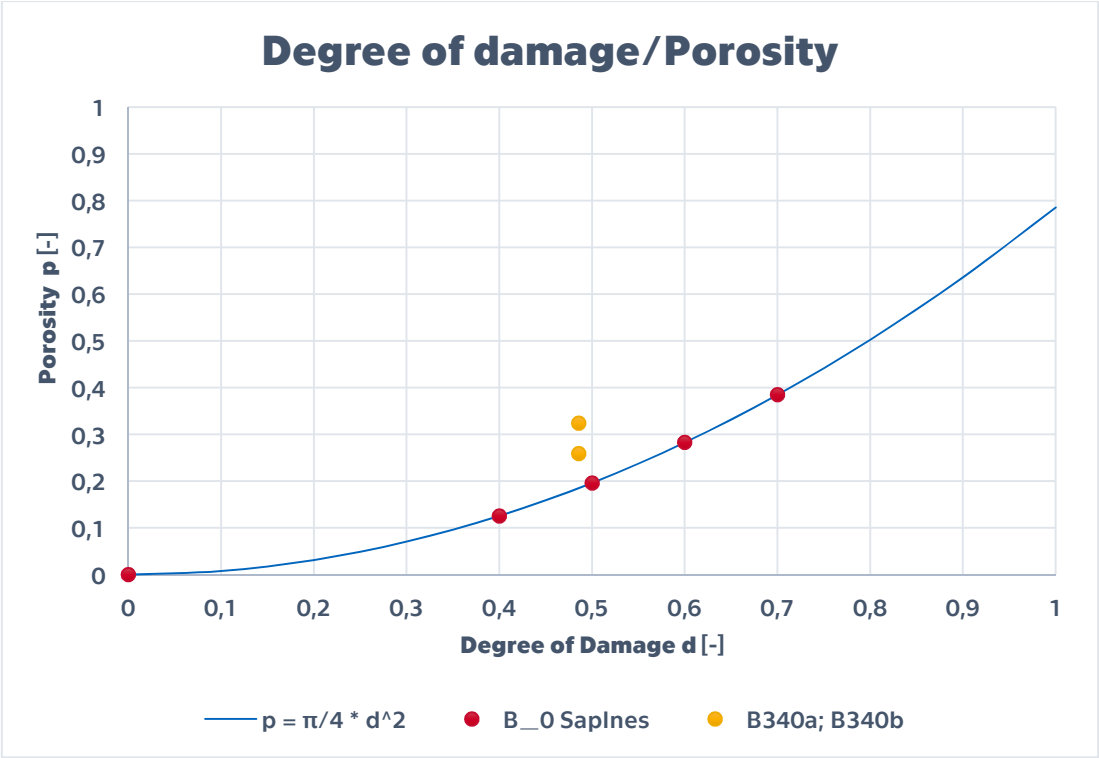

Chart 3-1 Degree of damage/Porosity relation

3.2.2.2 Samples

The set of samples contained 7 samples made of dry spruce wood. Samples were knot free and material was chosen to minimize influence of all possible defects of wood. Each sample had dimensions of *b* x *h* x *l* [mm] (70 x 70 x 220 mm) and different porosity *p* and degree of damage *d*.

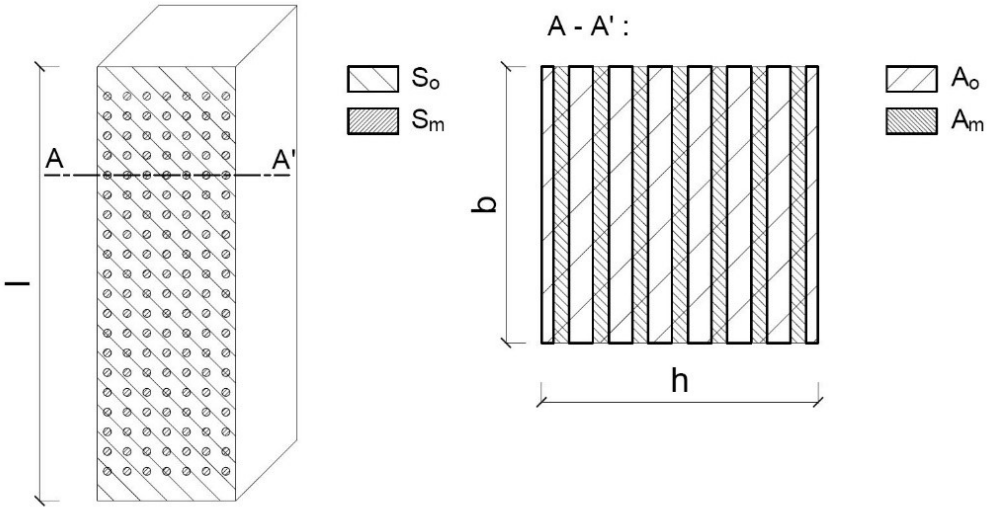

Figure 3-1 Geometry of B_0 samples

List of samples is shown by following Table 3-1:

Sample	Width	Depth	Length	Degree of Damage	Porosity
	b	*h*	*l*	*d*	*p*
	[mm]	[mm]	[mm]	[-]	[-]
BN_0	70	70	220	0,000	0,000
$B4_0$	70	70	220	0,600	0,126
$B5_0$	70	70	220	0,500	0,196
$B6_0$	70	70	220	0,400	0,283
$B7_0$	70	70	220	0,300	0,385
$B34_0$a	70	70	220	0,486	0,259
$B34_0$b	69	70	220	0,486	0,324

Table 3-1 Parameters of B_0 samples

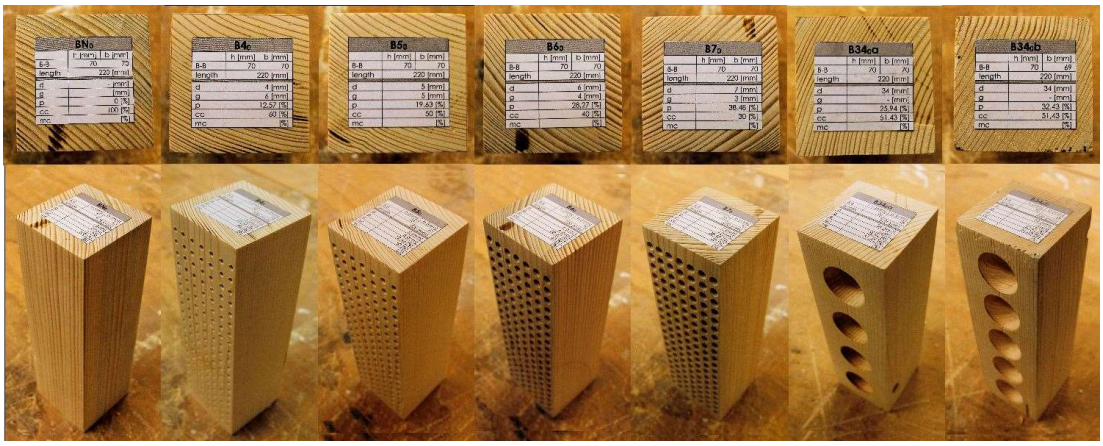

Photo 3–1 B_0 samples

3.2.2.3 Determination of the modulus of elasticity in a compression parallel to the grain

Tests were made on 29th November 2016 in laboratory of the Carinthia University of Applied Sciences in Villach, Austria under supervision of Prof. Dipl.-Ing. Dr.techn. Martin Schneider.

Conditions in laboratory:

Ari temperature: 19 °C

Air humidity 23 %rH

Condition of wood:

Moisture content: 14 %

Measuring device:

TesT GmbH

Model P114.250kN.H

No. 07.904286

Made in 2007

The modulus of elasticity was measured by a cycling strain controlled static load test. The speed of loading s was:

$$s = 0{,}00005\ [1/s] \cdot l = 0{,}00005 \cdot 220 \cdot 60\ [mm/min] = 0{,}66\ [mm/min]$$

The accuracy of measurement was in limit of 1 % of the load applied to the test piece and for loads less then 10 % of the applied maximum load under limit 0,1 % of the maximum applied load. Two extensometers were used and positioned to minimize the effect of distortion. Deformation was determined with accuracy of 0,02 mm. [7]

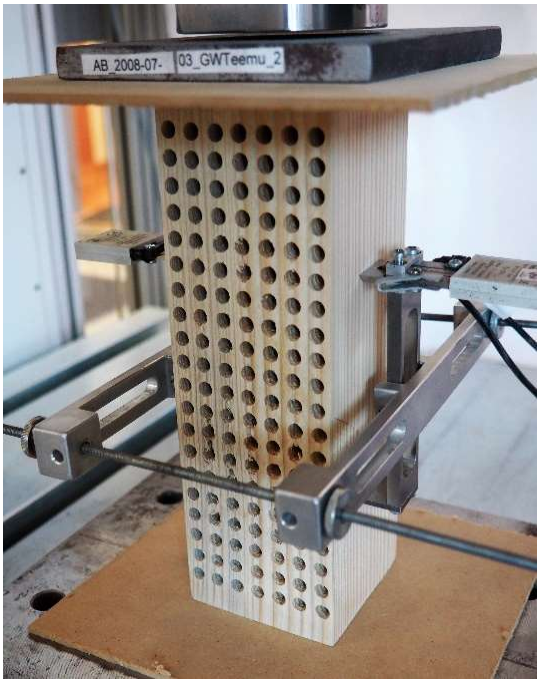

Photo 3–2 Extensometers on specimen $B6_0$

The modulus of elasticity in compression E was calculated by generally know Formula 3–4.

$$E = \frac{l\,(F_2 - F_1)}{A_N\,(w_2 - w_1)}$$

Formula 3–4 Modulus of elasticity

Limits F_1 and F_2 ware calculated based on assumption that wood used would have a compressive strength f_c = 21 [MPa]. Lower limit F_1 was calculated to cause stress of 10 % of f_c in the critical cross section of the specimen ($A_o - A_m$) and upper limit F_2 to cause 33 % of f_c.

Chart 3-2 four cycles of loading and unloading specimen $B5_0$:

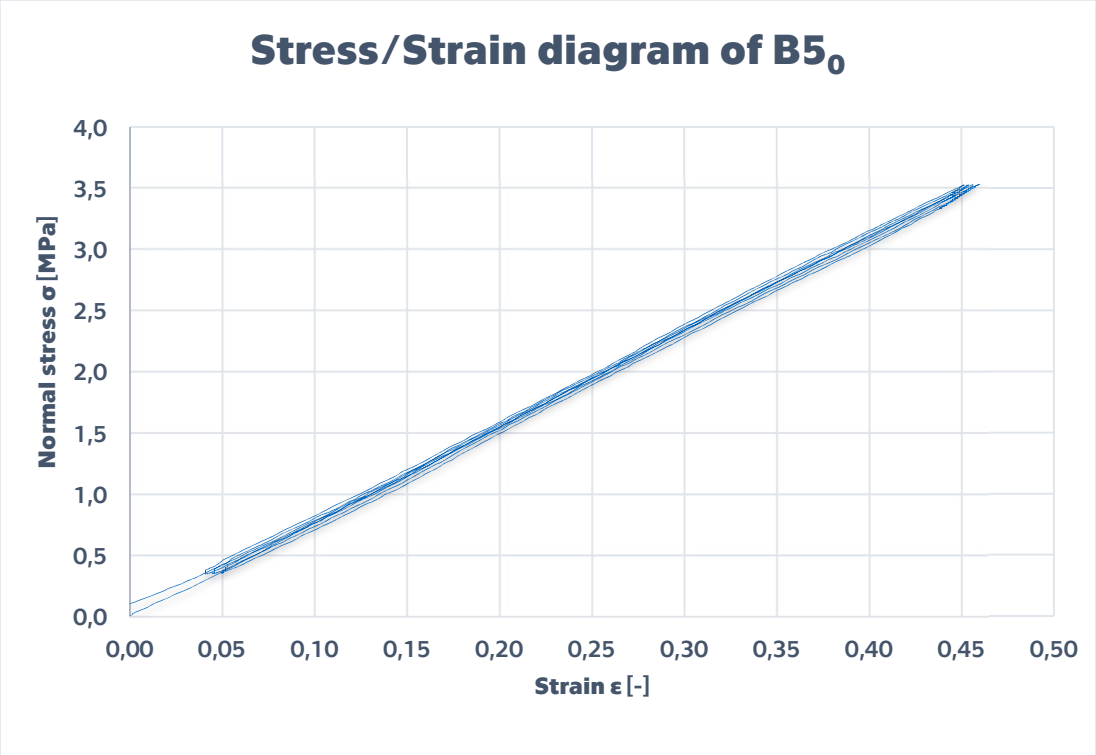

Chart 3-2 Stress / Strain diagram of specimen $B5_0$

3.2.2.4 Determination of compressive strength parallel to grain

Compressive strength was measured on the same set of samples used for determination of the modulus of elasticity. Also, the same device was used and measuring was done one day after on 30th November 2016 with practically unchanged laboratory conditions.

Strain controlled static load test was performed. Speed of loading s was 1 [mm/min]. Failures occurred in the time interval (100; 220) [s]. The normal stress σ was calculated from the measured force F:

$$\sigma = \frac{F}{A_o}$$

Formula 3–5 Normal stress

Strain ε was not measured during compressive strength test. It was calculated indirectly from measured time t , speed of loading s and the length of the sample according to Formula 3–6:

$$\varepsilon_{(t)} = \frac{t \cdot s}{l} \; [-]$$

Formula 3–6 Strain

A trend of decreasing compressive strength with increasing degree of damage is recognisable in the Chart 3-3. There is one exception in the trend. Specimen $B7_0$ performed higher in compressive strength test then less perforated specimen $B6_0$. The surface part of the specimen $B6_0$ suddenly buckled at one point (Annex 1 Photo 5–13). Probably because of relatively fast loading of specimens, decrease of stiffness is not very clear in the Chart 3-3:

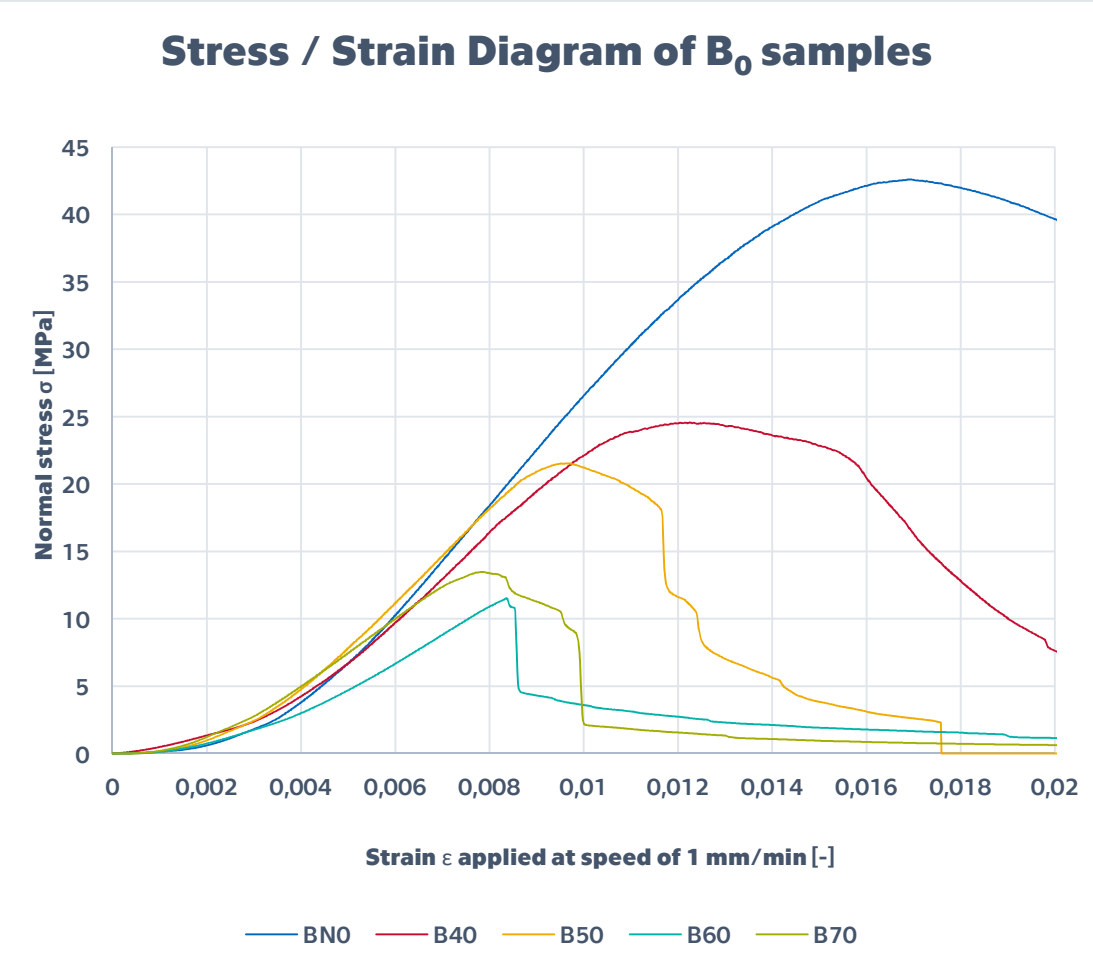

Chart 3-3 Stress / Strain diagram of B_0 samples

3.2.2.5 Measured material properties

Besides B specimens, there was one piece of another wood marked as FN_0. Its material properties were used in next calculations in chapter 0. Material of FN_0 had distinctly lower compressive strength, because of two facts. Wood was not dry enough (moisture content about 25 %) and relatively fast grown of the original tree.

Results of the experiments are in Table 3-2.

Material	Modulus of elasticity	Compressive strength
	[MPa]	[MPa]
BN_0	11110	42,6
$B4_0$	8567	25,6
$B5_0$	7337	21,3
$B6_0$	6006	17,0
$B7_0$	4651	12,8
$B34_0a$	8546	20,2
$B34_0b$	7349	19,3
FN_0	8944	19,2

Table 3-2 Measured material properties

It has to be stated that the assumed compressive strength $f_{c,N}$ = 21 [MPa] was lower then measured one $f_{c,N,m}$ = 42,6 [MPa]. It means that stress in the specimens was not in the range of 10% to 33% of f_c but in the range of 5% - 16,5% during the measurement of the modulus of elasticity.

3.2.3 ANALYSIS OF THE DATA

3.2.3.1 Compressive strength

Decrease of compressive strength with increase of degree of damage is linear in correspondence with the assumption:

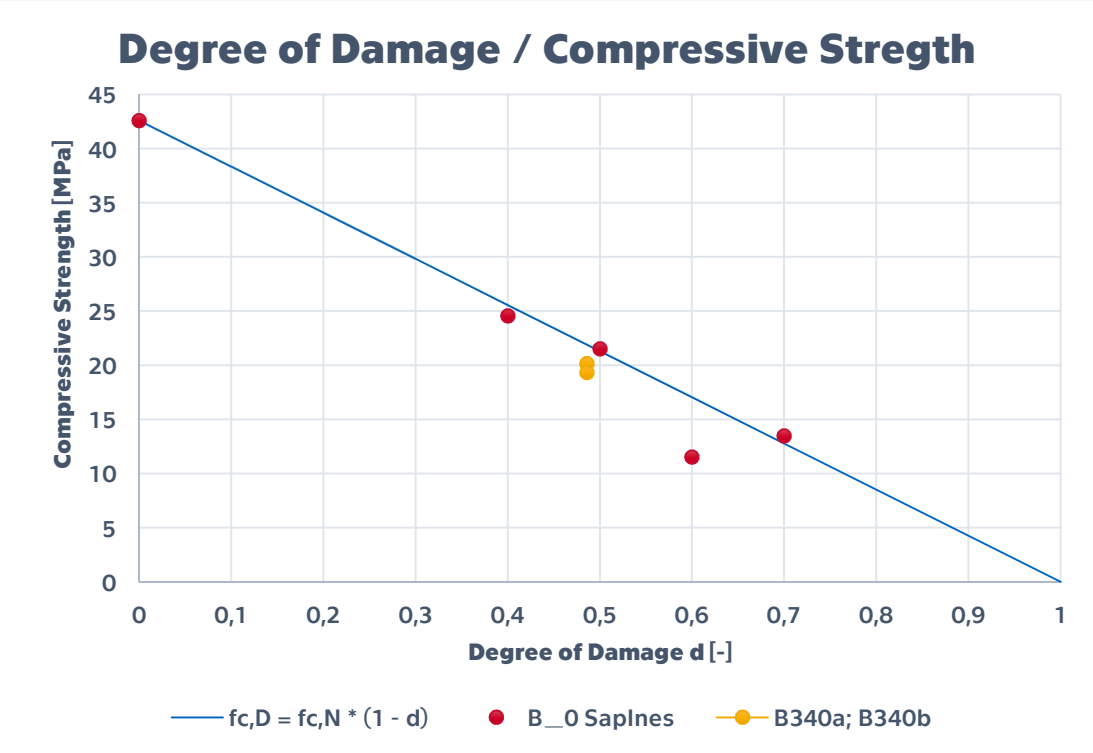

Chart 3-4 Degree of damage / Compressive strength of B_0 samples

As mentioned above, the sample $B6_0$ is little bit out of the trend. Resulting expression for the determination of the compressive strength of damaged wood is:

$$f_{c,D} = f_{c,N} \cdot (1-d)$$

Formula 3–7 Compressive strength of damaged wood

Relation between porosity p and compressive strength f_c is then given by relation between degree of damage d and porosity p (Chart 3-5).

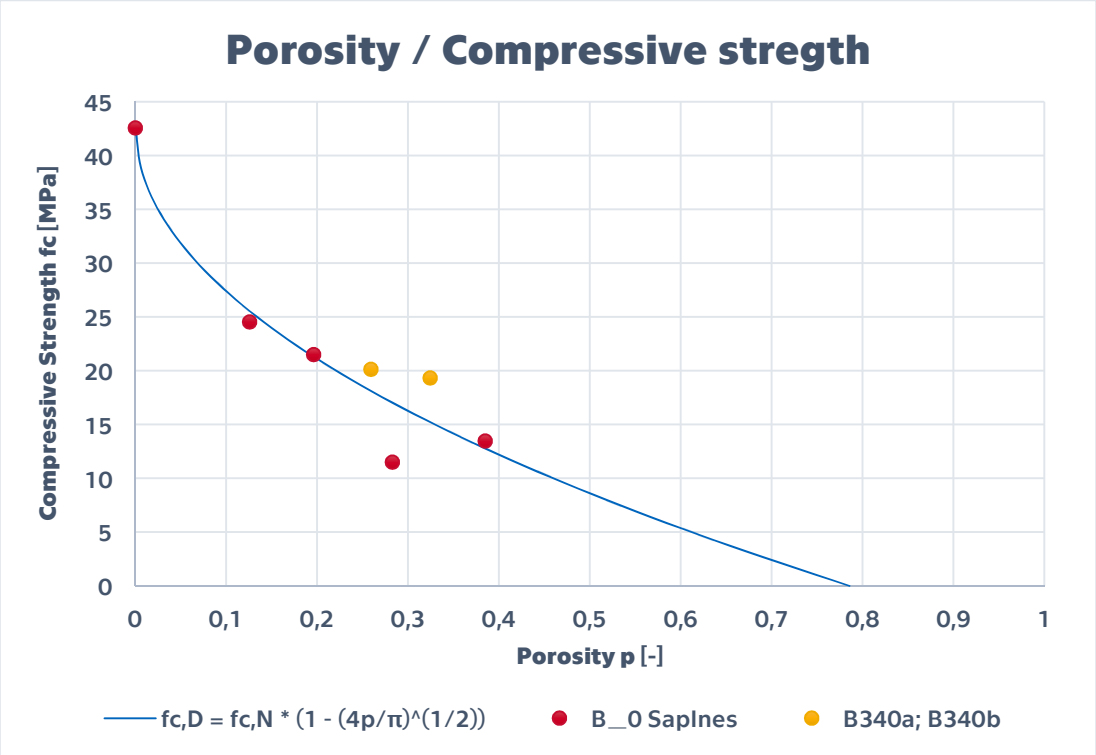

Chart 3-5 Porosity / Compressive strength of B_0 samples

The specimens $B34_0a$ and $B34_0b$ which had the same degree of damage, performed almost the same in the compressive strength test even though they had different porosity.

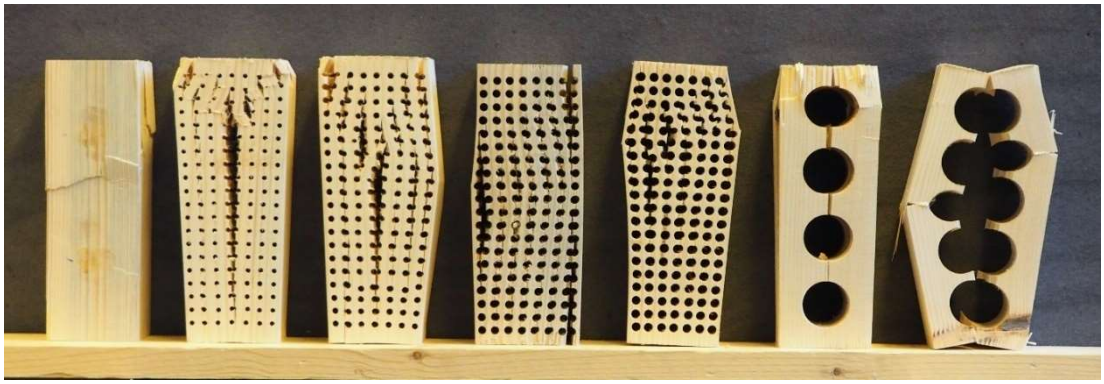

Photo 3–3 B_0 specimens after collapse

3.2.3.2 Modulus of elasticity

The decrease of the modulus of elasticity with the increase of the porosity is a crucial relation of the whole experimental part of this thesis. It's necessary to mention that all this theory is based on a direct measurement of just 5 specimens.

The result of optimization is the following Formula 3–8:

$$E_D = E_N \cdot e^{-p} \cdot (1-p)$$

Formula 3–8 Modulus of elasticity of damaged wood

Samples $B34_0a$ and $B34_0b$ were not taken into account for establishing this formula. Distribution of the porosity in these specimens is not similar to a real damage of wood.

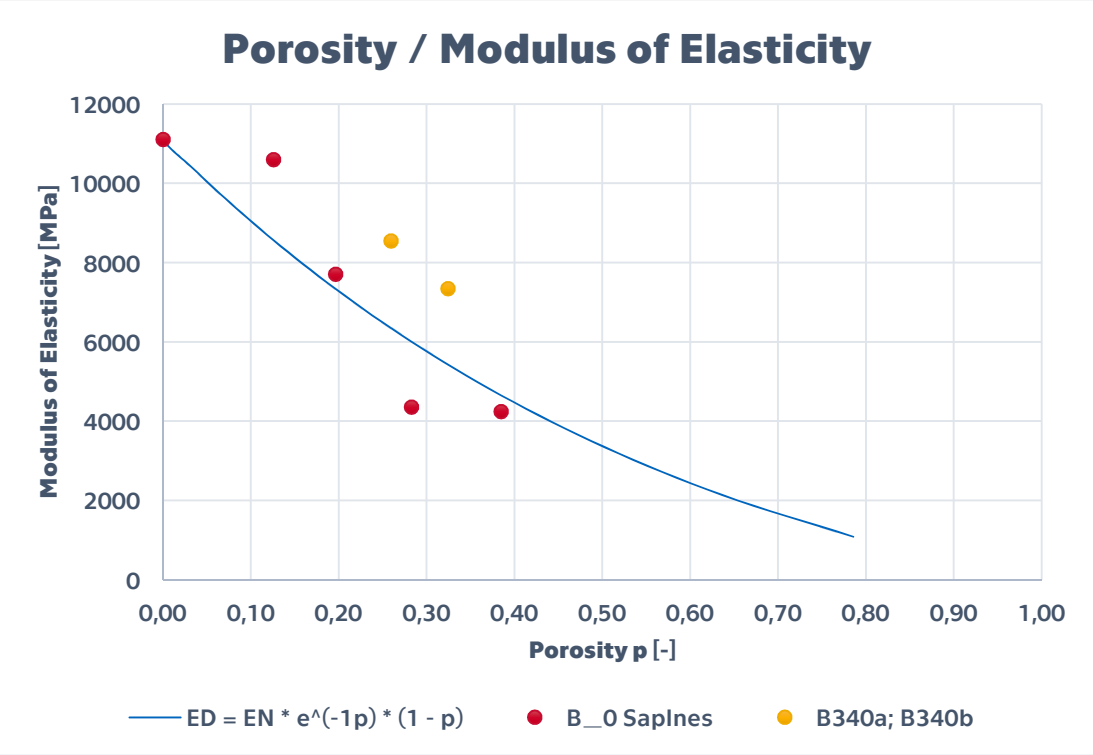

Chart 3-6 Porosity / Modulus of elasticity of B_0 samples

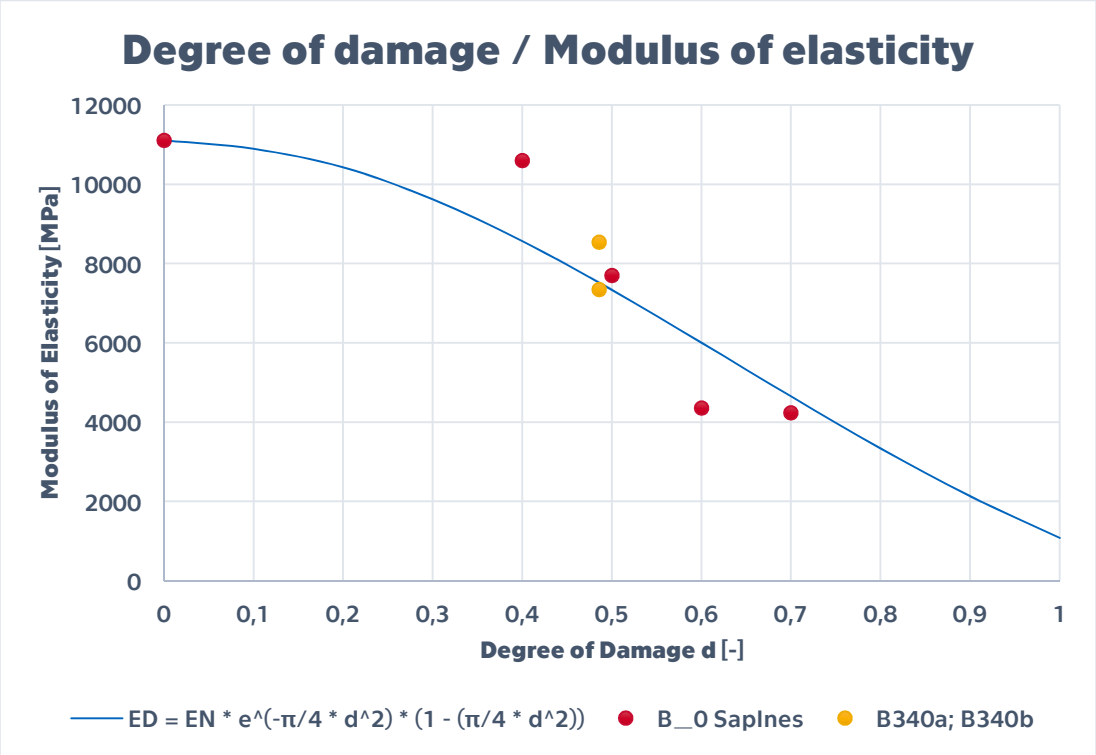

Chart 3-7 Degree of damage / Modulus of elasticity of B_0 samples

3.2.3.3 Transfer of simulation to real behaviour

For simulation of wood damage, rectangular homogeneously distributed net of circular holes through the specimens was used. Because of this method acc. to Chart 3-1 porosity p does not converge to 1 with degree of damage $d = 1$. Geometry is expressed in Figure 3-2:

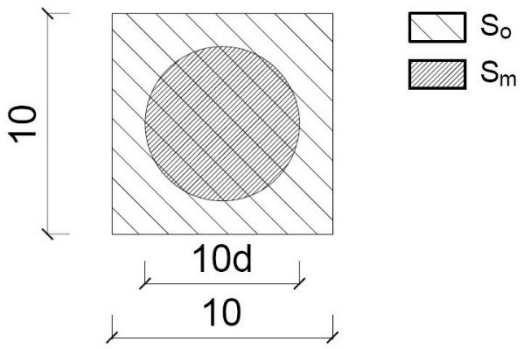

Figure 3-2 Geometry of circular holes

For the real behaviour of damaged wood, is expected that porosity p does converge to 1 with degree of damage $d = 1$ and correspond more to Figure 3-3 and Chart 3-8.

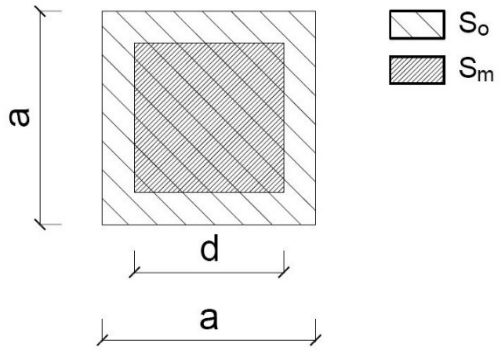

Figure 3-3 Geometry of square holes

Based on this assumption new relation for degree of damage d and real porosity p was derived. This method was further used for application on column S (naturally damaged wood).

$$p = d^2$$

Formula 3–9 Porosity for naturally damaged wood

The theory of material properties of naturally damaged wood is formed by Formula 3–9; Formula 3–8 and Formula 3–7. The following chards shows the relations of quantities:

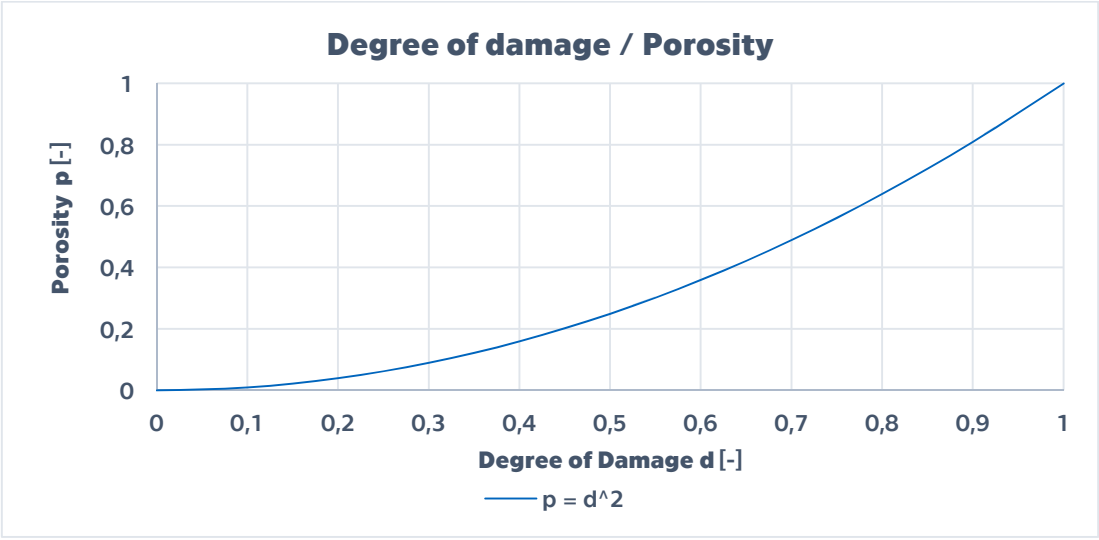

Chart 3-8 Degree of damage / Porosity for naturally damaged wood

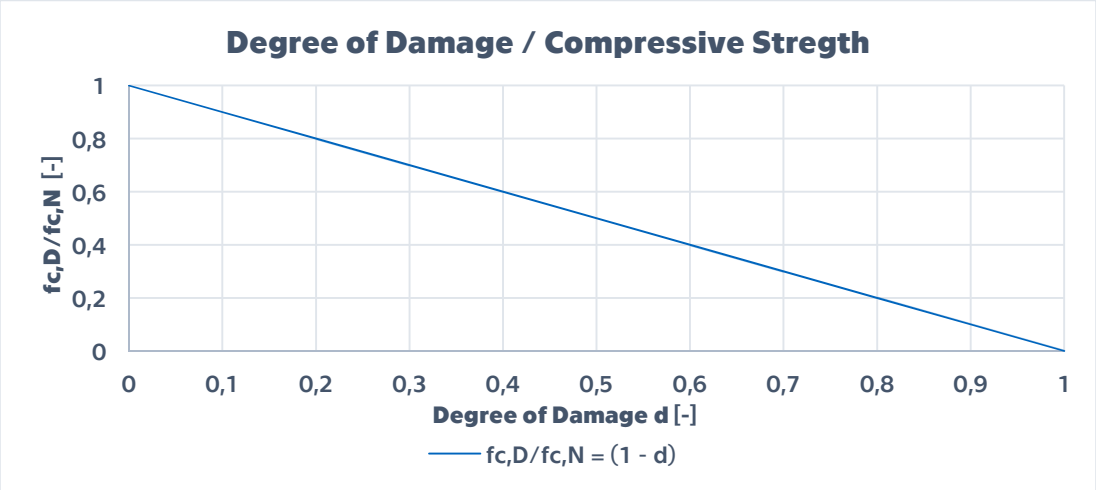

Chart 3-9 Degree of damage / Compressive strength for naturally damaged wood

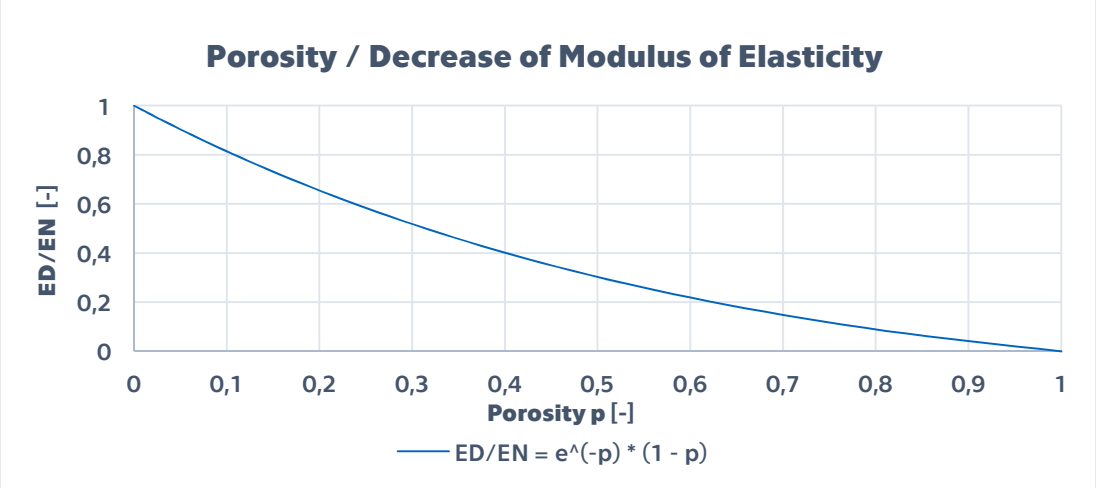

Chart 3-10 Porosity / Decrease of modulus of elasticity for naturally damaged wood

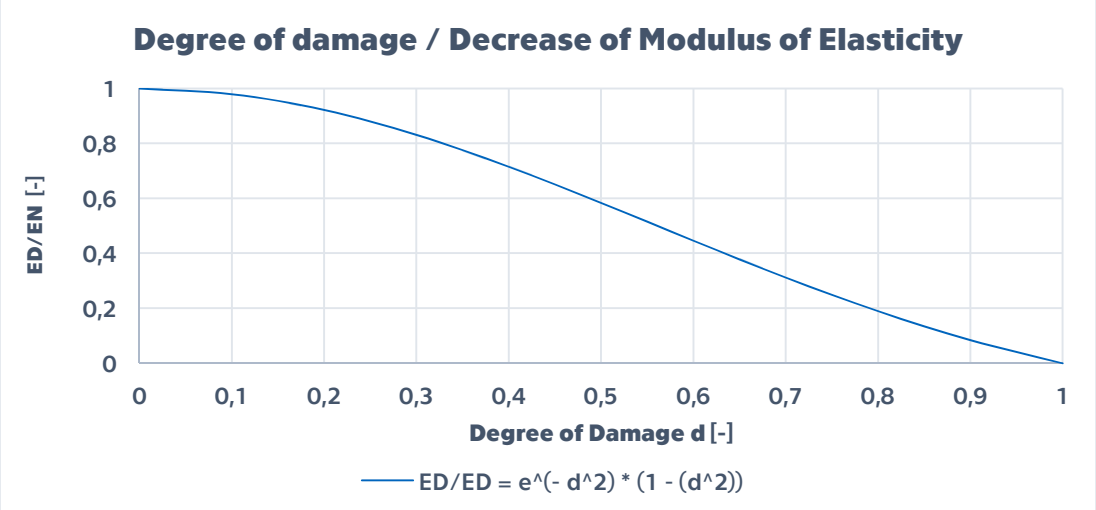

Chart 3-11 Degree of damage / Decrease of E for naturally damaged wood

3.2.4 Conclusion

Based on the results, formulas for calculation of the compressive strength of damaged material $f_{c,D}$ and modulus of elasticity of damaged wood E_D were established. Compressive strength of damaged wood depends on the original compressive strength $f_{c,N}$ and the degree of damage d. Modulus of elasticity of damaged wood depends on the original modulus of elasticity E_N and the porosity p.

If the Formula 3–9

$$p = d^2$$

is substituted in the Formula 3–8

$$E_D = E_N \cdot e^{-p} \cdot (1-p)$$

the product is exponential function for determination the modus of elasticity of damaged wood from the modus of elasticity of original undamaged wood and the form the degree of damage:

$$E_D = E_N \cdot e^{-(d^2)} \cdot (1- d^2)$$

Formula 3–10 Modulus of elasticity of naturally damaged wood

Expression for the compressive strength of naturally damaged wood stays Formula 3–7:

$$f_{c,D} = f_{c,N} \cdot (1-d)$$

The ratio between cross section dimension and length of specimens was not 1:6 as it is prescribed in norms for testing wood properties. Nevertheless, this ratio was the same for all the specimens so the results are comparable. Slight inaccuracy could be expected for determined properties of undamaged samples used in further calculations.

3.3 THE LOAD BEARING CAPACITY OF PARTIALLY PERFORATED COLUMNS

3.3.1 INTRODUCTION

In this chapter, results of calculations are compared with results of static load tests. Two sets of columns were examined. Each set consisted of 6 columns with the height of one meter. The height was just one meter because it was the limit for an accessible testing machine. The first set is named B. The wood was bought in a carpenter's shop. Second set is marked F and the material was kindly provided by a farmer Mr. Steinwender. The wood was spruce in both cases. The middle part of the most of the columns was damaged with certain porosity. Always one column was undamaged, marked with letter N, four were damaged by holes of diameter from 4 to 7 mm, and one had certain part cut out completely.

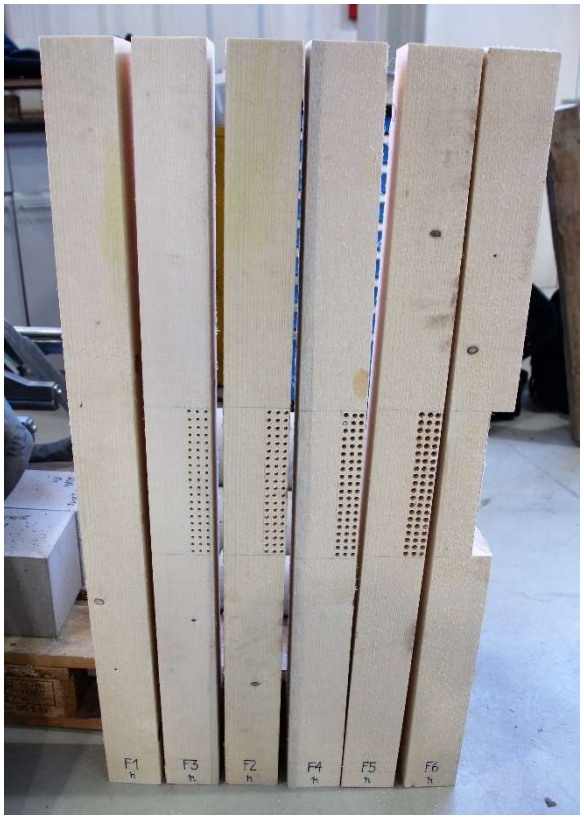

Photo 3–4 F samples

During cutting of the material the emphasis was put on avoiding knot and other defects in specimens. Static load tests were performed to show the influence of a damaged zone on the load bearing capacity of the tested columns.

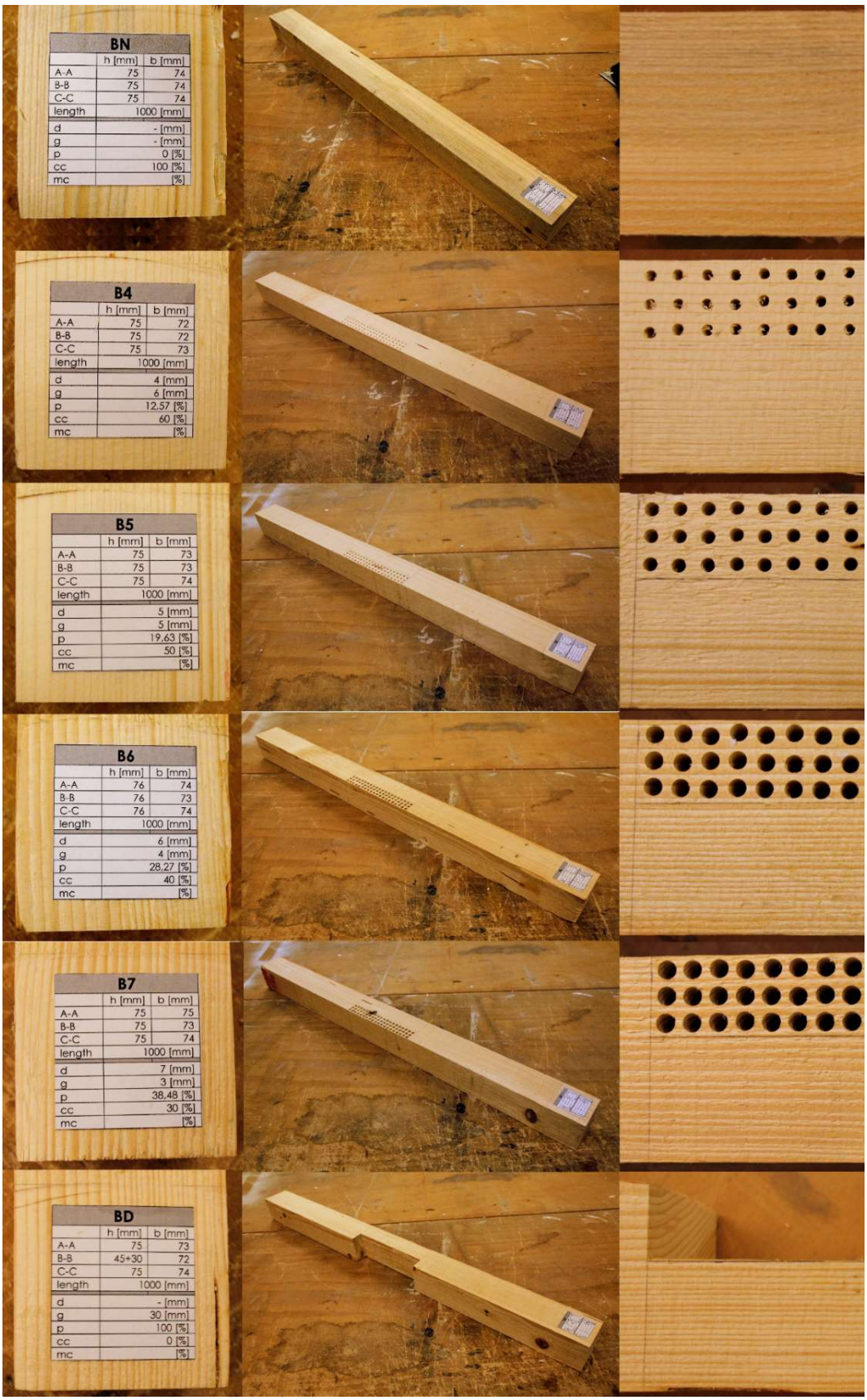

Photo 3–5 B samples

3.3.2 CALCULATION OF THE LOAD BEARING CAPACITY - COMPOSITE CROSS SECTION METHOD

Columns were judged by Eurocode EN 1995-1-1 procedure 6.3.2 - Columns subjected to either compression or combined compression and bending. [8] Composite cross section method with a fully connected parts of cross section ($\gamma = 1$) was used.

Material properties of undamaged wood were determined by direct measurement of the modulus of elasticity and the compressive strength of specimen BN_0 for B columns and FN_0 for F columns (Table 3-2). Properties of damaged wood was calculated from Formula 3–3, Formula 3–7 and Formula 3–8 derived in previous chapter of the thesis.

All partial factors for material properties and safety are not used (set equal to 1) as well as modification factor for duration of load, because this chapter is focused on the real behavior of wood members and not on designing structures.

3.3.2.1 Demonstrative calculation of load bearing capacity of the column B5:

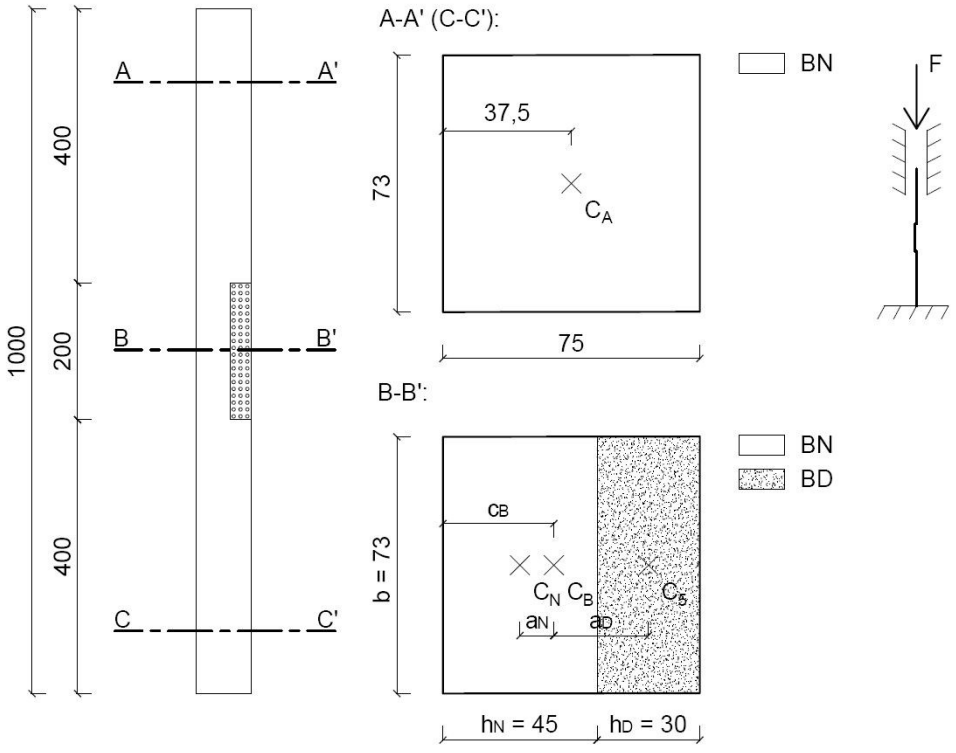

Figure 3-4 Geometry of B5 column

Effective length:

L_{ef} = **0,613 [m]**

(calculated by stability calculation in software Scia Engineer 16.0 Student)

To make results comparable with static load tests, supports were considered to be fixed in a rotation.

Material properties:

BN:

E_N = *11 110 [MPa]*

$f_{c,N}$ = *42,6 [MPa]*

BD:

d = *0,5 [-]*

circular holes porosity

$$p = \frac{\pi}{4} \cdot d^2 = \frac{\pi}{4} \cdot 0{,}5^2 = 0{,}196\ [-]$$

$$f_{c,D} = f_{c,N} \cdot (1-d) = 42{,}6 \cdot (1-0{,}5) = 21{,}3\ [MPa]$$

$$E_D = E_N \cdot e^{(-p)} \cdot (1-p) = 11110 \cdot e^{(-0{,}196)} \cdot (1-0{,}196) = 7343\ [MPa]$$

Slenderness:

Center of gravity:

$$c_B = \frac{\sum(E_i \cdot A_i \cdot c_i)}{\sum(E_i \cdot A_i)} = \frac{11110 \cdot 45 \cdot 73 \cdot 22{,}5 + 7343 \cdot 30 \cdot 73 \cdot 60}{11110 \cdot 45 \cdot 73 + 7343 \cdot 30 \cdot 73} = 33{,}96\ [mm]$$

Distances of partial centers of gravity to center of gravity of the cross section:

$$a_N = c_B \cdot \frac{h_N}{2} = 33{,}96 - 22{,}5 = 11{,}46\ [mm]$$

$$a_D = c_D - c_B = 60 - 33{,}96 = 26{,}04\ [mm]$$

Effective bending stiffness:

$\gamma = 1$ [-] (fully rigid connection)

$$EI_{c,ef} = \sum_{i=1}^{n} \left(E_i \cdot I_{y,i} + \gamma_i \cdot E_i \cdot A_i \cdot a_i^2\right) =$$

$$= E_N \cdot \frac{1}{12} \cdot b \cdot h_N^3 + 1 \cdot E_N \cdot b \cdot h_N \cdot a_N^2 + E_D \cdot \frac{1}{12} \cdot b \quad h_D^3 + 1 \cdot E_D \cdot b \quad h_D \cdot a_D^2 =$$

$$= 11110 \cdot 10^6 \cdot \frac{1}{12} \cdot 0{,}073 \cdot 0{,}045^3 +$$

$$+ 1 \cdot 11110 \cdot 10^6 \cdot 0{,}073 \cdot 0{,}045 \cdot 0{,}01146^2 +$$

$$+ 7343 \cdot 10^6 \cdot \frac{1}{12} \cdot 0{,}073 \cdot 0{,}03^3 +$$

$$+ 1 \cdot 7343 \cdot 10^6 \cdot 0{,}073 \cdot 0{,}03 \cdot 0{,}02604^2 =$$

$$= 2{,}305 \cdot 10^4 \ [Nm^2]$$

Effective area:

$$\Sigma EA_{c,tot} = E_N \cdot A_N + E_D \cdot A_D =$$

$$= 11110 \cdot 10^6 \cdot 0{,}073 \cdot 0{,}045 + 7343 \cdot 10^6 \cdot 0{,}073 \cdot 0{,}03 = 5{,}256 \cdot 10^7 \ [N]$$

Effective slenderness ration:

$$\lambda_{c,ef} = l_{ef} \cdot \sqrt{\frac{\Sigma EA_{c,tot}}{EI_{c,ef}}} = 0{,}613 \cdot \sqrt{\frac{5{,}256 \cdot 10^7}{2{,}305 \cdot 10^4}} = 29{,}27 \ [-]$$

Undamaged part:

Relative slenderness:

$$\lambda_{rel,N} = \frac{\lambda_{c,ef}}{\pi} \cdot \sqrt{\frac{f_{c,N}}{E_N}} = \frac{29{,}27}{\pi} \cdot \sqrt{\frac{42{,}6}{11110}} = 0{,}577 > 0{,}3 \rightarrow \text{stability check} \ [-]$$

$\beta_c = 0{,}2$ [-] (solid timber)

$$k_N = 0{,}5 \cdot \left[1 + \beta_c \cdot \left(\lambda_{rel,N} - 0{,}3\right) + \lambda_{rel,N}^2\right] = 0{,}5 \cdot \left[1 + 0{,}2 \cdot (0{,}577 - 0{,}3) + 0{,}577^2\right] = 0{,}694 \ [-]$$

$$k_{c,N} = \frac{1}{k_N + \sqrt{k_N^2 - \lambda_{rel,N}^2}} = \frac{1}{0{,}694 + \sqrt{0{,}694^2 - 0{,}577^2}} = 0{,}926 \ [-]$$

Condition 6.23 EN 1995 – 1 -1:

$$\frac{\sigma_{c,N}}{k_{c,N} \cdot f_{c,N}} = 1 \quad / \quad \sigma_{c,N} = \frac{E_N \cdot F_N}{\Sigma EA_{c,tot}}$$

$$\frac{\frac{E_N \cdot F_N}{\Sigma EA_{c,tot}}}{k_{c,N} \cdot f_{c,N}} = 1$$

$$F_N = \frac{k_{c,N} \cdot f_{c,N} \cdot \Sigma EA_{c,tot}}{E_N} = \frac{0{,}926 \cdot 42{,}6 \cdot 10^6 \cdot 5{,}256 \cdot 10^7}{11110 \cdot 10^6} = 186\,609\ [N] = 187\ [kN]$$

Damaged part:

Relative slenderness:

$$\lambda_{rel,D} = \frac{\lambda_{c,ef}}{\pi} \cdot \sqrt{\frac{f_{c,D}}{E_D}} = \frac{29{,}27}{\pi} \cdot \sqrt{\frac{21{,}3}{7343}} = 0{,}534 > 0{,}3 \rightarrow \text{stability check}\ [-]$$

$\beta_c = 0{,}2\ [-]$ (solid timber)

$$k_N = 0{,}5 \cdot \left[1 + \beta_c \cdot (\lambda_{rel,D} - 0{,}3) + \lambda_{rel,D}^2\right] = 0{,}5 \cdot \left[1 + 0{,}2 \cdot (0{,}534 - 0{,}3) + 0{,}534^2\right] = 0{,}666\ [-]$$

$$k_{c,D} = \frac{1}{k_D + \sqrt{k_D^2 - \lambda_{rel,D}^2}} = \frac{1}{0{,}666 + \sqrt{0{,}666^2 - 0{,}534^2}} = 0{,}940\ [-]$$

Condition 6.23 EN 1995 – 1 -1:

$$\frac{\sigma_{c,D}}{k_{c,D} \cdot f_{c,D}} = 1 \quad / \quad \sigma_{c,D} = \frac{E_D \cdot F_D}{\Sigma EA_{c,tot}}$$

$$\frac{\frac{E_D \cdot F_D}{\Sigma EA_{c,tot}}}{k_{c,D} \cdot f_{c,D}} = 1$$

$$F_D = \frac{k_{c,D} \cdot f_{c,D} \cdot \Sigma EA_{c,tot}}{E_D} = \frac{0{,}94 \cdot 21{,}3 \cdot 10^6 \cdot 5{,}256 \cdot 10^7}{7434 \cdot 10^6} = 143\,440\ [N] = 143\ [kN]$$

Load bearing capacity of column B5:

$F_{MAX,c} = MIN\ (F_N; F_D) = MIN\ (187; 143) = 143\ [kN]$

The influence of the bending moment caused by eccentricity of the load in the middle part was neglected in the condition 6.23. The change of position of the axis in the middle part of the member is expressed by extended effective length of the column. Column B5 should buckle under the force about 143 [kN].

3.3.2.2 Calculated load bearing capacity of specimens:

Column	Damage zone		Dimensions		Effective length	**Maximal normal force**
	d	*p*	*b*	*h*	l_{ef}	$F_{MAX,c}$
	[-]	[%]	[mm]	[mm]	[m]	**[kN]**
BN	0,0	0,00%	74,0	75,0	0,595	**221,7**
B4	0,4	12,57%	72,0	75,0	0,590	**154,5**
B5	0,5	19,63%	73,0	75,0	0,613	**143,4**
B6	0,6	28,27%	73,0	76,0	0,665	**131,4**
B7	0,7	38,48%	73,0	75,0	0,631	**116,8**
BD	1,0	100,00%	72,0	75,0	0,780	**76,7**
FN	0,0	0,00%	79,0	80,0	0,584	**118,9**
F4	0,4	12,57%	83,5	79,0	0,595	**88,8**
F5	0,5	19,63%	79,0	80,0	0,601	**79,2**
F6	0,6	28,27%	83,5	80,0	0,610	**77,4**
F7	0,7	38,48%	81,0	80,5	0,623	**69,0**
FD	1,0	100,00%	82,0	50,5	0,730	**68,1**

Table 3-3 Calculated load bearing capacity of B and F columns

3.3.3 STATIC LOAD TESTS OF B AND F COLUMNS

Tests were made 30th November 2016 in the laboratory of the Carinthia University of Applied Sciences in Villach, Austria.

Conditions in laboratory:

Ari temperature: 18 °C

Air humidity 25 %rH

Condition of wood:

Moisture content: 14 % (B)

Measuring device:

TesT GmbH

Model P114.250kN.H

No. 07.904286

Made in 2007

Static load test was strain controlled. Speed of loading s was 1 mm/min as well as in the case of determination of compressive strength test of BN_0 and FN_0. Failures occurred in the time interval (180; 270) [s]. The normal stress σ was recalculated from measured force F acc. Formula 3–5.

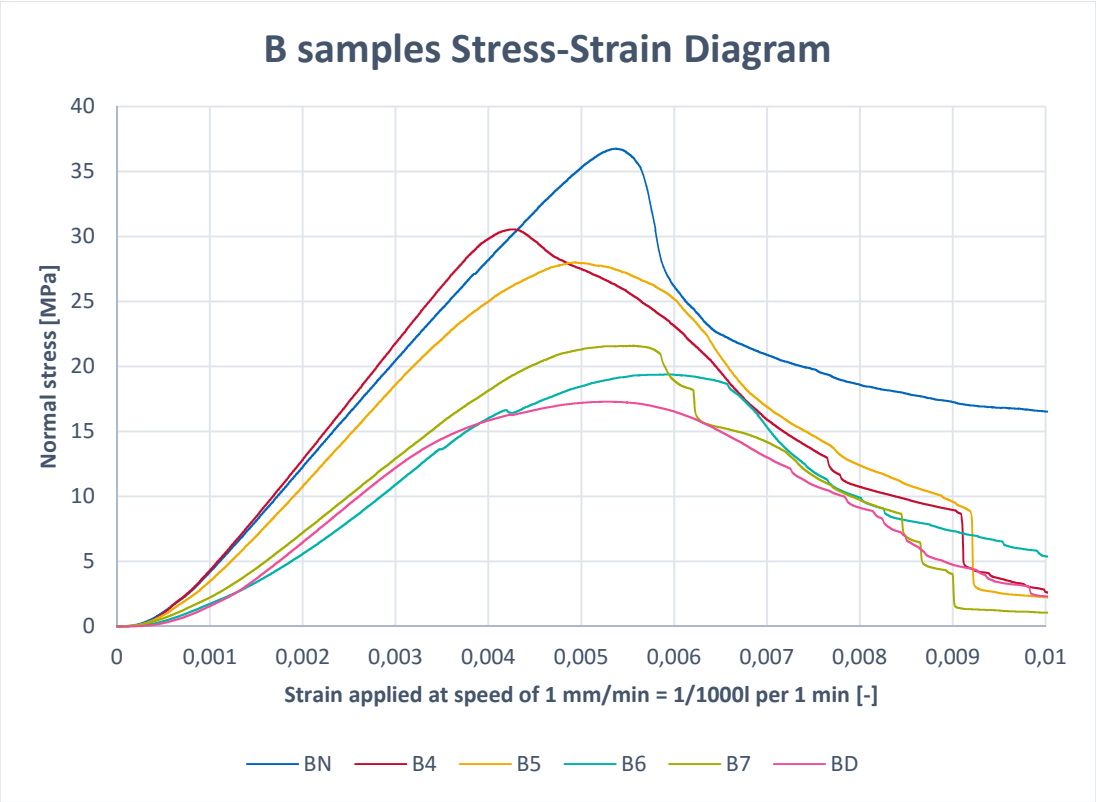

Chart 3-12 Stress / Strain diagram of B columns

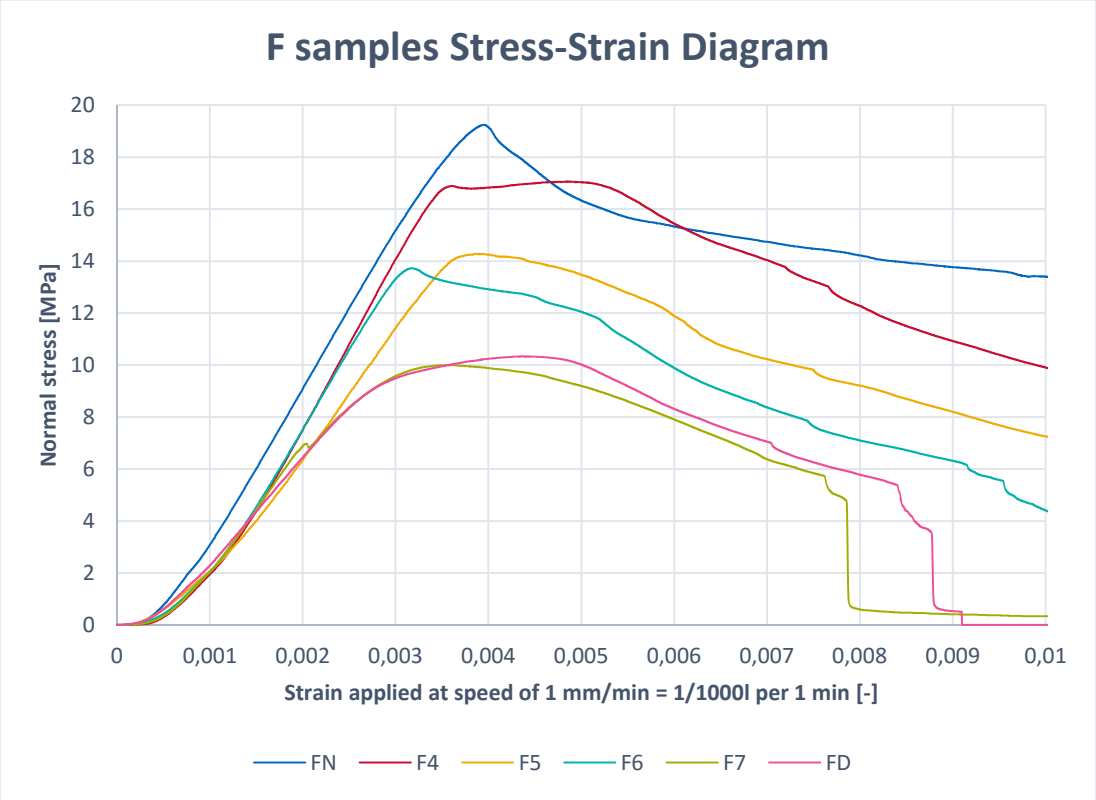

Chart 3-13 Stress / Strain diagram of F columns

3.3.4 CONCLUSION:

The comparison of the results of calculated and measured load bearing capacity is displayed in Chart 3-14:

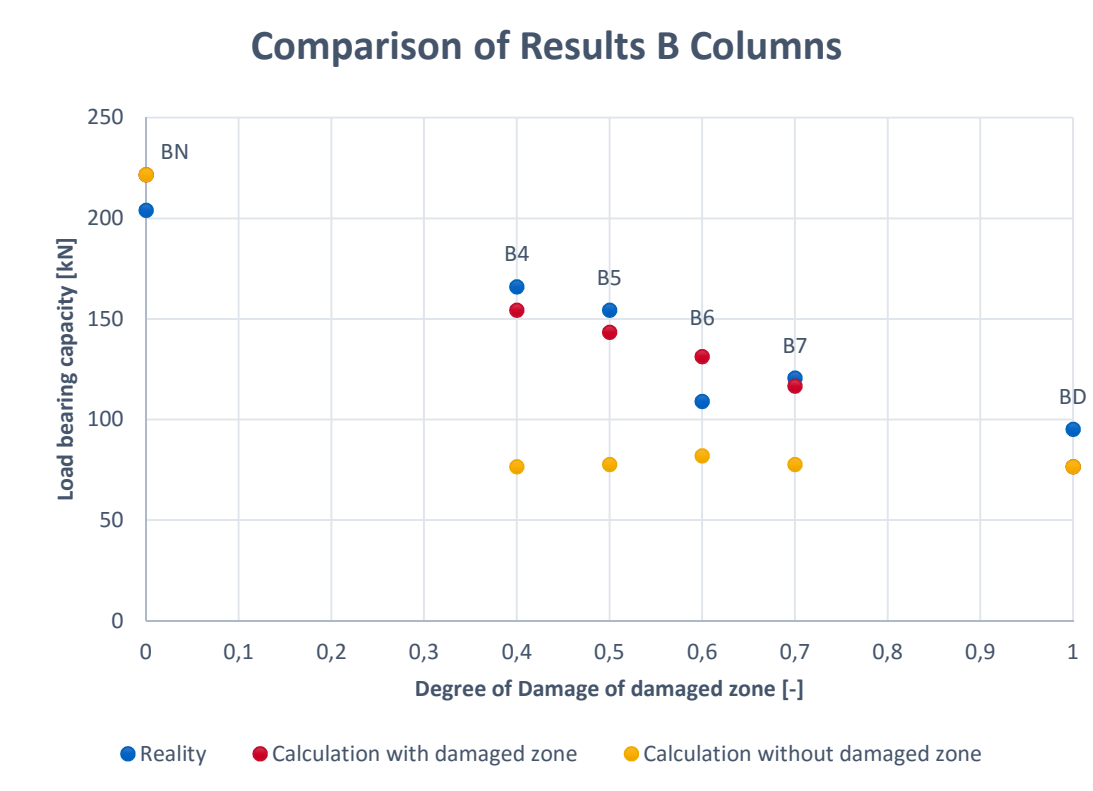

Chart 3-14 Comparison of results B columns

From difference of blue (measured values) and red (calculated values) points it is possible to see accuracy of the method. An error of calculation c (Formula 3–11) was determined for all samples. The average value was 11%.

$$c = \left| 1 - \frac{F_{MAX,c}}{F_{MAX,m}} \right|$$

Formula 3–11 Error of calculation

Yellow points represent load bearing capacity calculated by conservative procedure which does not take into account the damaged parts of structures regardless of its stage of damage. Of course it is on the safe side but e.g. for the B5 column, which has the degree of damage of the damaged zone d = 0,5 [-] and porosity p = 19,6 [%], the load bearing capacity is just half of the measured value.

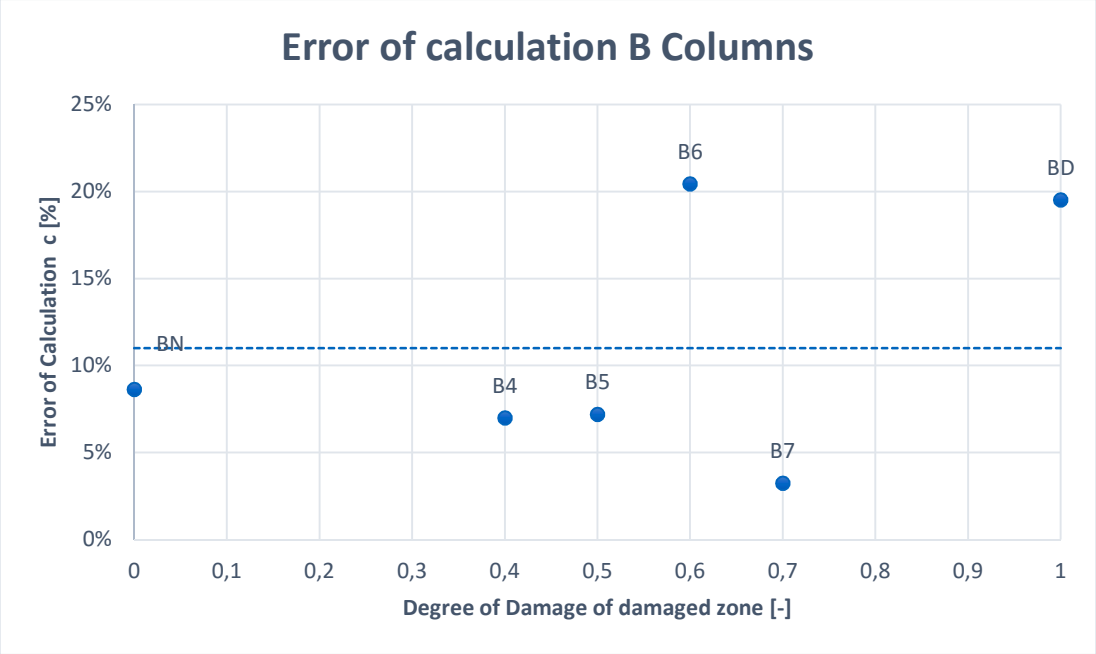

Chart 3-15 Error of calculation B Columns

Column	Reality	Calculation with damaged zone	Calculation without damaged zone
	[kN]	[kN]	[kN]
BN	**204,1**	221,7	221,7
B4	**166,1**	154,5	76,7
B5	**154,5**	143,4	77,8
B6	**109,1**	131,4	82,1
B7	**120,7**	116,8	77,8
BD	**95,3**	76,7	76,7
FN	**121,6**	118,9	118,9
F4	**107,8**	88,8	*66,4*
F5	**93,7**	79,2	*64,7*
F6	**91,4**	77,4	*68,4*
F7	**65,0**	69,0	*67,3*
FD	**68,0**	68,1	68,1

Table 3-4 Load bearing capacity of columns

3.4 THE LOAD BEARING CAPACITY OF THE NATURALLY DAMAGED COLUMN

3.4.1 INTRODUCTION

This chapter is focused on one piece of fir wood marked as column S. It is 1m long with cross section dimensions 85 x 90 mm. It was originally used as a backing lath. It was partially damaged by rot and that is why it was chosen for this experiment.

One task of this thesis is to provide procedure of calculation load bearing capacity of an naturally damaged column. In this chapter the procedure developed in previous chapter was combined with resistance drilling for localization and rating of the degree of damage and kiln dry method for determination of the strength class of the undamaged material. The column S was the subject of the last static load test and the result of calculation was compared with the result of measured load bearing capacity. At the end, the specimen was cut into parts for diagnosis of the accuracy of the localization of damage (Annex 1 Chapter 5.3).

3.4.2 LOCALIZATION AND RATING OF DAMAGED ZONES IN THE COLUMN S

3.4.2.1 Used device - Resistograph® R650-PR

Carinthia University of Applied Sciences provided Resistograph® R650-PR for this project. It is a battery powered resistance drilling machine produced by RINNTECH e.K., Germany.

Parameters:

- Maximal drilling length 50 cm
- 25 measured values per millimeter(10Bit)
- Automatically maximized thrust up to 2 cm/sec
- Used needle diameter of 1.5 mm and 3.0 mm tip

Photo 3–6 Resistograph® R650-PR

3.4.2.2 Interpretation of resulting diagrams

The result of each drilling is a diagram which has distance (depth of drilling) on the x axis and relative resistance of wood on the axis y. This relative resistance is based on energy consumption of the motor responsible for rotating the needle.

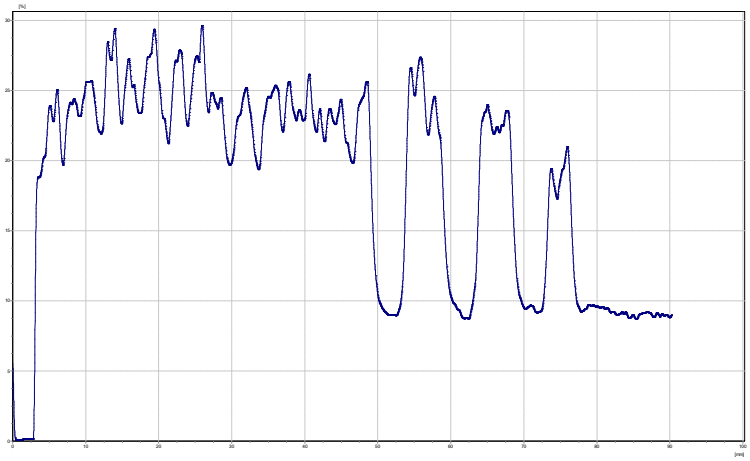

Chart 3-16 Example of a diagram from Resistograph® (drilling B5.2)

Measured resistance is relative so it is not possible to determine any material properties of the object directly. From the difference in resistance it is possible to locate damaged zones and estimate the degree of damage d.

Procedure of diagram analysis (example of B5 sample):

This example diagram is from drilling in the middle part of the column B5 started in the undamaged side going perpendicular to the member surface:

1) First step is to divide the cross section into damaged and undamaged part
    a. Put a line on lower limits of resistance in the area which is supposed to be undamaged. (The non-zero angle is coursed by an increase of resistance due to friction of the needle.)
    b. Where the resistance is below this line, the zone is considered to be damaged. The number of zones and the step of division are given by the required accuracy of calculation. Here the cross section was divided into two zones (undamaged and damaged) with step of division 5 [mm].
    c. Make another line parallel to first one so that the new line intersects the curve of resistance by the end of the cross section. This is the base line of zero resistance.

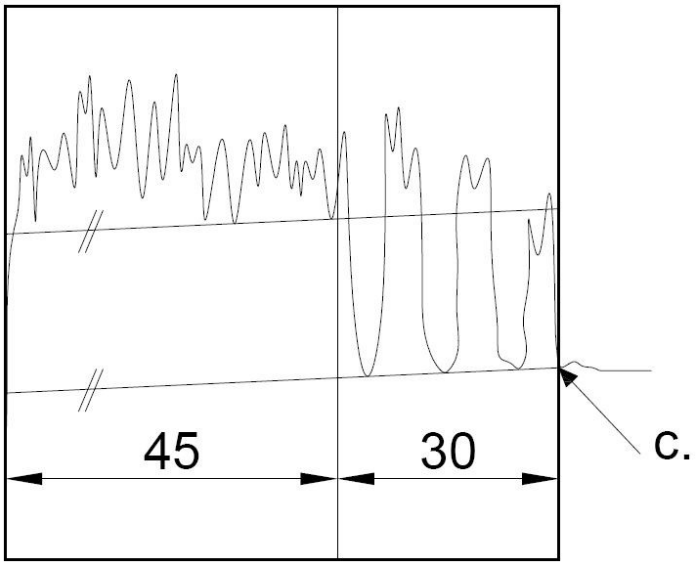

Figure 3-5 Interpretation of resistance drilling diagram 1

2) Areas under the curve

a. If it is necessary, area under the curve has to be calculated by integration or by graphical method, but in practice the average relative resistance is just estimated.

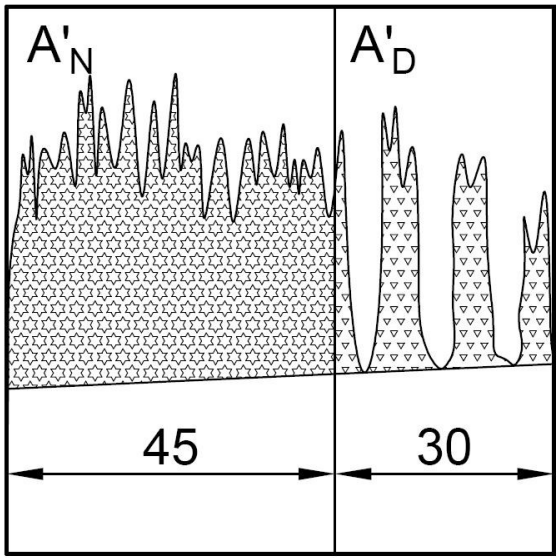

Figure 3-6 Interpretation of resistance drilling diagram 2

b. Area serves to determine the average relative resistance of a part of the cross section R

$$R_i = \frac{A'_i}{h_i}$$

Formula 3–12 Average relative resistance of a part of a cross section

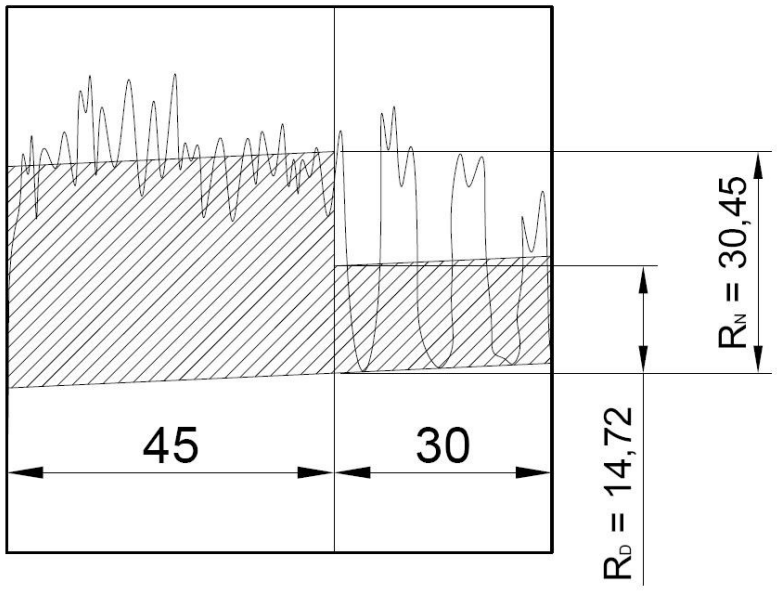

Figure 3-7 Interpretation of resistance drilling diagram 3

3) **Degree of damage**

a. **From the average relative resistance of a part R_i and undamaged part R_N the degree of damage d is calculated acc. Formula 3–13, or it is estimated acc. to Figure 3-8:**

$$d_i = \frac{R_{D,i}}{R_N}$$

Formula 3–13 Degree of damage from the diagram

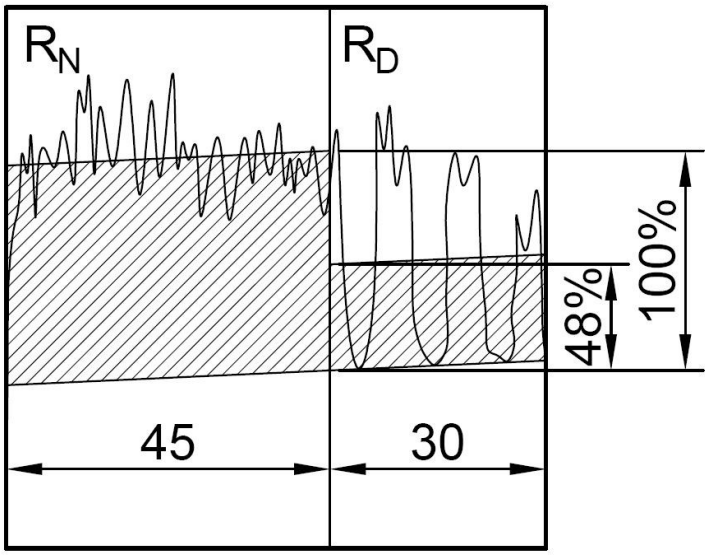

Figure 3-8 Interpretation of resistance drilling diagram 4

Degree of damage d in this case based on calculation is equal:

$$d = \frac{R_D}{R_N} = \frac{\frac{A'_D}{h_D}}{\frac{A'_N}{h_n}} = \frac{\frac{441,6}{30}}{\frac{1370,3}{45}} = 0,483\ [-]$$

Area A_D and A_N was calculated by Autodesk AutoCAD 2016 Student.

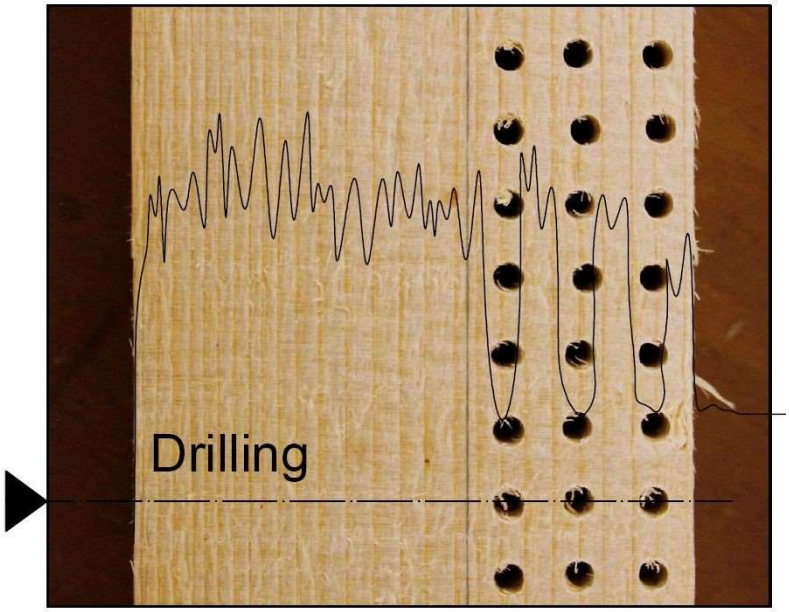

Figure 3-9 Resistance drilling diagram on the photo of specimen B5

Real degree of damage acc. to Formula 3–1 is equal:

$$d = \frac{A_m}{A_o} = \frac{3 \cdot 5 \cdot 75}{30 \cdot 75} = 0{,}5 \ [-]$$

Accuracy is satisfactory and this procedure was used for analysing diagrams of the column S.

3.4.2.3 Analyse of damage of the column S

Column S was inspected by 30 drillings in 10 cross sections. Each cross section was divided into 3 strips (one per drilling) and each strip into 9 fields. Together 270 volume blocks of dimensions 10 x 30 (25) x 100 mm. For each block the degree od damage d was determined.

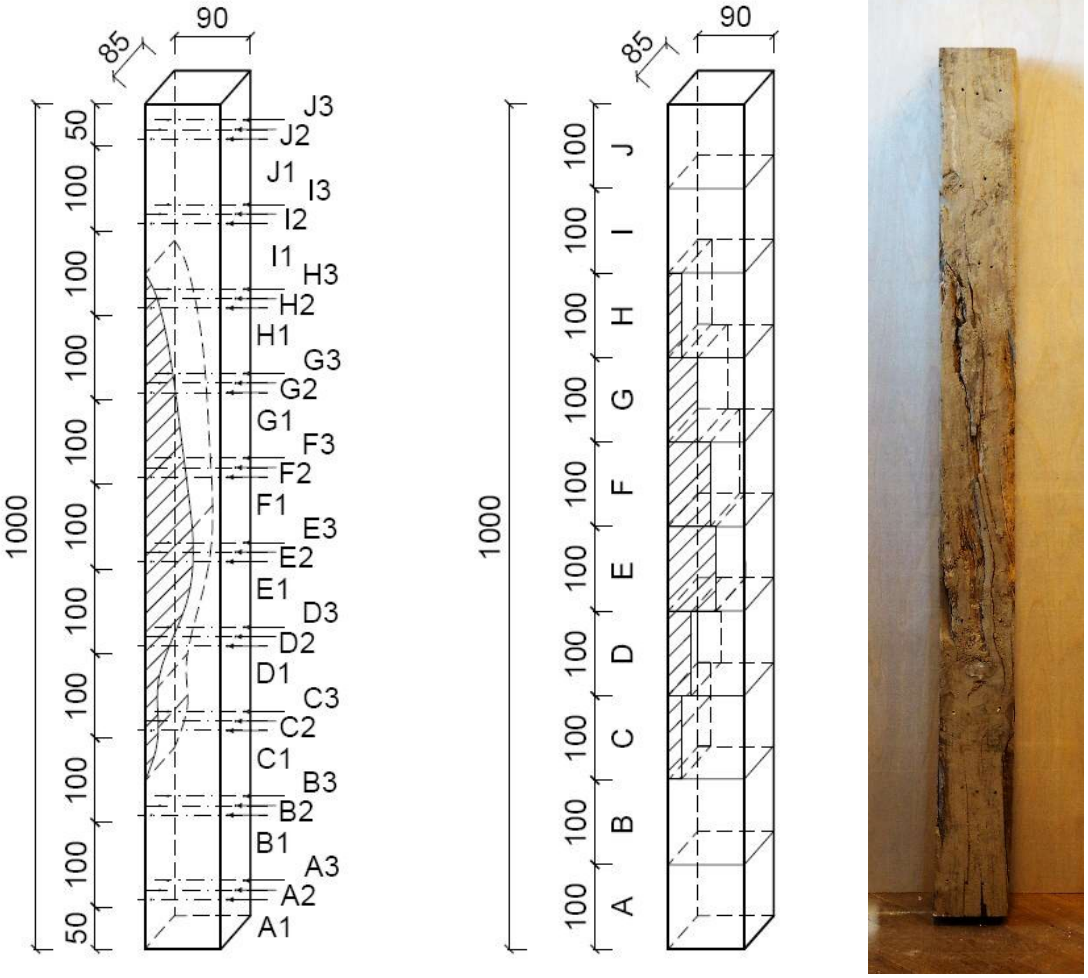

Figure 3-10 Geometry of the column S

Photo 3–7 Damaged surface of the column S

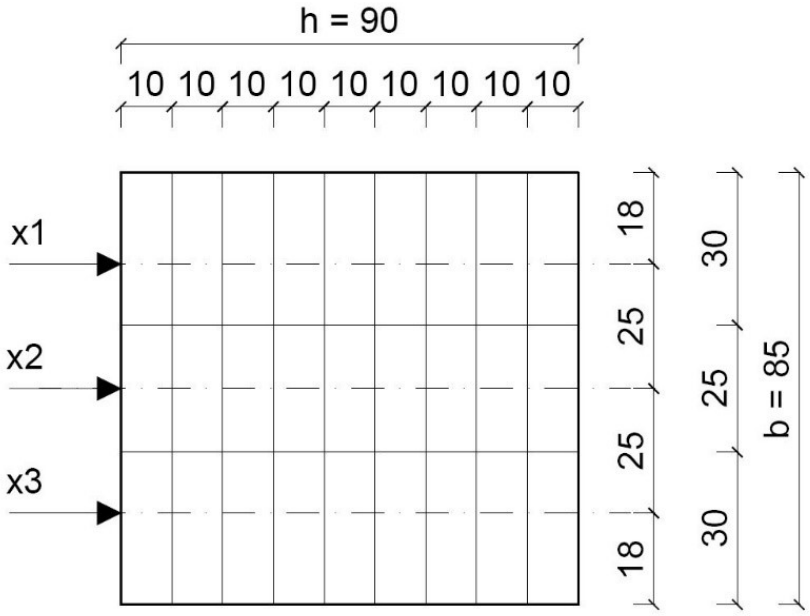

Figure 3-11 Cross section of the column S

Example analysis of diagrams in the cross section G:

Black lines are the minimum resistance of undamaged wood and the base line, green line represents the average resistance of the undamaged part of the cross section, yellow and orange horizontal lines represents the average resistance of the discovered damaged parts of the cross section and vertical lines divides the cross section Each strip was divided into 9 one-centimeter fields starting from the beginning of the cross section which is not in coincide with the beginning of a diagram. That is why vertical lines do not seem to be in the optimal spots.

G1:

- First 3 cm are undamaged
- 4. and 5. cm has degree of damage d = 0,3 [-]
- 6. and 7. cm is without any decay
- 8. and 9. cm in damaged up to the d = 0,5 [-]

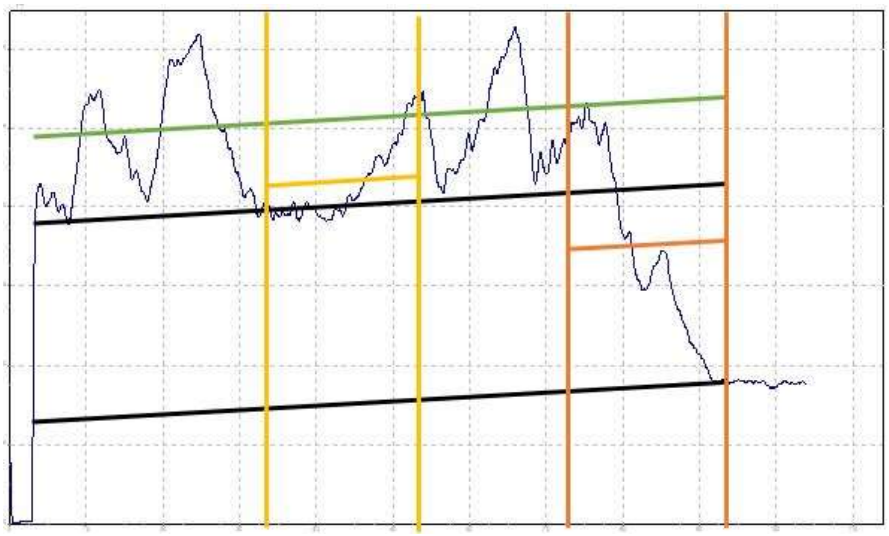

Figure 3-12 Analyse of the diagram G1

G2:

- First 4 cm are undamaged
- 5. - 7. cm has degree of damage d = 0,3 [-]
- 8. and 9. cm in damaged up to the d = 0,5 [-]

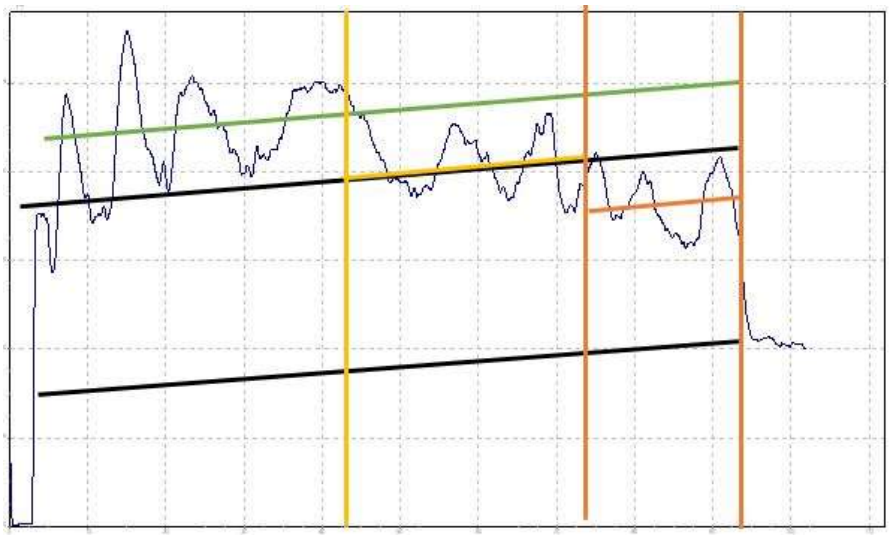

Figure 3-13 Analyse of the diagram G2

G3:

- First 6 cm are undamaged
- 7. - 9. cm is almost destroyed with the d = 0,8 [-]

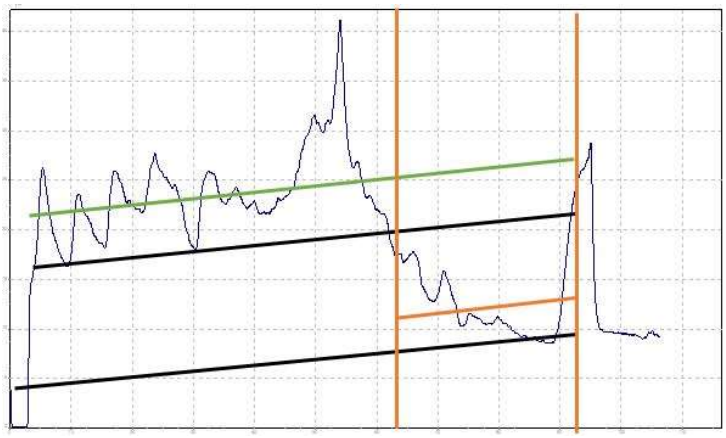

Figure 3-14 Analyse of the diagram G3

Summary of the damaged zones in the column S

Results of resistance drilling more or less correspond with the expectation based on visual check of the column.

		1	2	3	4	5	6	7	8	9
A	1	0,0	0,0	0,0	0,1	0,1	0,1	0,0	0,0	0,0
	2	0,0	0,0	0,0	0,0	0,0	0,0	0,2	0,2	0,2
	3	0,0	0,0	0,0	0,0	0,0	0,0	0,0	0,0	0,0

		1	2	3	4	5	6	7	8	9
B	1	0,0	0,0	0,0	0,0	0,0	0,0	0,0	0,0	0,0
	2	0,0	0,0	0,0	0,0	0,0	0,0	0,0	0,2	0,2
	3	0,0	0,0	0,0	0,0	0,0	0,0	0,0	0,0	0,0

		1	2	3	4	5	6	7	8	9
C	1	0,0	0,0	0,0	0,0	0,0	0,0	0,0	0,0	0,0
	2	0,0	0,0	0,0	0,0	0,0	0,0	0,0	0,0	0,0
	3	0,0	0,0	0,0	0,2	0,2	0,0	0,0	0,0	0,0

		1	2	3	4	5	6	7	8	9
D	1	0,0	0,0	0,0	0,0	0,0	0,0	0,4	0,4	0,4
	2	0,0	0,0	0,0	0,0	0,0	0,0	0,5	0,5	0,5
	3	0,0	0,0	0,0	0,0	0,0	0,0	0,5	0,5	0,5

		1	2	3	4	5	6	7	8	9
E	1	0,0	0,0	0,3	0,3	0,3	0,3	0,3	0,6	0,6
	2	0,0	0,0	0,1	0,1	0,1	0,1	0,5	0,5	0,5
	3	0,0	0,0	0,0	0,0	0,0	0,0	0,5	0,5	0,5

		1	2	3	4	5	6	7	8	9
F	1	0,0	0,2	0,2	0,2	0,2	0,0	0,0	0,4	0,4
	2	0,0	0,0	0,0	0,0	0,0	0,2	0,2	0,4	0,4
	3	0,0	0,0	0,3	0,3	0,3	0,0	0,0	0,7	0,7

		1	2	3	4	5	6	7	8	9
G	1	0,0	0,0	0,0	0,3	0,3	0,0	0,0	0,5	0,5
	2	0,0	0,0	0,0	0,0	0,3	0,3	0,3	0,5	0,5
	3	0,0	0,0	0,0	0,0	0,0	0,0	0,8	0,8	0,8

		1	2	3	4	5	6	7	8	9
H	1	0,0	0,0	0,1	0,1	0,1	0,0	0,0	0,0	0,0
	2	0,0	0,0	0,0	0,0	0,2	0,2	0,2	0,2	0,2
	3	0,0	0,0	0,0	0,0	0,0	0,0	0,4	0,4	0,4

		1	2	3	4	5	6	7	8	9
I	1	0,0	0,0	0,0	0,0	0,0	0,0	0,0	0,0	0,2
	2	0,0	0,0	0,0	0,0	0,0	0,0	0,0	0,2	0,2
	3	0,0	0,0	0,0	0,0	0,0	0,0	0,0	0,0	0,0

		1	2	3	4	5	6	7	8	9
J	1	0,0	0,0	0,0	0,2	0,2	0,2	0,0	0,0	0,0
	2	0,0	0,0	0,0	0,0	0,0	0,0	0,0	0,0	0,2
	3	0,0	0,0	0,0	0,0	0,0	0,0	0,0	0,2	0,2

Table 3-5 Inspection of the damage in the column S

3.4.3 MATERIAL PROPERTIES OF THE COLUMN S

3.4.3.1 Undamaged wood S_N

Material properties were determined indirectly from the density. Three specimens were taken from the end of the piece before it was cut into precise length of 1 m. Kiln dry method for calculation of density was used and material was ranked acc. to Table 3-8.

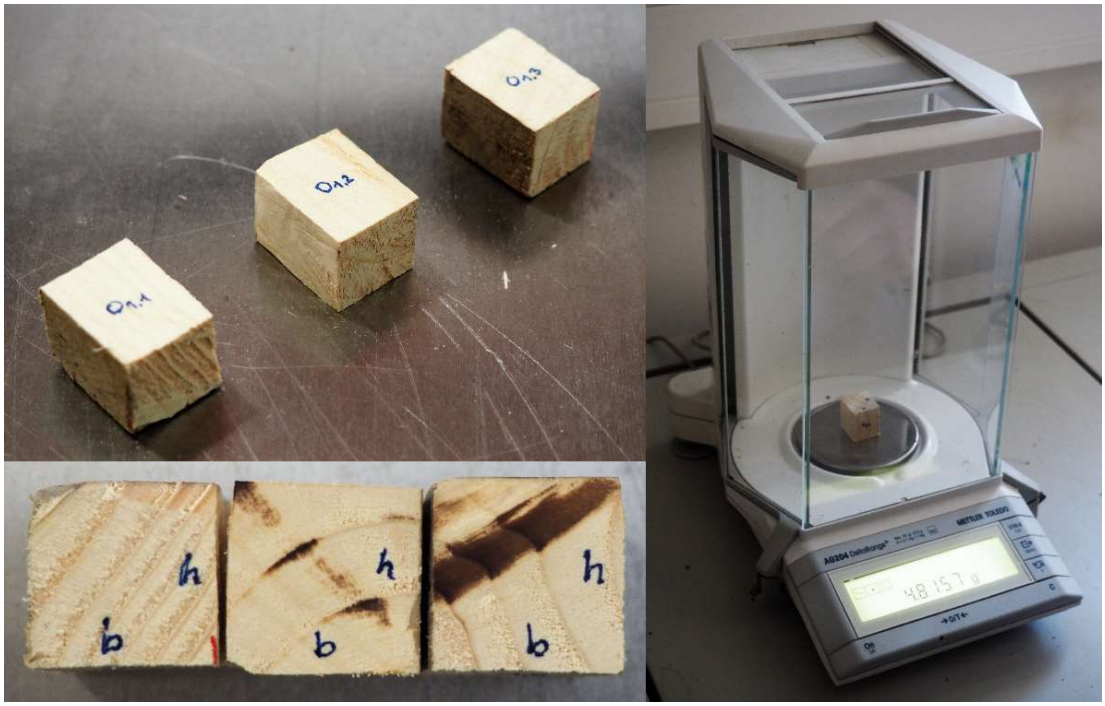

Photo 3–8 Specimens for calculation of the density of the material S_N

Measured values are displayed in Table 3-6:

Sample	Dimensions			Weight			
	b	*h*	*l*	$g_{t=0h}$ 6.12.2016 10:30	$g_{t=24h}$ 7.12.2016 10:30	$g_{t=29h}$ 7.12.2016 15:30	$g_{t=24h} - g_{t=29h}$
	[mm]			[g]			
S1.1	20,5	20,5	27,0	3,7165 g	3,4135 g	3,4158 g	-0,0023
S1.2	21,5	20,0	26,0	3,9687 g	3,6150 g	3,6148 g	0,0002
S1.3	21,0	21,5	27,0	4,2639 g	3,9110 g	3,9128 g	-0,0018

Table 3-6 Dimensions and weights of samples of S_N wood

Moisture content and density are calculated in the Table 3-7. Final density is recalculated to the moisture content 12 %. It corresponds to the state of storing in 20°C and humidity 65 %. The mean value of density of the undamaged material S_N was averaged from three specimens.

Sample	Moisture content	Density						Strength class of wood
	MC	$\rho_{t=0h}$	$\rho_{t=0h}$ Average	$\rho_{MC=0\%}$	$\rho_{MC=0\%}$ Average	$\rho_{MC=12\%}$	$\rho_{MC=12\%}$ Average	
	[%]	[kg/m3]						
S1.1	8,9%	328	344	301	315	337	353	C14
S1.2	9,8%	355		323		362		
S1.3	9,0%	350		321		359		

Table 3-7 Moisture content and density of samples of S_N wood

The wood of the column S was rated in the class C14. It comes from relatively fast grown fir and that is probably the reason why it was primarily separated from construction timber and was used just as backing lath.

Table 1 – Strength classes – Characteristic values from ČSN EN 338 [9]:

		Jehličnaté dřeviny												Listnaté dřeviny							
		C14	C16	C18	C20	C22	C24	C27	C30	C35	C40	C45	C50	D18	D24	D30	D35	D40	D50	D60	D70
Pevnostní vlastnosti (v N/mm²)																					
Ohyb	$f_{m,k}$	14	16	18	20	22	24	27	30	35	40	45	50	18	24	30	35	40	50	60	70
Tah rovnoběžně s vlákny	$f_{t,0,k}$	8	10	11	12	13	14	16	18	21	24	27	30	11	14	18	21	24	30	36	42
Tah kolmo k vláknům	$f_{t,90,k}$	0,4	0,4	0,4	0,4	0,4	0,4	0,4	0,4	0,4	0,4	0,4	0,4	0,6	0,6	0,6	0,6	0,6	0,6	0,6	0,6
Tlak rovnoběžně s vlákny	$f_{c,0,k}$	16	17	18	19	20	21	22	23	25	26	27	29	18	21	23	25	26	29	32	34
Tlak kolmo k vláknům	$f_{c,90,k}$	2,0	2,2	2,2	2,3	2,4	2,5	2,6	2,7	2,8	2,9	3,1	3,2	7,5	7,8	8,0	8,1	8,3	9,3	10,5	13,5
Smyk	$f_{v,k}$	3,0	3,2	3,4	3,6	3,8	4,0	4,0	4,0	4,0	4,0	4,0	4,0	3,4	4,0	4,0	4,0	4,0	4,0	4,5	5,0
Tuhostní vlastnosti (v kN/mm²)																					
Průměrná hodnota modulu pružnosti rovnoběžně s vlákny	$E_{0,mean}$	7	8	9	9,5	10	11	11,5	12	13	14	15	16	9,5	10	11	12	13	14	17	20
5% kvantil modulu pružnosti rovnoběžně s vlákny	$E_{0,05}$	4,7	5,4	6,0	6,4	6,7	7,4	7,7	8,0	8,7	9,4	10,0	10,7	8,0	8,5	9,2	10,1	10,9	11,8	14,3	16,8
Průměrná hodnota modulu pružnosti kolmo k vláknům	$E_{90,mean}$	0,23	0,27	0,30	0,32	0,33	0,37	0,38	0,40	0,43	0,47	0,50	0,53	0,63	0,67	0,73	0,80	0,86	0,93	1,13	1,33
Průměrná hodnota modulu pružnosti ve smyku	G_{mean}	0,44	0,5	0,56	0,59	0,63	0,69	0,72	0,75	0,81	0,88	0,94	1,00	0,59	0,62	0,69	0,75	0,81	0,88	1,06	1,25
Hustota (v kg/m³)																					
Hustota	ρ_k	290	310	320	330	340	350	370	380	400	420	440	460	475	485	530	540	550	620	700	900
Průměrná hodnota hustoty	ρ_{mean}	350	370	380	390	410	420	450	460	480	500	520	550	570	580	640	650	660	750	840	1080
POZNÁMKA 1 Výše uvedené hodnoty pro pevnost v tahu, pevnost v tlaku, pevnost ve smyku, 5% modul pružnosti, průměrný modul pružnosti kolmo k vláknům a průměrný modul pružnosti ve smyku byly vypočteny na základě vztahů uvedených v příloze A.																					
POZNÁMKA 2 Tabelované vlastnosti odpovídají dřevu s vlhkostí při teplotě 20 °C a relativní vlhkosti 65 %.																					
POZNÁMKA 3 Dřevo vyhovující třídám C45 a C50 nemusí být snadno dostupné.																					
POZNÁMKA 4 Charakteristické hodnoty pro pevnost ve smyku jsou uvedeny pro dřevo bez trhlin, podle EN 408. Účinek trhlin může být zahrnut v normách pro navrhování.																					

Table 3-8 Table 1 – Strength classes – Characteristic values from ČSN EN 338 [9]

3.4.3.2 Material properties of damaged wood in the column S

Material properties which were used for calculations of the load bearing capacity of the columns S are in the Table 3-9. Formula 3–9, Formula 3–8 and Formula 3–7, were used.

Material	Degree of damage	Porosity	Modulus of Elasticity	Compressive Strength
	d	*p = d2*	*ED = EN * e-1p * (1 - p)*	$fc_{,D} = fc_{,N} * (1 - d)$
	[-]	[%]	[MPa]	[MPa]
SN	0,0	0,0%	**7000**	**16,0**
S1	0,1	1,0%	6861	14,4
S2	0,2	4,0%	6457	12,8
S3	0,3	9,0%	5822	11,2
S4	0,4	16,0%	5011	9,6
S5	0,5	25,0%	4089	8,0
S6	0,6	36,0%	3126	6,4
S7	0,7	49,0%	2187	4,8
S8	0,8	64,0%	1329	3,2

Table 3-9 Material properties of S wood

3.4.4 MODEL OF THE COLUMN S

For the calculation of the load bearing capacity of a column, it is necessary to know the effective length. That was obtained by EFM in the software SCIA Engineer 16.0 Student.

To follow support conditions of static load test, column S is modeled with both supports preventing rotation in all directions. Column consists of 10 connected members. Each member has different cross section acc. to Table 3-5. Eccentricity of members is set up to keep the surface flat. This eccentricity of members caused by damage of cross sections leads to extended effective length compared with both ends clamped straight column. Linear stability calculation of effective length was performed.

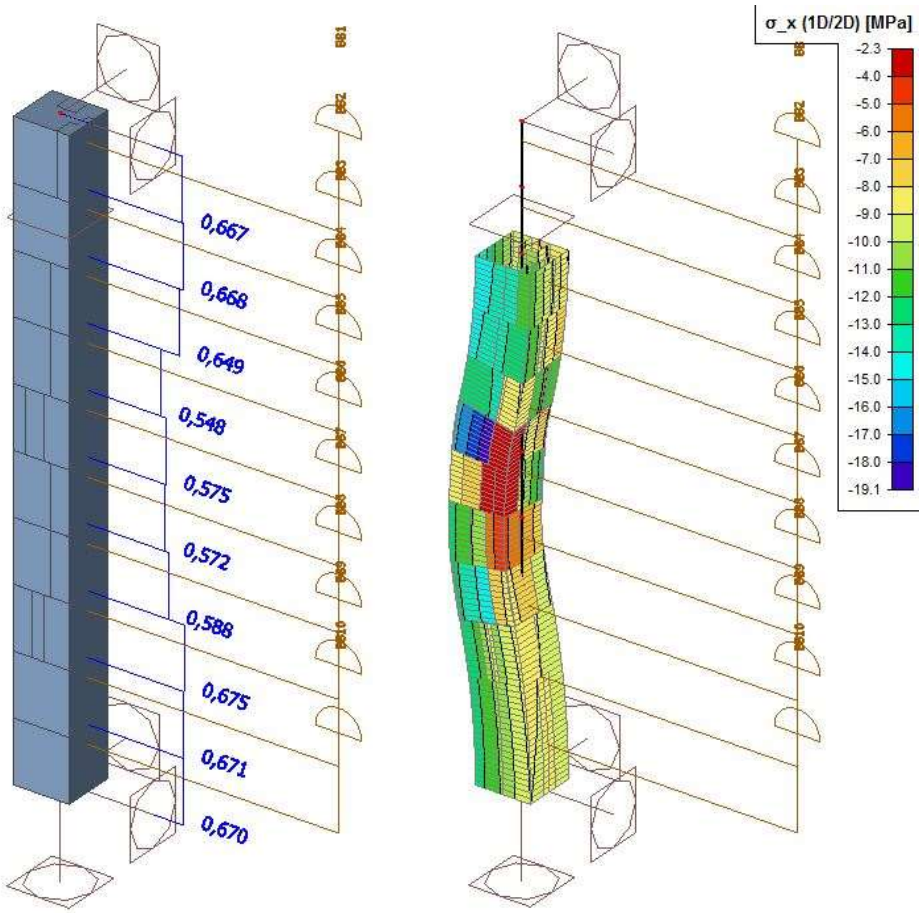

Figure 3-15 Model of the column S, effective length l_{ef} (left)

Normal stress under force F = 85 [kN] (right)

Effective lengths of cross sections are stated in Table 3-11.

On the right side of the Figure 3-15, it is possible to see the distribution of stress in the column S. Red color represents normal stress $\sigma_{x,D,0,8} < 4$ [MPa] which occurs in most damaged zones of the column. It means that these parts are not able to transfer a lot of force. Normal stress in a similar column with no damage and loaded by the same force would be $\sigma_{x,N}$ = 11,1 [MPa]. Here, it is possible see maximal stress $\sigma_{x,D,MAX}$ = 19,1 [MPa] in the cross section G. Nevertheless, these values of stress were not used in any point of the thesis. The figure is stated to show the behavior of the model.

3.4.5 LOAD BEARING CAPACITY OF THE COLUMN S

One of the products of this thesis is an excel spreadsheet which serves for calculation of the load bearing capacity of a cross section in a wood column with defined distribution od degree of damage d. Effective length, cross section dimensions, material properties of undamaged wood and distribution of damage has to be filled in as inputs. This spreadsheet follows the procedure described in chapter 3.3. It is possible to divide the cross section into 27 zones. The spreadsheet also calculates just in one direction so it is necessary to decide in which direction will the column buckle most likely. If it is not clear it is possible to make calculation in second direction by redefining the distribution of the degree of damage.

3.4.5.1 Calculation of the loadbearing capacity of the cross section G

Calculation MS Excel 2016:

The load bearing capacity of damaged cross section in wood column:

Composite cross section by EN 1995 - 1 - 1

1. Inputs

1.1 Material properties of undamaged wood

Compressive strength:	$f_{c,k}$ =	16	[MPa]	=	1,6E+07	[Pa]
Modulus of elasticity:	E_{mean} =	7000	[MPa]	=	7,0E+09	[Pa]
	$E_{0,05}$ =	7000	[MPa]	=	7,0E+09	[Pa]
Imperfection:	β_c =	0,2	[-]			

1.2 Geometry

Height:	h =	90	[mm]	=	0,09	[m]
Width:	b =	85	[mm]	=	0,085	[m]
Effective length:	l_{ef} =	548	[mm]	=	0,548	[m]
Degree od damage:	d =	<0;1>	[-]			

Fill the distribution in the zones

0,0	0,0	0,0	0,3	0,3	0,0	0,0	0,5	0,5	30,0
0,0	0,0	0,0	0,0	0,3	0,3	0,3	0,5	0,5	25,0
0,0	0,0	0,0	0,0	0,0	0,0	0,8	0,8	0,8	30,0
10	10	10	10	10	10	10	10	10	[mm]

85

90

Σd = 5,9 [-]

2. Material properties of damaged wood

$E_D = E_N * e^{-d^2} * (1-d^2)$

$f_{c,D} = f_{c,N} * (1- d)$

3.Calculation

3.1 Center of gravity

$c_y =$ 0,0388 [m]

3.2 Effective bending stiffness

$\Sigma EI_{c,el} =$ 2,527E+04 [Nm²]

3.3 Effective area

$\Sigma EA_{c,tot} =$ 4,365E+07 [N]

3.4 Effective slenderness ratio

$\lambda_{c,el} =$ 22,78 [-]

98,7	98,7	98,7	83,6	83,6	98,7	98,7	85,0	85,0
98,7	98,7	98,7	98,7	83,6	83,6	83,6	85,0	85,0
98,7	98,7	98,7	98,7	98,7	98,7	103,8	103,8	103,8

Maximal force:

$F_{MAX} =$ 83,6 [kN]

2. Material properties of damaged wood

$E_D = E_N * e^{-d^2} * (1-d^2)$

$f_{c,D} = f_{c,N} * (1- d)$

3.Calculation

3.1 Center of gravity

$c_y =$ 0,0388 [m]

3.2 Effective bending stiffness

$\Sigma EI_{c,el}$ = 2,527E+04 [Nm²]

3.3 Effective area

$\Sigma EA_{c,tot}$ = 4,365E+07 [N]

3.4 Effective slenderness ratino

$\lambda_{c,el}$ = 22,78

98,7	98,7	98,7	83,6	83,6	98,7	98,7	85,0	85,0
98,7	98,7	98,7	98,7	83,6	83,6	83,6	85,0	85,0
98,7	98,7	98,7	98,7	98,7	98,7	103,8	103,8	103,8

Maximal force:

F_{MAX} = 83,6 [kN]

Table 3-10 Calculation of the loadbearing capacity of the cross section G

3.4.5.2 Calculated load bearing capacity of all cross sections in the column S

Cross section	Effective length	Total damage	Load bearing capacity
	lef	$\Sigma d \in \langle 0; 27 \rangle$	*FMAX*
	[m]	[-]	[kN]
A	0,670	0,9	109,5
B	0,671	0,4	110,1
C	0,675	0,4	110,1
D	0,588	4,2	94,9
E	0,572	6,1	90,3
F	0,575	5,1	88,6
G	0,548	5,9	**83,6**
H	0,649	2,5	96,5
I	0,668	0,6	103,7
J	0,667	1,2	102,8

Table 3-11 List of calculated load bearing capacity of cross sections in column S

3.4.6 STATIC LOAD TEST OF THE COLUMN S

Tests was made 30th November 2016 in laboratory of the Carinthia University of Applied Sciences in Villach, Austria.

Conditions in laboratory:	**Measuring device:**
Ari temperature: 18 °C	TesT GmbH
Air humidity 25 %rH	Model P114.250kN.H
Condition of wood:	No. 07.904286
Moisture content: 17,7 %	Made in 2007

Static load test was strain controlled. Speed of loading was 1 mm/min. Failure occurred in time t = 463 [s].

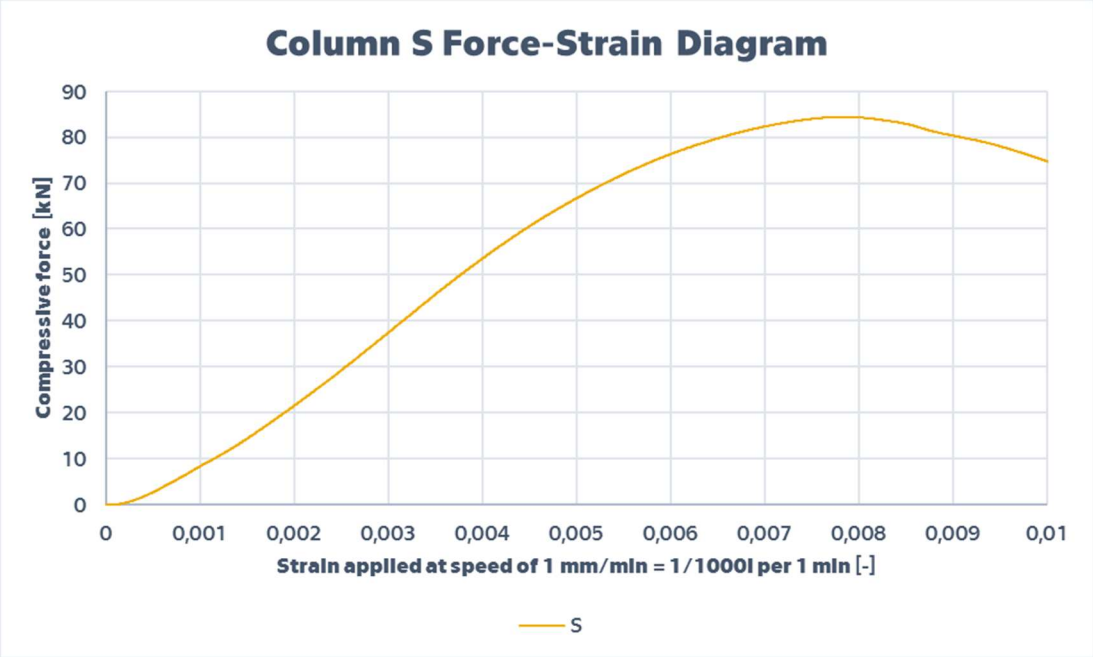

Chart 3-17 Force-strain diagram of the column S

Measured load bearing capacity of the column S is F_{MAX} = 84,4 [kN].

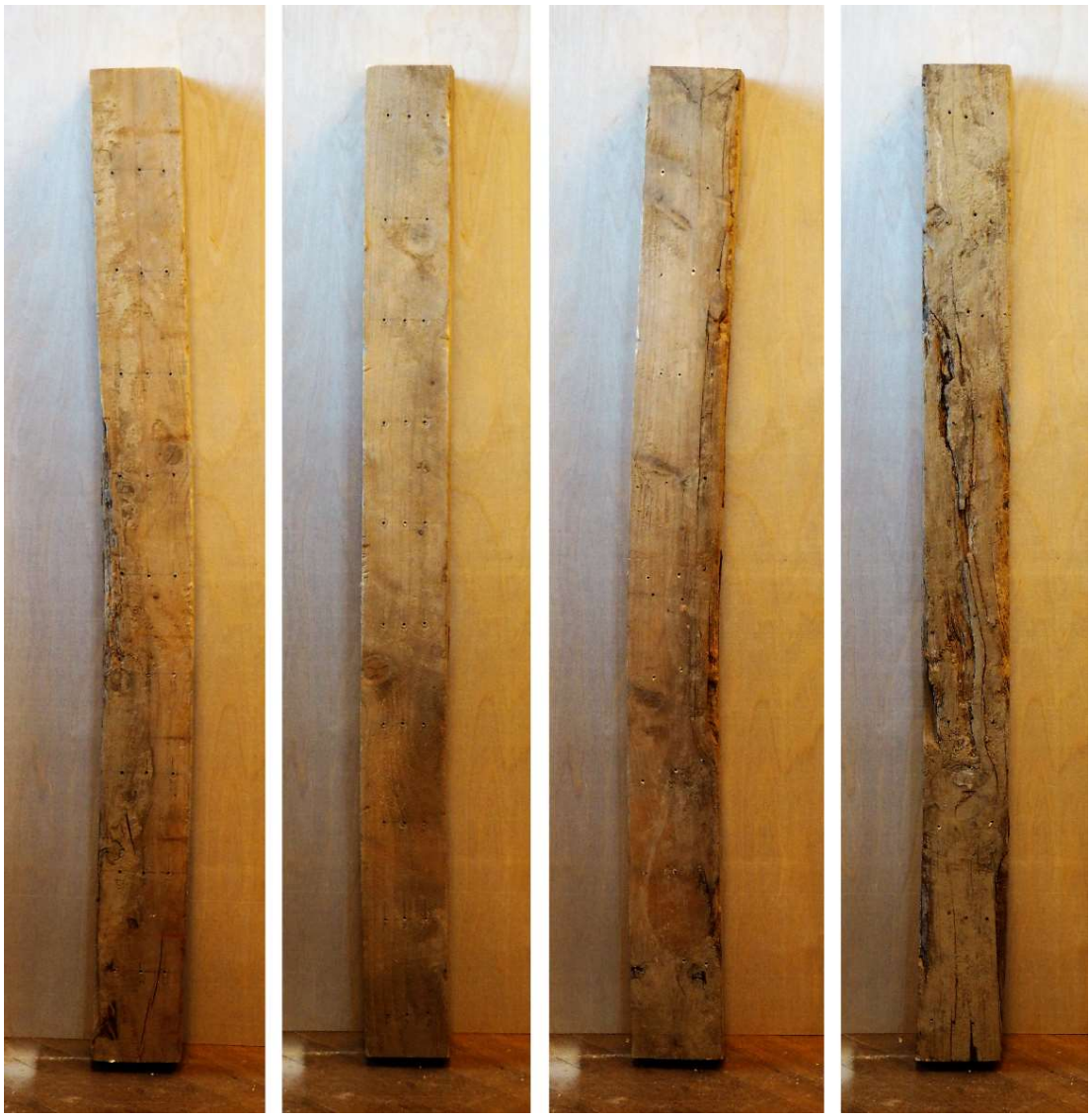

Photo 3–9 The Column S after the static load test

3.4.7 CONCLUSION

If the calculated and measured load bearing capacity is compared, product is acc. Formula 3–11 almost unbelievable error of calculation c = 1%.

$$c = \left|1 - \frac{F_{MAX,c}}{F_{MAX,m}}\right| = \left|1 - \frac{83,6}{84,4}\right| = 0,01\ [-]$$

If the column S had had no damaged zones, it would have collapsed in the compressive failure mode under the force of about 120 [kN]. It means that its damage (displayed in the Annex 1 chapter 5.3) made a difference in the load bearing capacity of about 36 [kN].

3.5 USE OF THE DEVELOPED PROCEDURE FOR A REAL-SIZED COLUMN

To analyse the influence of damaged zones in a real-sized wood column, another theoretical sample R was examined. This time 3m long with a cross section dimensions 160 x 160 mm, material timber C24 and supports allowing rotation of the ends of the column. As an environment, the service class 2 was selected. Load consists of 50% of dead load and 50% of live load with medium term action.

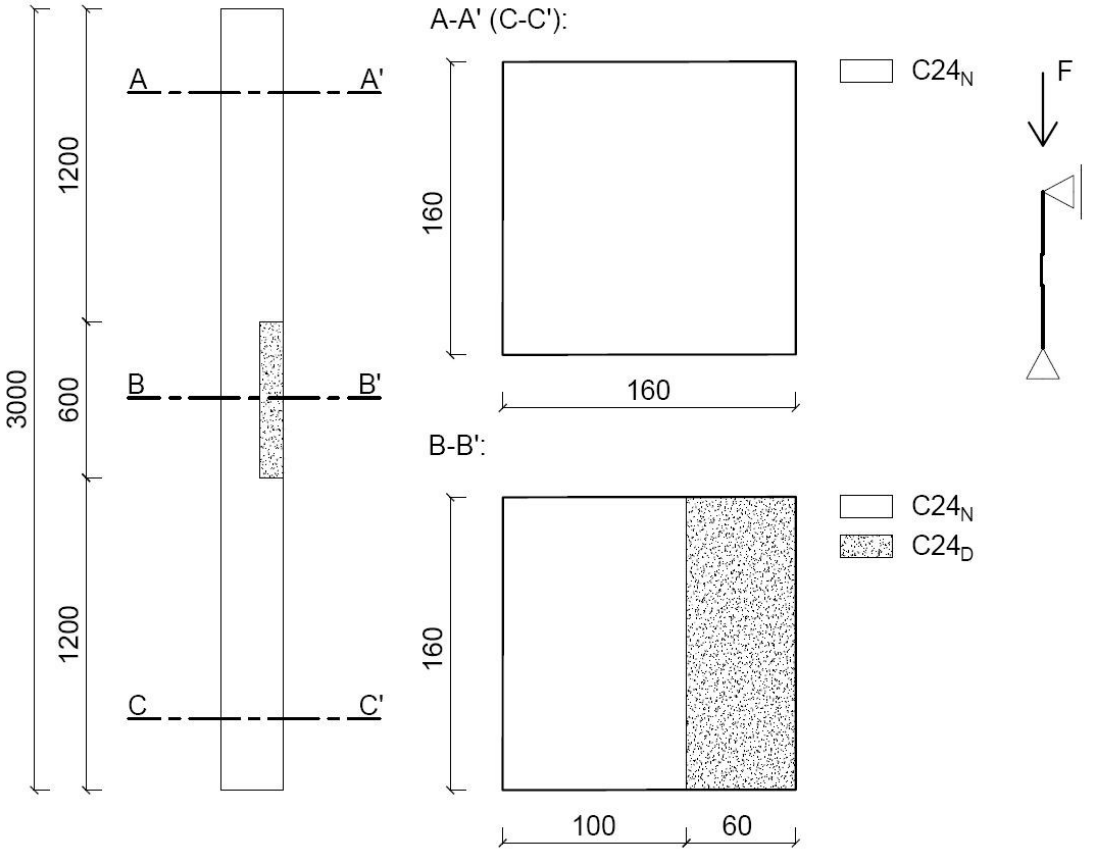

Figure 3-16 Geometry of column R

The theoretical column R was assed eleven times, always with different degree of damage of the selected zone.

$d \in \{0;0,1;0,2;0,3;0,4;0,5;0,6;0,7;0,8;0,9;1\}$

Effective length was calculated again by software SCIA Engineer 16.0 Student. Excel spreadsheet from chapter 3.4.5.1 was used. Calculation of design value of maximal compressive force was done according to Eurocode Formula 3–14 and Formula 3–15. For ultimate limit states, where the distribution of member forces and moments is affected by the stiffness distribution in the structure, the final mean value of modulus of elasticity $E_{mean,fin}$ should be calculated from Formula 3–14. [5]

$$E_{mean,fin,i} = \frac{E_{mean,i}}{(1+\Psi_2 \cdot k_{def})}$$

Formula 3–14 Formula 2.10 from EN 1995-1-1 [5]

$$f_{c,d} = k_{mod} \cdot \frac{f_{,c,k}}{\gamma_M}$$

Formula 3–15 Formula 2.14 from EN 1995-1-1 [5]

For chosen conditions, material and load duration the applied values were:

k_{mod}=0,8 [-] γ_M=1,3 [-]

k_{def}=0,8 [-] Ψ_2=0,6 [-]

Results of calculations are displayed in Table 3-12:

Degree of damage damaged zone	Design load bearing capacity		Fd/Fd'
	with damaged zone	without damaged zone	
d	Fd	Fd'	
[-]	**[kN]**	[kN]	[-]
0	**182,4**	182,4	**1,0**
0,1	**170,9**	29,5	**5,8**
0,2	**160,2**	29,5	**5,4**
0,3	**148,9**	29,5	**5,0**
0,4	**137,4**	29,5	**4,7**
0,5	**124,7**	29,5	**4,2**
0,6	**109,2**	29,5	**3,7**
0,7	**89,7**	29,5	**3,0**
0,8	**67,1**	29,5	**2,3**
0,9	**46,1**	29,5	**1,6**
1	**29,5**	29,5	**1,0**

Table 3-12 Load bearing capacity of the R column

Conclusions are summarized in the following chapter.

3.6 CONCLUSION OF THE EXPERIMENTAL PART

The aim of the experimental part of this thesis was to examine the influence of damaged zones in a timber column on its load bearing capacity.

Frist chapter is focused on material properties of damaged timber. Products of the series of experiments are formulas for determining the compressive strength and the modulus of elasticity of damaged material. (Formula 3–7 and Formula 3–8). The number of specimens was limited by time consuming drilling. Much more samples should be tested to confirm or to refute this theory.

Anyway, for the purpose of this thesis the theory was used in the next experiment. Two sets of columns were subjected to a static load test and the resulting load bearing capacity was compared with the calculated one. Determination of the maximal compressive force was based on Eurocode EN 1995-1-1 procedure for composite cross sections in members subjected to stability issues. The average error of calculation is 11%. Interestingly, the average error of calculation would be significantly higher, if the linear decrease of the modulus of elasticity with the linear increase of the degree of damage would have been used. The load bearing capacity obtained by this assumption generates unacceptably unsafe results. The average error of calculation would be about 20% and the estimate is always higher than real measured load bearing capacity. Turquoise color in Chart 3-18.

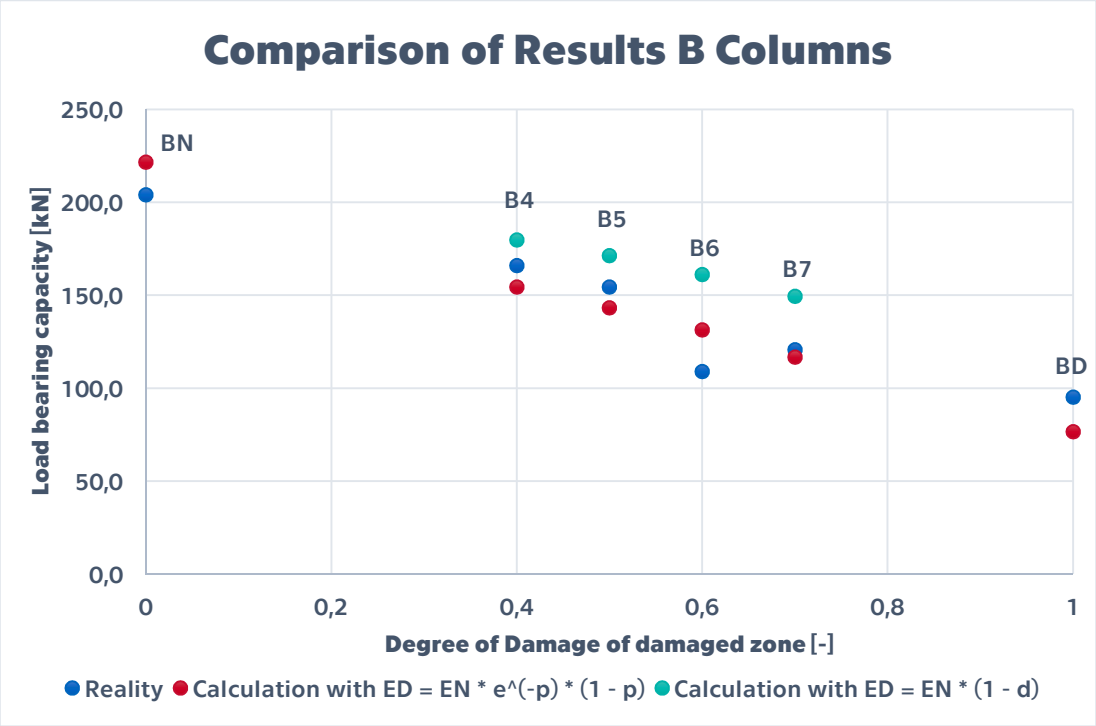

Chart 3-18 Difference in results based on used function of E_D

Third task was to apply the developed theory to a naturally damaged member. At this point it is necessary to use a method for localization and rating of the distribution of damage in the subject. Resistance drilling was considered to be best option and was used. The material properties of undamaged wood had to be determined for application of the developed theory. For this purpose, an indirect method based on determining the density of the wood was used. Combination of these methods and the developed theory of material properties led to a very precise result. It was just one specimen and it could have been only a coincidence. However, for the purpose of the thesis the whole procedure was considered to be verified.

In the last chapter of the experimental part, this procedure was used for calculation of load bearing capacity of the theoretical real-sized column R (Figure 3-16). On this subject the influence of the damaged zone in the middle part of the column was analyzed. The slenderness of a real column is normally higher then slenderness of B or F columns examined in the chapter 3.3. That is the reason for even bigger influence of the damaged zone in such a member.

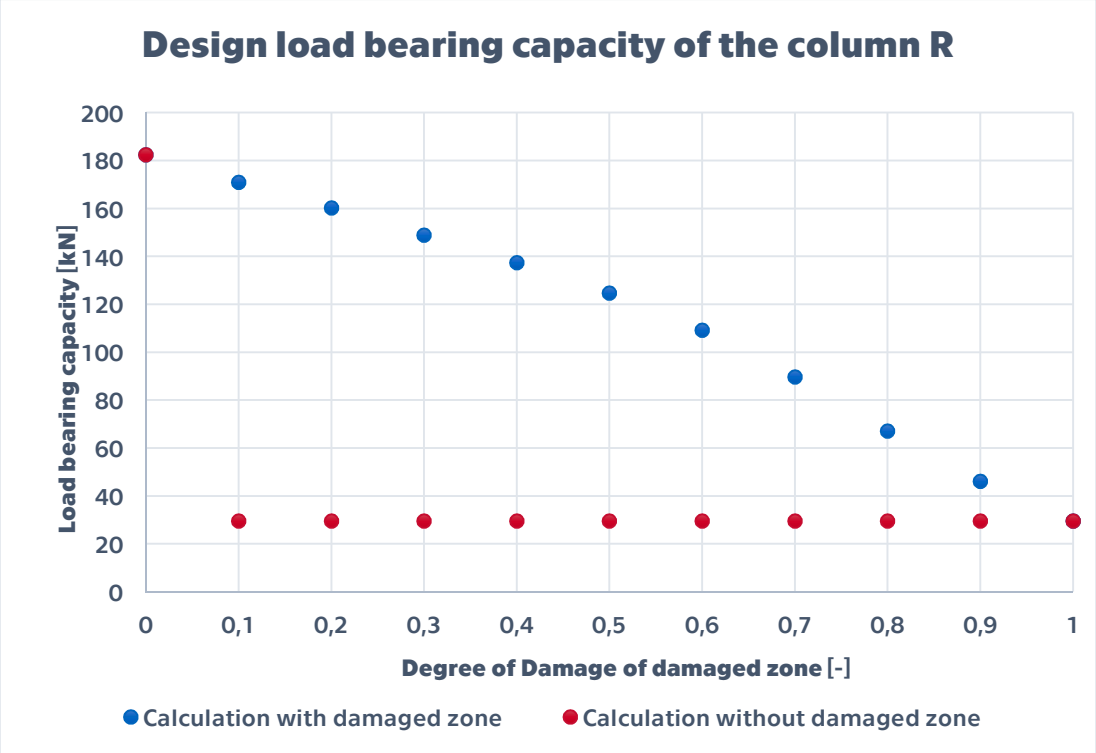

Chart 3-19 Load bearing capacity of the theoretical column R

Design load bearing capacity of the undamaged variant of the column R is about 180 [kN]. If one quarter of the cross section is completely missing in the middle part, the design load bearing capacity drops to the 30 [kN]. Partially because of reduced cross section area and partially because of increased effective length. If the zone of damage had been very short and had had on influence on the effective length, the resistance of such a column would have been about 60 [kN].

Difference of the design load bearing capacity between blue and red points expresses the influence of the damaged material. This influence is significant for the specified geometry of the member. Even for the degree of damage of the decayed zone d = 0,8 (which corresponds to an advanced stage of brown rot) the design load bearing capacity is more then doubled compared to the one obtained by discarding the damaged zone out of the calculation.

PRACTICAL PART

THE INSPECTION OF THE OLD ROOF STRUCTURE

4.1 INTRODUCTION

Practical part of this thesis is focused on a brief inspection of a historical roof structure. The aim of this work is to become acquainted with the roof structure, try to find week parts and inspect them by micro-resistance drilling. This thesis does not analyze static of the roof. It is focused on the condition of members only.

4.2 OBJECT DESCRIPTION

Photo 4–1 The public elementary school Khevenhüller

The public elementary school Khevenhüller is located in the Khevenhüller street 16 in Villach (Austria). The studied object is the roof of freestanding three-storey building with a E-shaped floor. It was built during the second half of the 19th century and the last general renovation took place in 1984. [10]

4.3 ROOF DESCRIPTION

The roof consists of two main asymmetric gable parts, two main hips/valleys by the corners of the plan and in the middle there is another smaller gable roof covering the staircase. The roof can be classified as a double roof (rafter, purlin system). The external wall closer to the yard of the building (right oh the Photo 4–2) terminates lower then the opposite one. According to Figure 4-2 the longer rafters are 9,5m in the length and except for the wall pale they are supported by two field purlins and the top purlin. External rafters (5,6 m) have just one support in the middle of the span.

Photo 4–2 Demonstrative photo of the roof structure

Vast majority of the members are original from the 19th century. There are just few replaced parts of wall plates and rafters.

At the first sight members of the roof seems to be in quiet good condition.

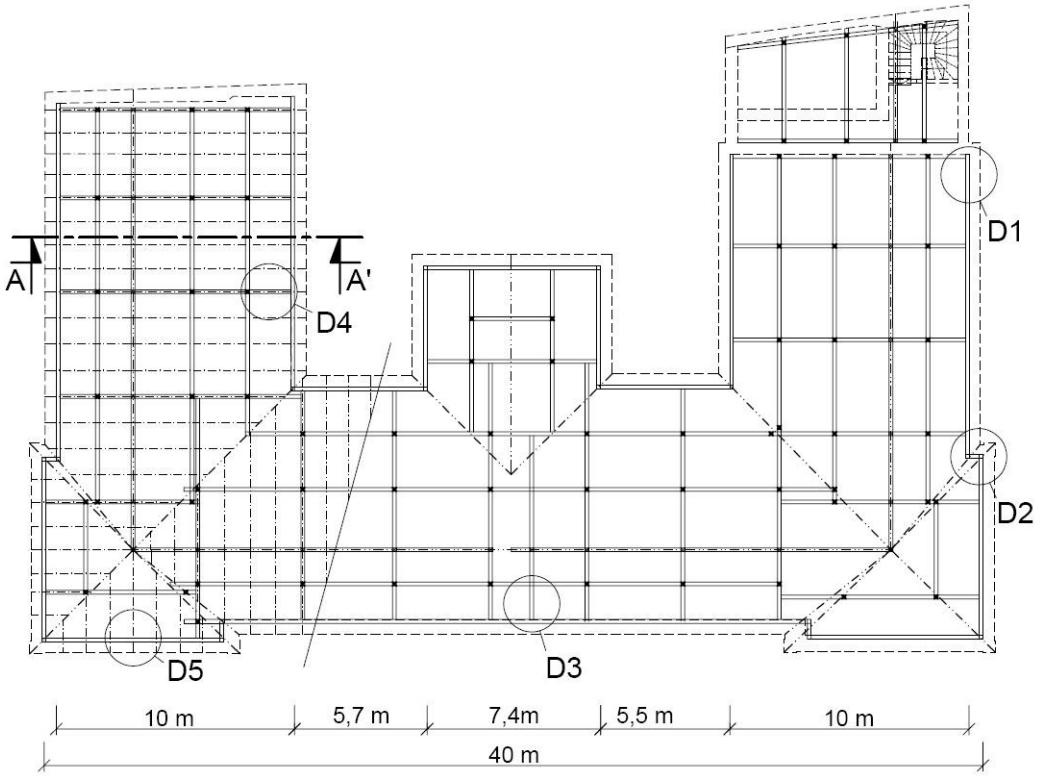

Figure 4-1 Schematic plan of the roof

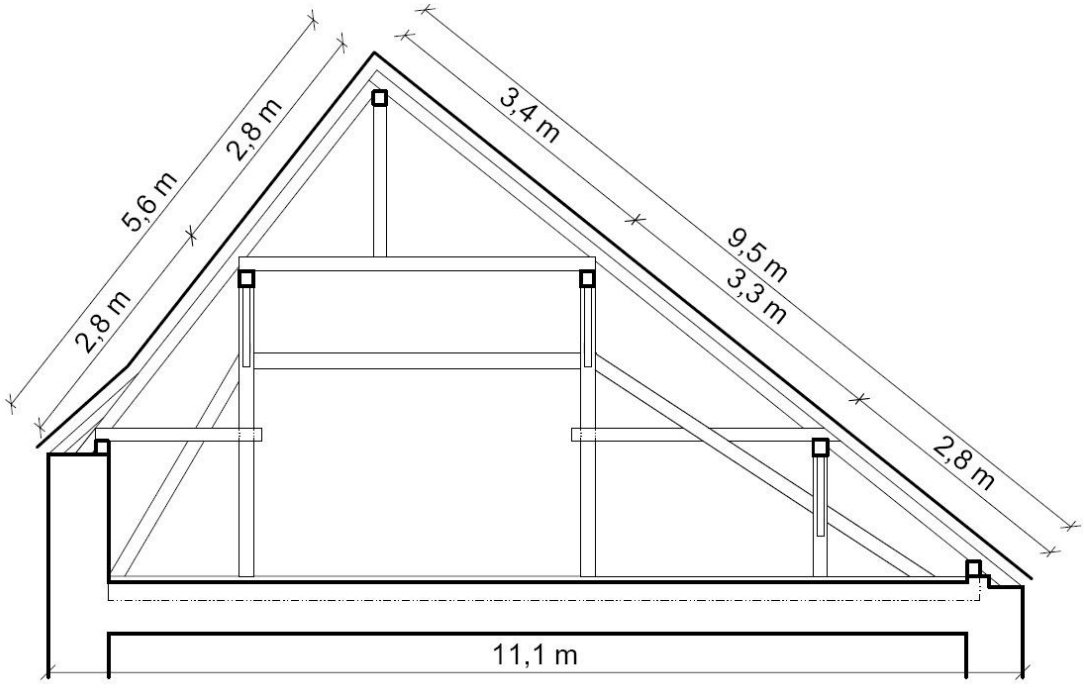

Figure 4-2 Schematic cross section A-A'

4.4 INSPECTION OF THE ROOF MEMBERS

4.4.1 INTRODUCTION

The inspection was performed during the November 2016. It was done in a team of two people, me and my colleague BSc Sebastian Gigli.

At first, it was necessary to measure the geometry of the whole roof. The only sources of information were The chronicle of Khevenhüller school and floor plans. There was no plan of the roof. When the structure was drawn, macroscopic analysis could have started.

Detail visual check discovered several problematic spots of the structure. They are marked in the Figure 4-1 as details D1 to D5. There were more problematic members in the roof but the task of this thesis is not to provide a complete documentation of the roof condition. Only the specific representative details are investigated in the thesis.

Selected details were inspected by Resistograph®.

4.4.2 DETAIL D1 – ROTTEN WALL PLATE

At the southwest corner of the roof a wet wall plate was found, which responded by a hollow sound after knocking on its surface. Furthermore, discolorations and fungi were spotted.

Photo 4–3 Detail D1

The following sketch shows the locations of the drillings:

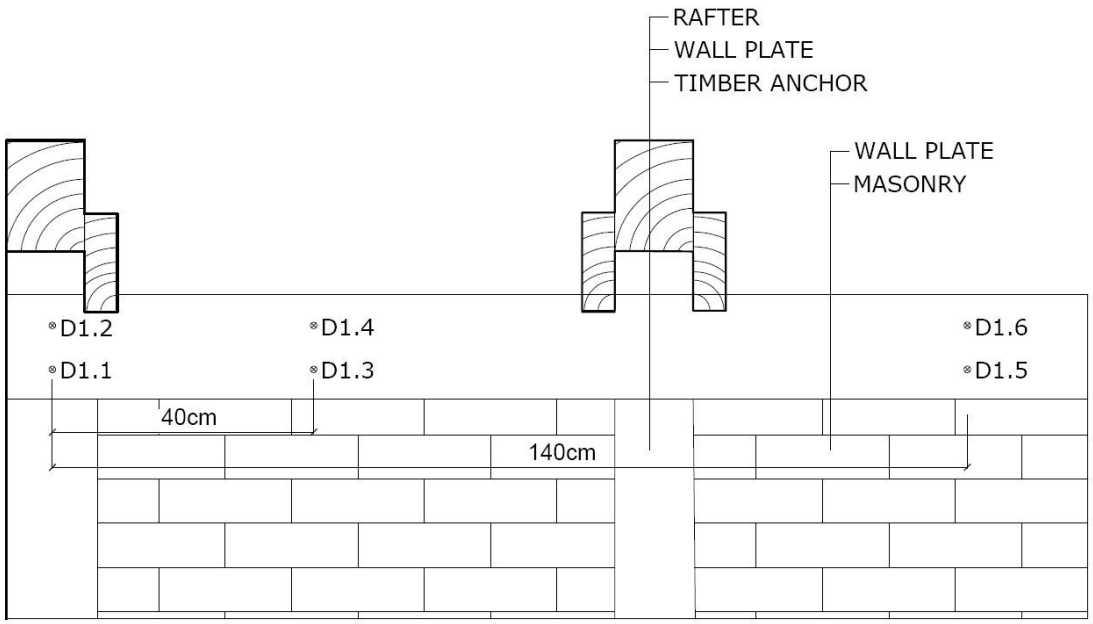

Figure 4-3 Detail D1 – Section longitudinal to the wall plate

4.4.2.1 Drilling D1.1

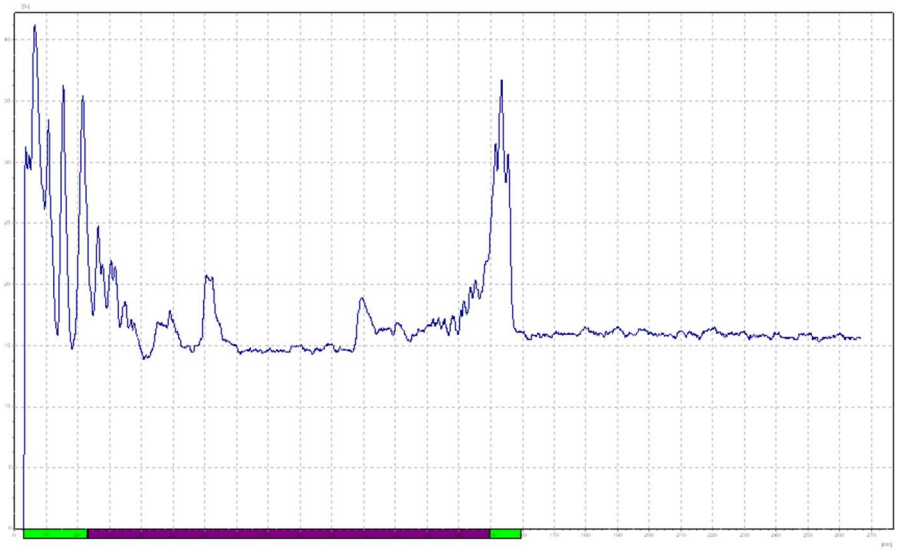

Chart 4-1 Drilling D1.1

According to the assumption, there is almost no resistance about 3 cm under the surface. The reason could be a leak in the roof, which has destroyed the wall plate over the years.

4.4.2.2 Drilling D1.2

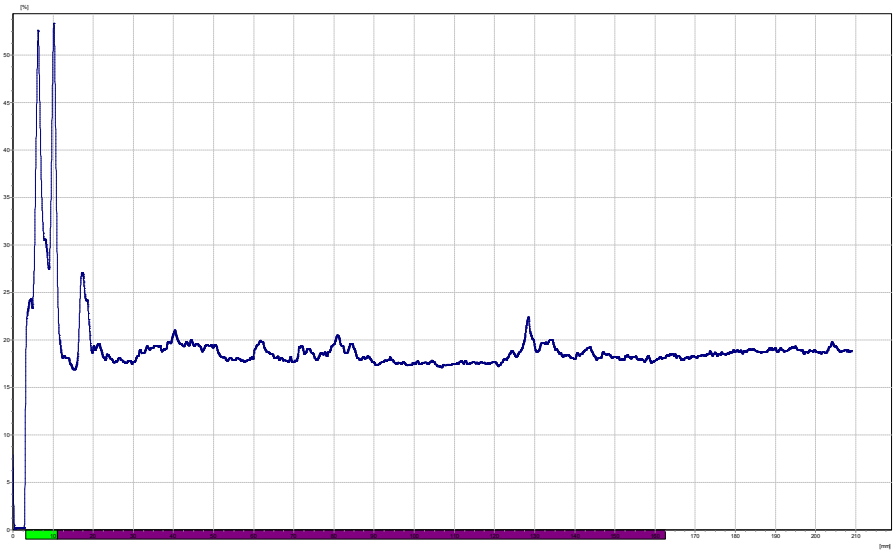

Chart 4-2 Drilling D1.2

Similar to the previous drilling D1.1, there is no resistance after 1-2 cm. Almost whole cross-section is destroyed.

4.4.2.3 Drilling D1.3

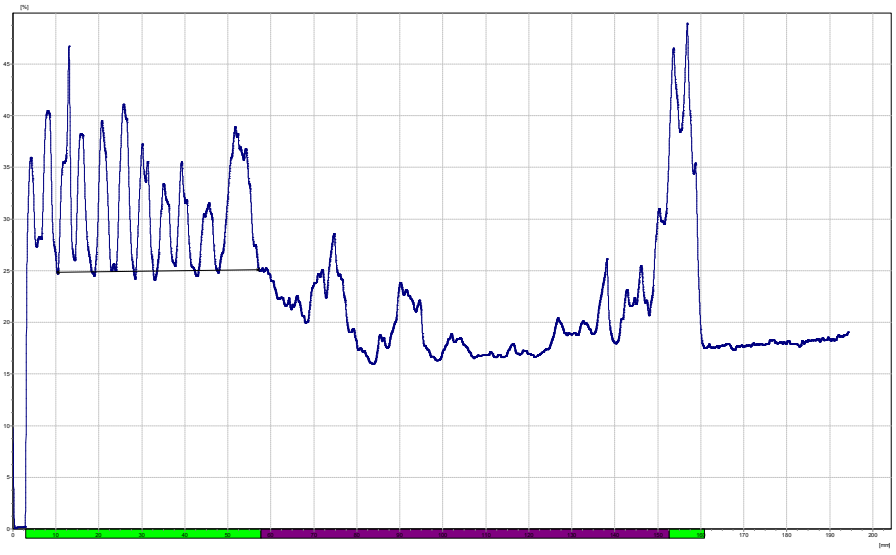

Chart 4-3 Drilling D1.3

The drilling D1.3 shows a slight increase of the resistance. However, 60% of the cross-section is damaged.

4.4.2.4 Drilling D1.4

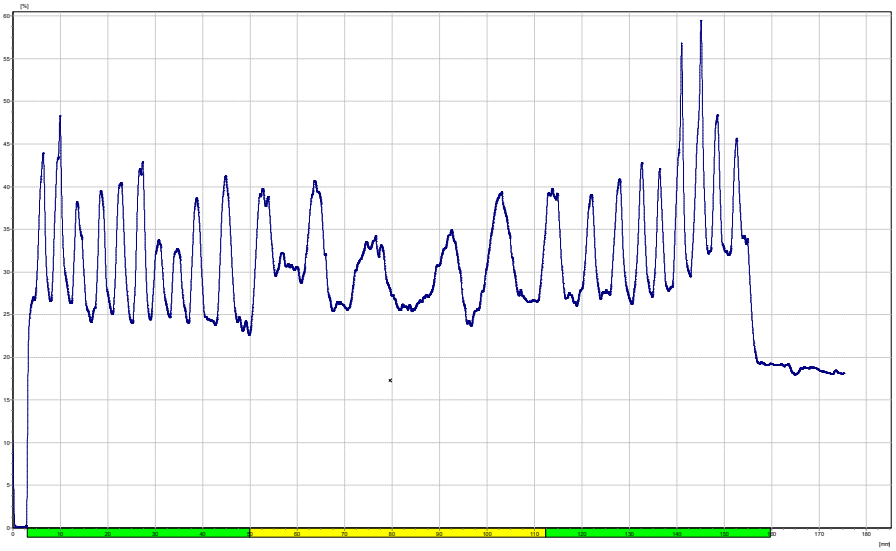

Chart 4-4 Drilling D1.4

Despite the fact that the bore D1.4 has been carried out only 10 cm above the point D1.3, a clear increase of the resistance can be seen.

4.4.2.5 Drilling D1.5

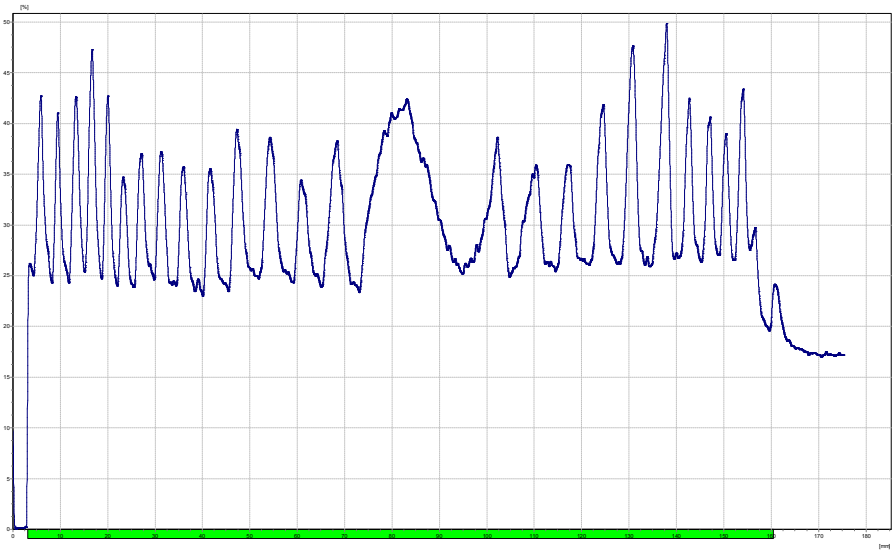

Chart 4-5 Drilling D1.5

This resistance measurement is located 1,40 m away from the D1.1 and D1.2. The diagram provides the prove that at this point the wood is not damaged.

Drilling D1.6 confirmed this fact.

4.4.2.6 Recommendation

In the course of possible refurbishments of the roof, the roof cladding has to be fixed and the wall plate must be replaced in this area to keep the roof serviceable. In addition, there is no structural separation between the wooden components and the masonry throughout the roof area. Further design of remediation should focus on this fact.

4.4.3 DETAIL D2 – DAMAGED VALLEY CORNER

As can be seen in the Photo 4–4 Detail D2Photo 4–4, a reduction in the wood substance can be determined on the basis of the visual survey in detail D2. The Figure 4-4 shows the locations of the drillings.

Photo 4–4 Detail D2

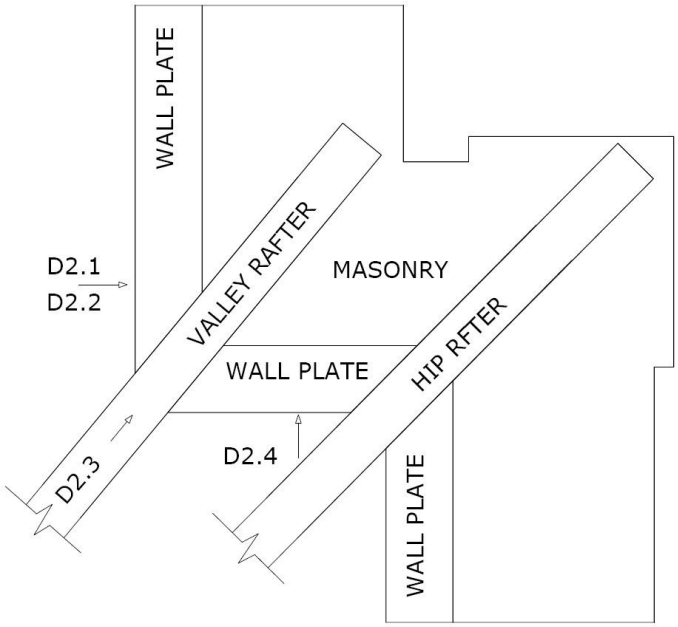

Figure 4-4 Detail D2 – Top view of the corner

4.4.3.1 Drilling D2.1

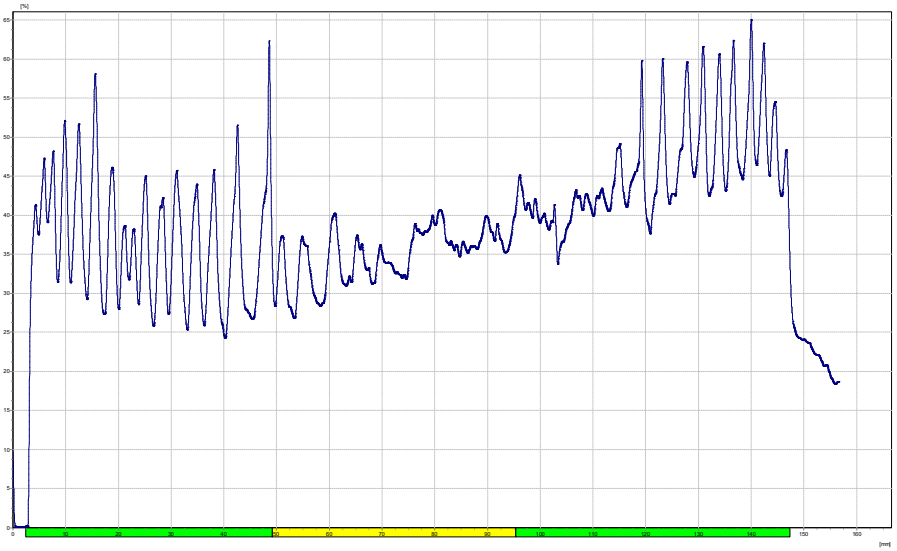

Chart 4-6 Drilling D2.1

The diagram in detail D2.1 shows disturbed structure of the material in the middle area of the wall plate. Towards the end, the annual ring density looks good again.

4.4.3.2 Drilling D2.2

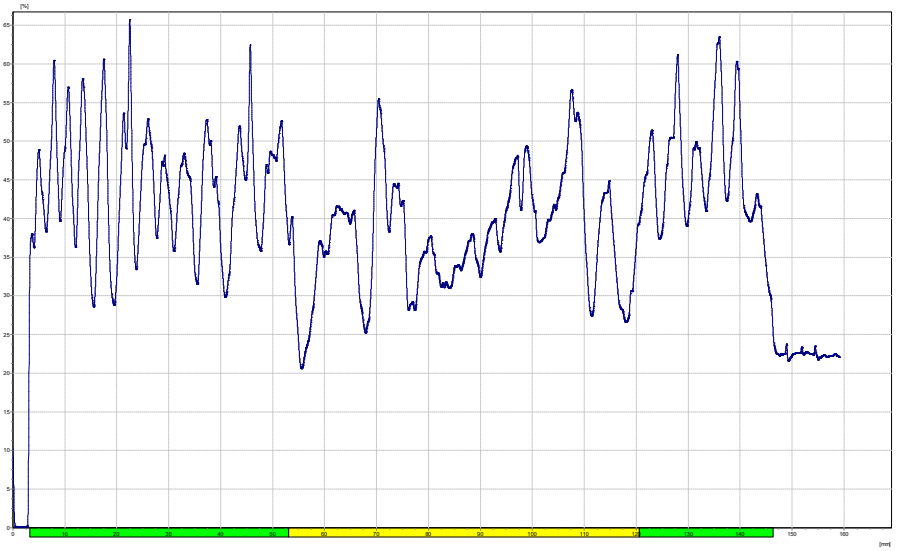

Chart 4-7 Drilling D2.2

The resistance measurement in detail D2.2 shows even clearer differences in strength and indicates a problem in the central part of the member.

4.4.3.3 Drilling D2.3

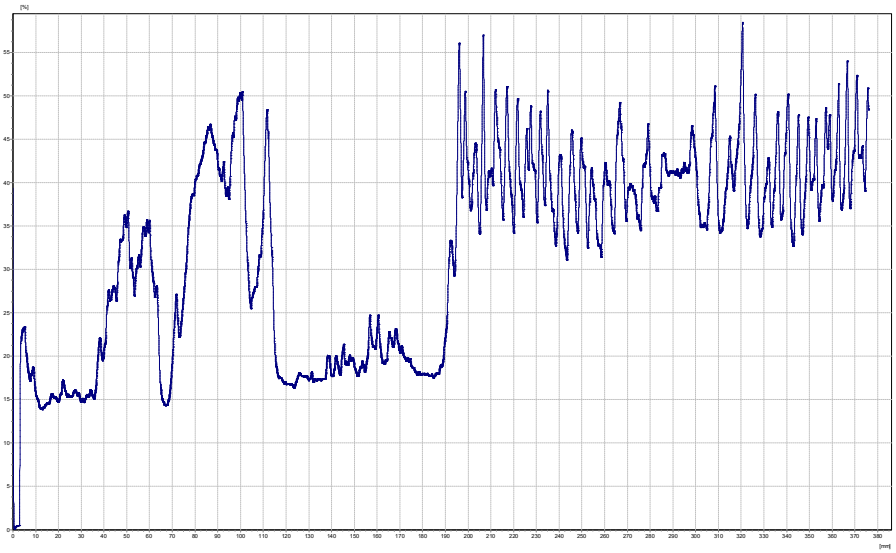

Chart 4-8 Drilling D2.3

This diagram is a product of the drilling made in the direction displayed on the Photo 4–4. It shows the differences in the strength of the wall plate and the rafter. Decrease in the drilling resistance is evident in the wall plate and the rafter seems to be intact.

4.4.3.4 Drilling D2.4

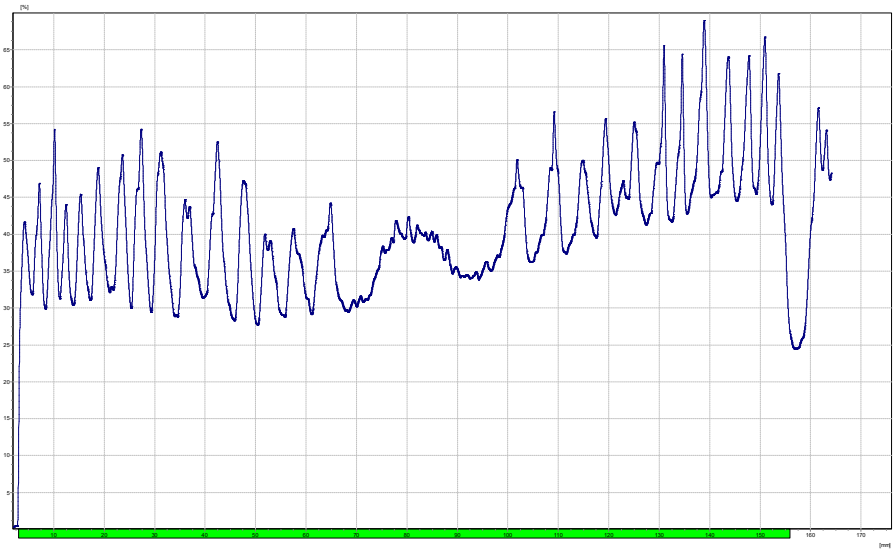

Chart 4-9 Drilling D2.4

The D2.4 is located about 40 cm away from the damaged spot (corner). The diagram shows an intact material.

4.4.3.5 Recommendation

The investigation in the detail D2 showed that the damage is located directly in the corner of the wall plate under the valley-rafter. The wall plate should be replaced in this area.

4.4.4 DETAIL D3 – SURFACE DAMAGED BY INSECTS

Damage caused by insects was found in a strut in the middle part of the roof. This member supports the top purlin in the spot, where it is interrupted. Damaged zone was found close to the floor.

Photo 4–5 Detail D3

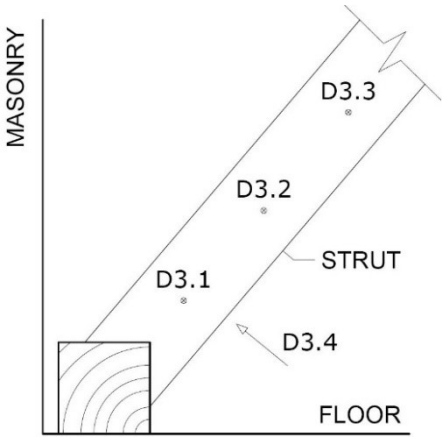

Figure 4-5 Detail D3 – Part of the cross section

4.4.4.1 Drilling D3.1

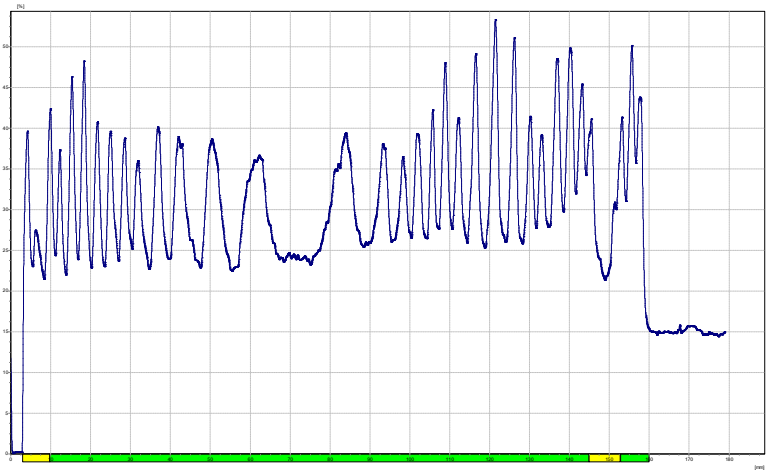

Chart 4-10 Drilling D3.1

The bore D3.1 is located directly in the area, where burrows of insects were found. The damage can be seen in the first external centimeters of the cross-section only. According to the chapter 2.1.2 the damage can by classified as shallow. Damage is affecting the mechanical properties of wood but the degree of damage is very low in this case.

4.4.4.2 Drilling D3.2

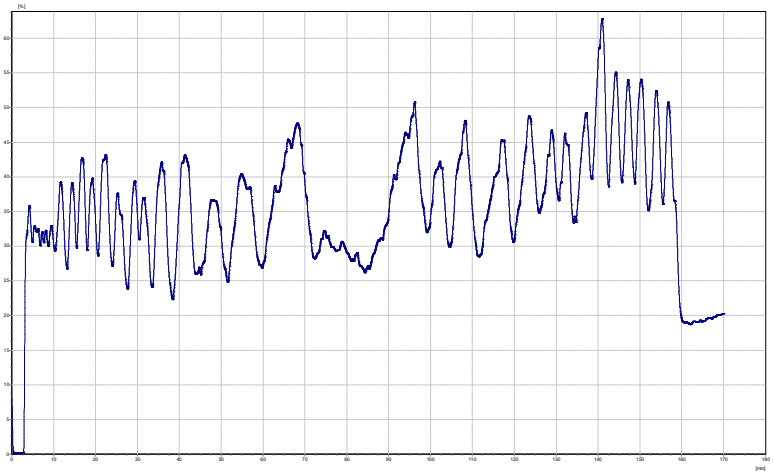

Chart 4-11 Drilling D3.2

Again the front surface is decayed but just in the depth of 1 cm. In the central part of the cross section the drill probably penetrated the member close to the original center of the tree in the tangential direction. Extending distance of hitting the annual rings to both sides from the center is in correspondence with this explanation.

4.4.4.3 Drilling D3.3

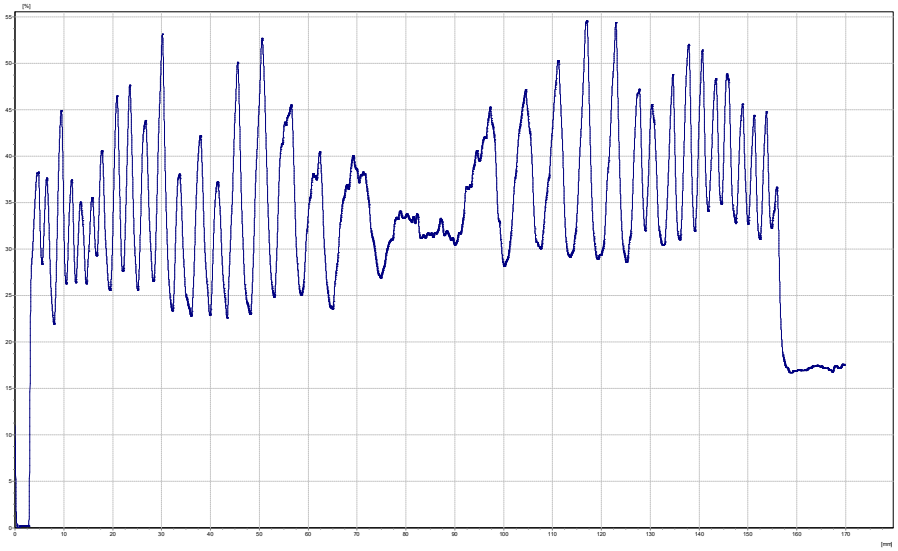

Chart 4-12 Drilling D3.3

This drilling was done 1m away from D3.1 where the wood seemed to be intact. Diagram confirmed the assumption as well as the explanation of the diagram D3.2.

4.4.4.4 Drilling D3.4

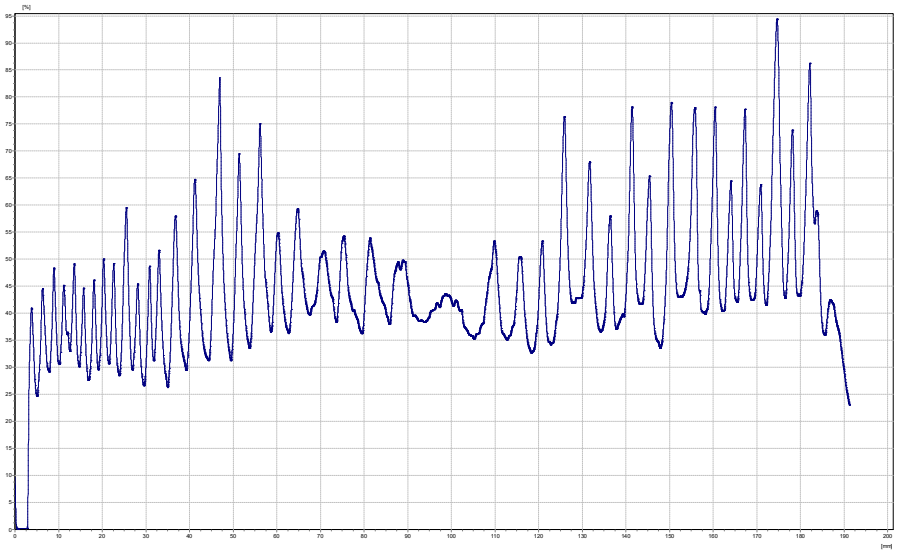

Chart 4-13 Drilling D3.4

Drilling D3.4 was made in the same cross section as D3.1, but in the perpendicular direction. Both front and posterior surfaces were not damaged. Resistance curve shows the intact intra-annual density of the timber and confirms the location of the tree center in the middle of the cross section.

4.4.4.5 Recommendation

No beetles were spotted in the time of the brief inspection, but this region of the roof should be examined by an expert in the field of wood decaying insect. Assuming a good treatment of the wood, the strut could probably stay in the service.

4.4.5 DETAIL D4 – WET AND MOLDY RAFTER

Wet and moldy surface was found on the rafter which is a part of the main bond. The rafter is situated next to a roof window. Several drillings were made to determinate the internal condition of the rafter. The wall palate is affected by a mold as well.

Photo 4–6 Detail D4

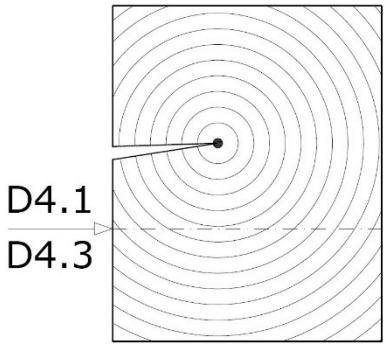

Figure 4-6 Cross section of the rafter

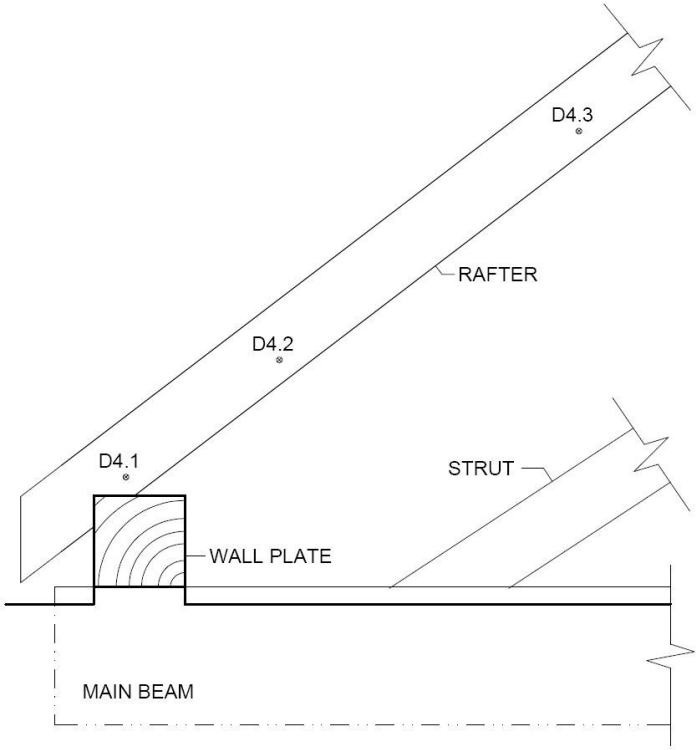

Figure 4-7 Detail D4 – Part of the cross section

4.4.5.1 Drilling D4.1

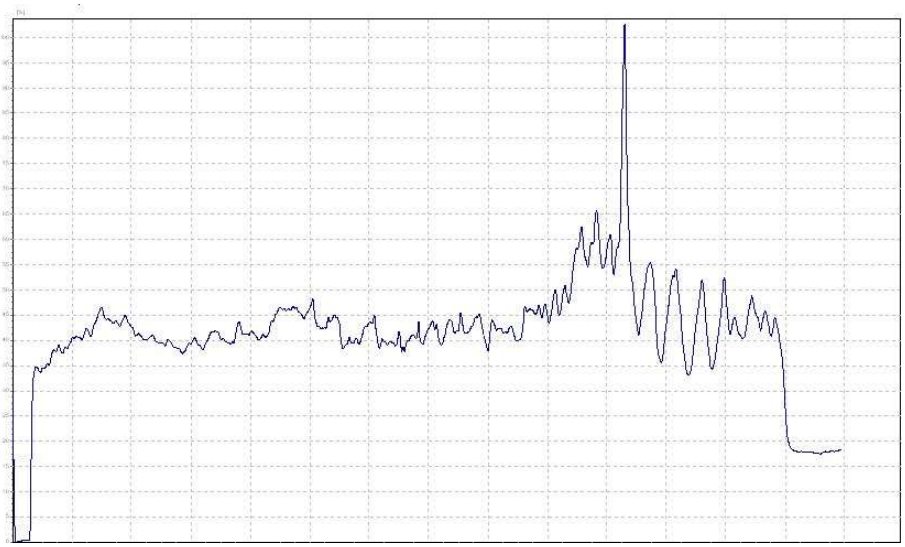

Chart 4-14 Drilling D4.1

Interpretation of the diagram D4.1 is not conclusive. The material still had some strength, but the difference of the resistance is not significant through the annual rings. It can mean two things, a problem of material or a tangential direction of drilling. In this case acc. to Figure 4-6 it could be combination

of both. First few centimeters were damaged, then the borer entered the spring wood.

The product of drilling D4.2 in the distance of 50 cm away from the wall palate is very similar to the diagram D4.1.

4.4.5.2 Drilling D4.3

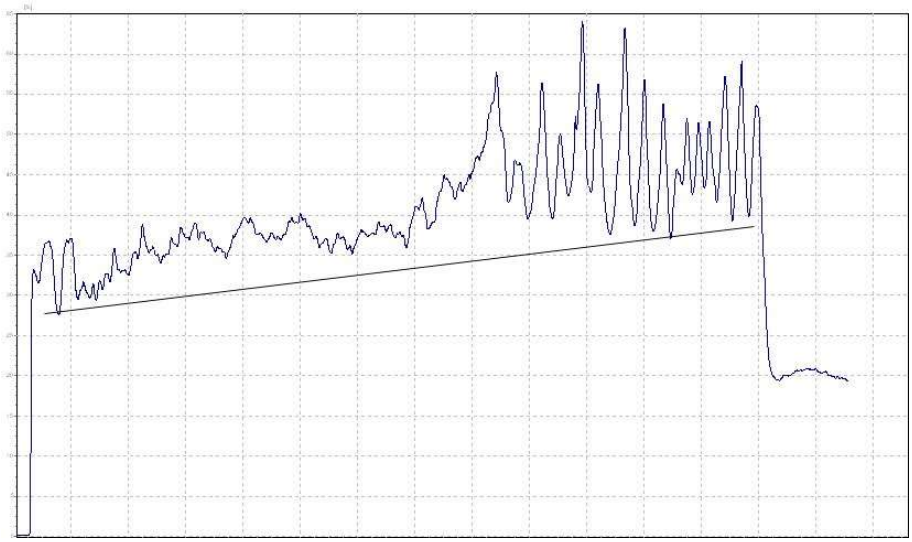

Chart 4-15 Drilling D4.3

This drilling was done about 1,5m away from the wall plate where the rafter seemed to be undamaged. At the beginning two annual rings were hit and then the fluctuations of resistance are not significant again. It further contributes to the possibility of tangential direction of drilling, so the material of the rafter could be in a good condition at this point.

4.4.5.3 Recommendation

The cause of moisture has to be found and solved in any case. The rafter should be subjected to further examination.

4.4.6 DETAIL D5 – RESISTANCE OF UNDAMAGED HISTORICAL WOOD

In the detail D5 the wall plate, which has been exchanged probably during the general renovation in 1984, and original rafter from 19th century is compared. This drilling was made so that it contained an intact historical wood and a newer timber in one diagram. From the diagram is not possible to determinate any absolute value of any quantity such as strength or modulus of elasticity, but it can provide the relative comparison of densities.

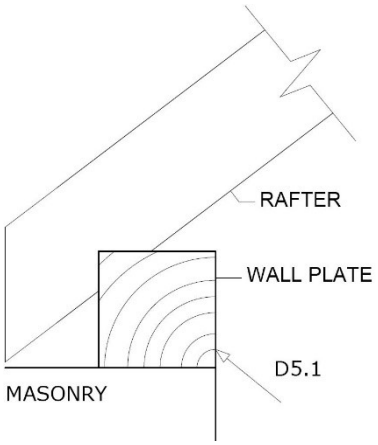

Figure 4-8 Detail D5 Part of the cross section

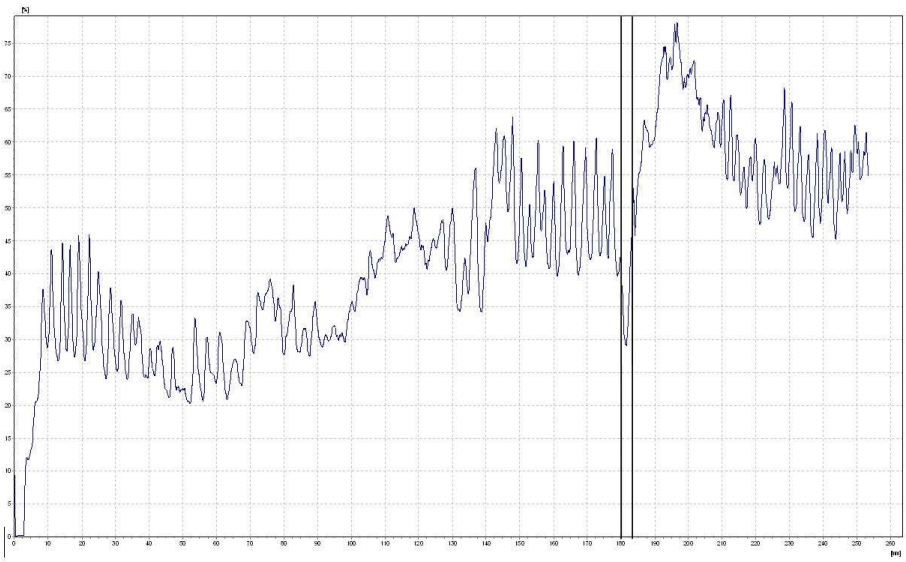

Chart 4-16 Drilling D5.1

The resistance of the historical wood is comparable to and even higher then the resistance of the wood from 1984.

4.5 CONCLUSION OF THE PRACTICAL PART

This part of the thesis provides examples of historical damaged wood members. The examination was carried out using micro-resistance drilling. This method can expose the inner condition of a wood member in a few minutes. Sometimes it is necessary to make a detailed analysis of the diagram in a computer in bigger scale, but the most of the first assumptions based on the resistance printed live during drilling were correct. This possibility of analyzing results saves time during the process of inspection. A typical example can be the determination of the longitudinal span of a damage in a member. It is possible to continue making drillings until a diagram shows an intact resistance of the wood.

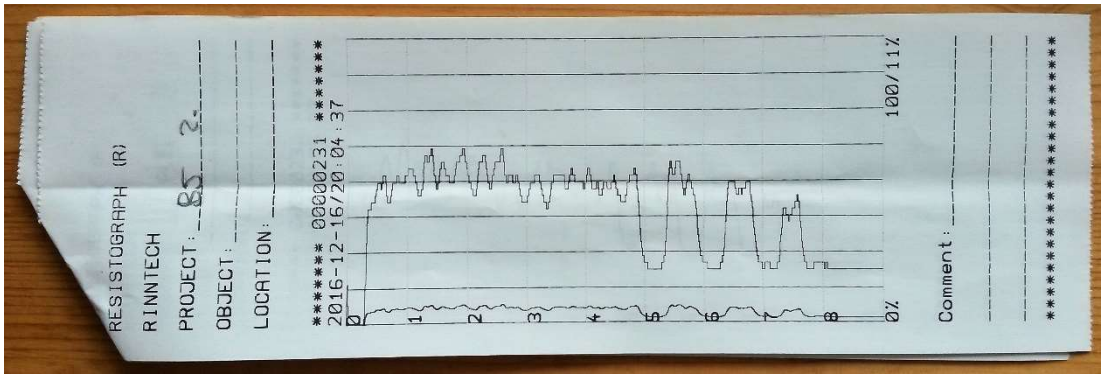

Photo 4–7 Example of printed diagram (B5.2 Chart 3-16)

The main benefit of my work was a contribution to the project of a complete inspection of the roof structure. My personal benefit is the experience I gained during the work.

8th January 2017

Jakub Mareš
jakubmares21@gmail.com

REFERENCES

[1] GIBSON, L. J. and ASHBY, M. F. *Cellular solids, Structure and properties – Second edition*; Cambridge Solid State Science Series; 1999; ISBN 0-521-49911-9

[2] STRAKA, B.; VANĚREK, J. and VEJPUSTEK, Z. *Conclusions from analysis and rehabilitation of existing timber roof structures*; Technical University in Brno

[3] KOUKAL, M., NOVOTNÝ, V., ZDENĚK, M. *Ochrana dřeva, dřevěných výrobků a konstrukcí*; Dům technicky ČSVTS České Budějovice, 1987, 173p., number of publication 24-13.13/60/740/87

[4] WASSERBAUER, R. *Biologické znehodnocení staveb*. ABF Praha, 2000, ISBN 80-86165-30-2.

[5] RINN, F. *Basics of micro-resistance drilling for timber inspection*; Accessible from: http://docplayer.org/6626894-Basics-of-micro-resistance-drilling-for-timber-inspection.html

[6] RINN, F. *Typical Trends in Resistance Drilling Profiles of Trees*; Arborist•News www.isa-arbor.com February 2014

[7] *Timber structures – Structural timber and glued laminated timber – Determination of some physical and mechanical properties*; RRICTISQ RRICTISQ, na, BST 2005; ISBN 0 580 24284 6

[8] *EN 1995-1-1:2004 (E) Eurocode 5 – Design of timber structures; Part 1-1: General – Common rules and rules for buildings;* 2004-11-01; Technical Committee CEN/TC250

[9] *ČSN EN 338 – Konstrukční dřevo – Třídy pevnosti*; May 2010; Czech Office for Standards, Meteorology and Testing

[10] *The chronicle of Khevenhüller school*

[11] *Floor plans of Khevenhüller school (pdf)*

[12] MAGNUS I. *Historic timber roof structures, construction technology and structural behaviour*, Master thesis; Catholic University Of Leuven Faculty Of Engineering

[13] KLOIBER M., KOTLÍNOVÁ M. *Porovnání dynamického a statického modulu pružnosti poškozeného dřeva*; Applied mechanics 206; 8th International scientific conference

[14] F´ATRAI G. *Historic roof structures*; Széchenyi István University, Department of Architecture and Building Construction

[15] HOATH J. *Repairing Historic Roof Timbers*

[16] ORTNER J. *Instandsetzungshandbuch für historische Dachwerke und deren Verbindungen*; Institut für Holzbau und Holztechnologie Technische Universität Graz; MA-4-04/2014

[17] RINN, F., From *wood anatomy to tree-biomechanics*; © RINTECH e.K. HARDTSTR. 20-22 69126 HEIDELBERG GERMANY; 2015

[18] RINN, F., Practical *application of micro-resistance drilling for timber inspection*; Sonderdruck aus Holztechnologie

[18] BODIG J. JAYNE B. A., M*echanics of Wood and Wood Composites*; © Van Nostrand Reinhold Company; 1982; ISBN 0-442-00822-8

[20] *Roofs - A Guide to The Repair of Historic Roofs;* Government Publications Sales Office; © Government of Ireland 2010; ISBN 0-7557-7540-6

[21] ČUNDERLÍK I., *Štruktúra dreva*; Technická Univerzita Vo Zvolene, Drevárska Fakulta; 2009; © prof. Ing. Igor Čunderlík, CSc.; ISBN 978-80-228-2061-5

ANNEX 1

PHOTO DOCUMENTATION OF EXPERIMENTAL SPECIMENS

This annex serves for detailed display of tested specimens and their possible defects such as knots and resin channels.

5.1 B_0 SPECIMENS

Specimens used for measuring material properties of wood with certain porosity.

Photo 5–1 B_0 specimens

5.1.1 BN_0

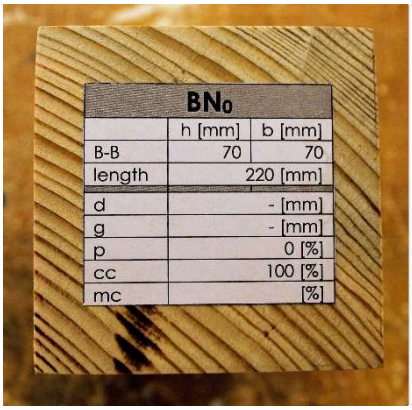

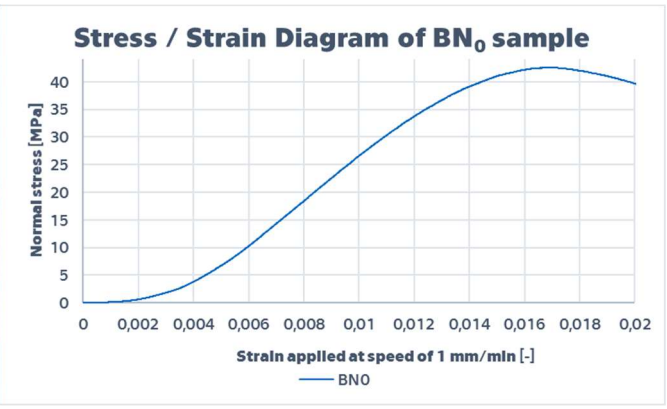

Photo 5–2 BN_0 label; Chart 5-1 Stress / Strain diagram BN_0

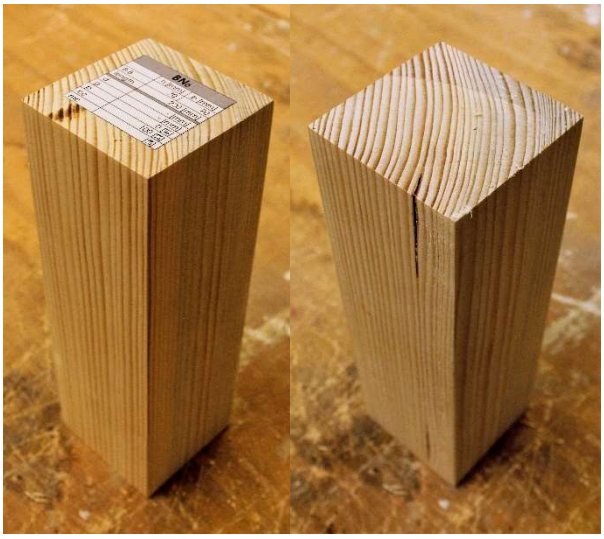

Photo 5–3 BN_0 before test

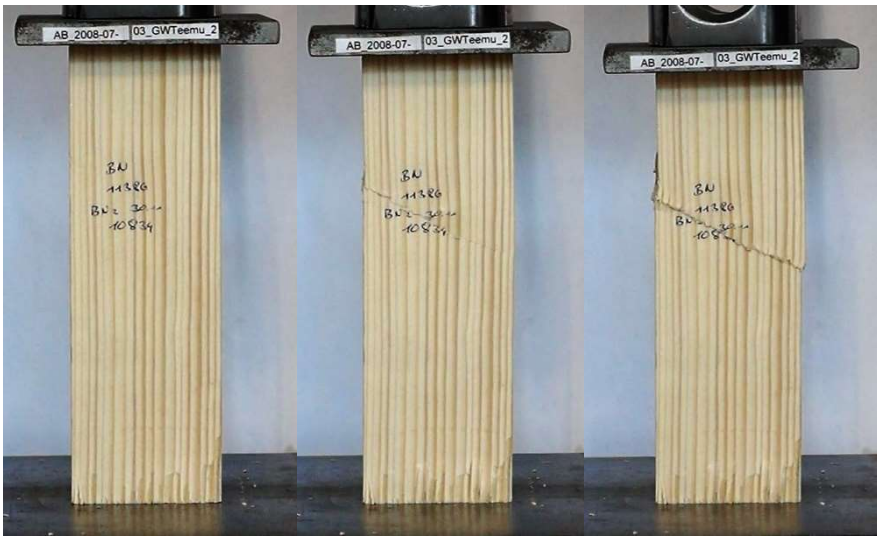

Photo 5–4 BN_0 compressive strength test

5.1.2 $B4_0$

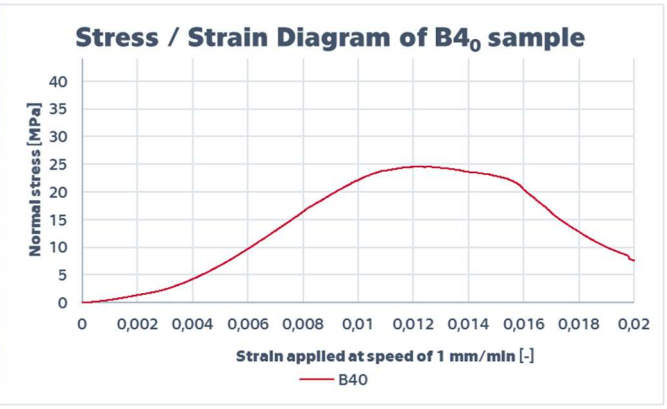

Photo 5–5 $B4_0$ label; Chart 5-2 Stress / Strain diagram $B4_0$

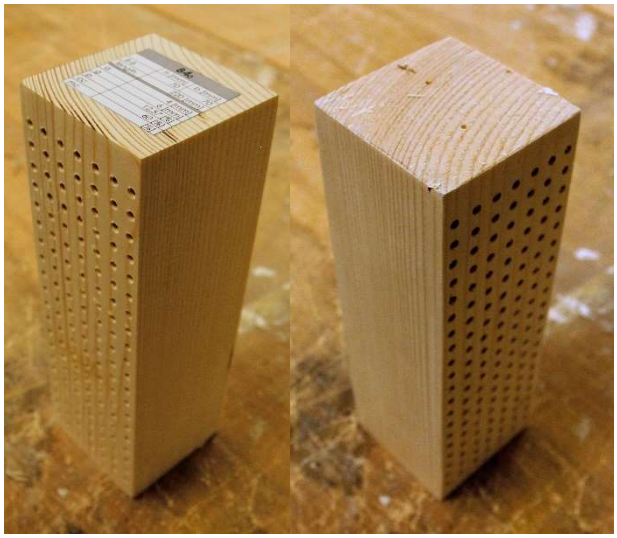

Photo 5–6 $B4_0$ before test

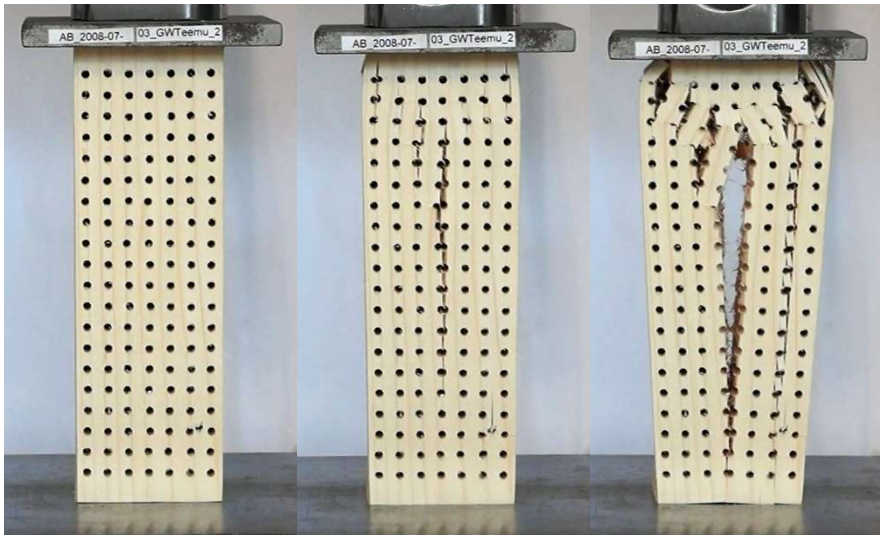

Photo 5–7 $B4_0$ compressive strength test

5.1.3 $B5_0$

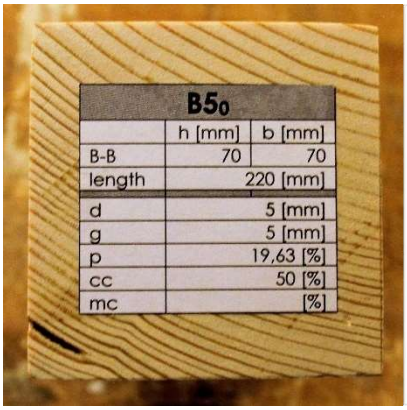

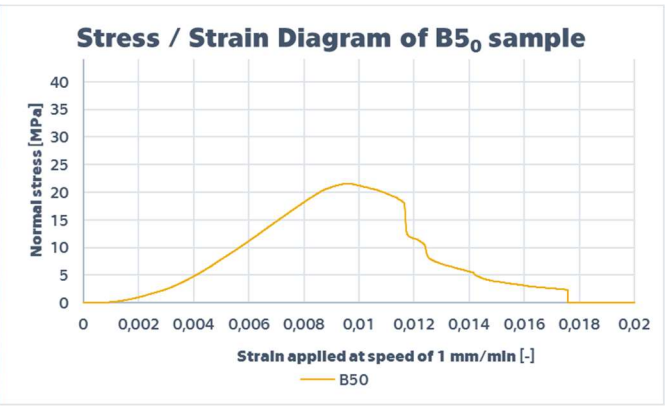

Photo 5–8 $B5_0$ label; Chart 5-3 Stress / Strain diagram $B5_0$

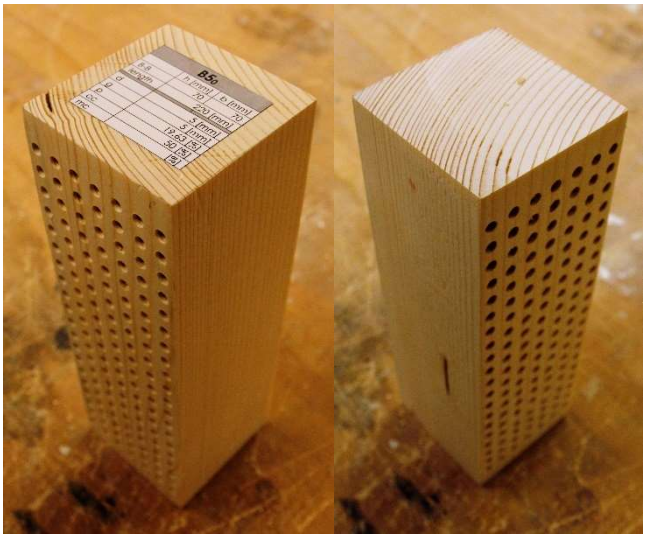

Photo 5–9 $B5_0$ before test

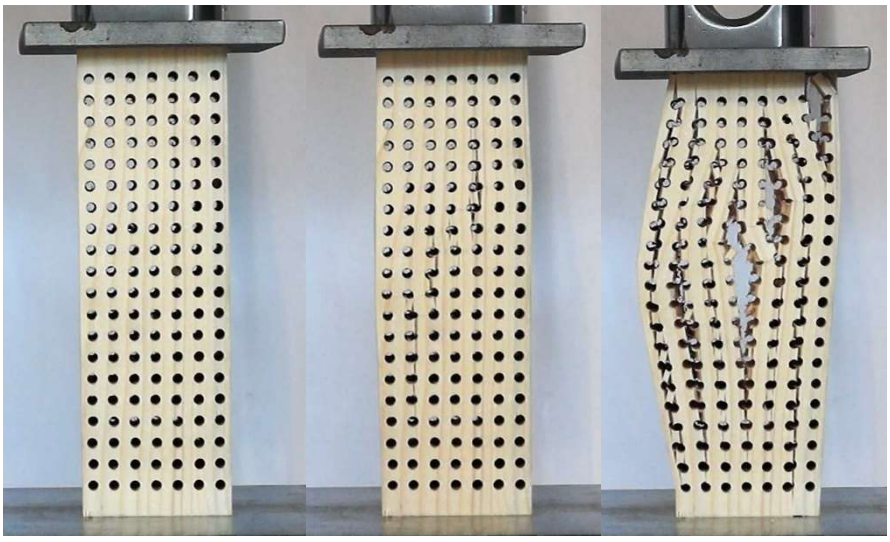

Photo 5–10 $B5_0$ compressive strength test

5.1.4 $B6_0$

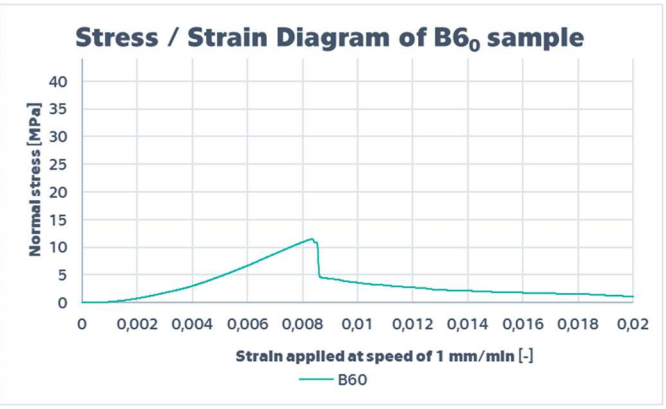

Photo 5–11 $B6_0$ label; Chart 5-4 Stress / Strain diagram $B6_0$

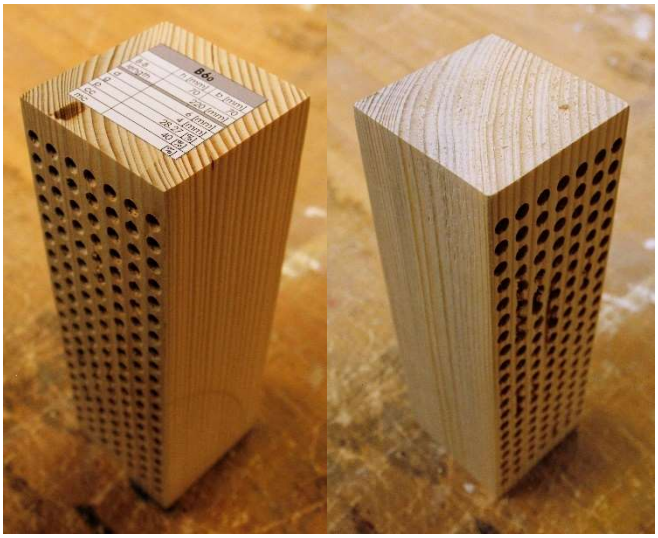

Photo 5–12 $B6_0$ before test

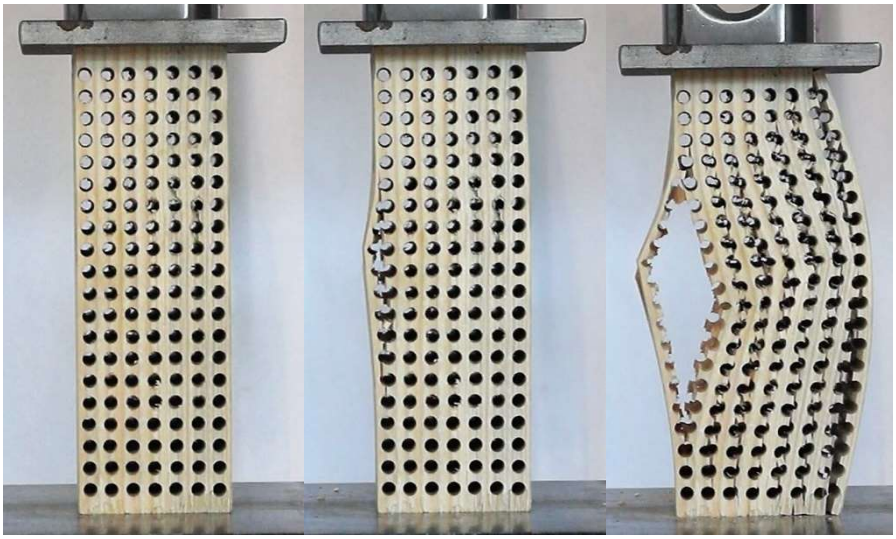

Photo 5–13 $B6_0$ compressive strength test

5.1.5 $B7_0$

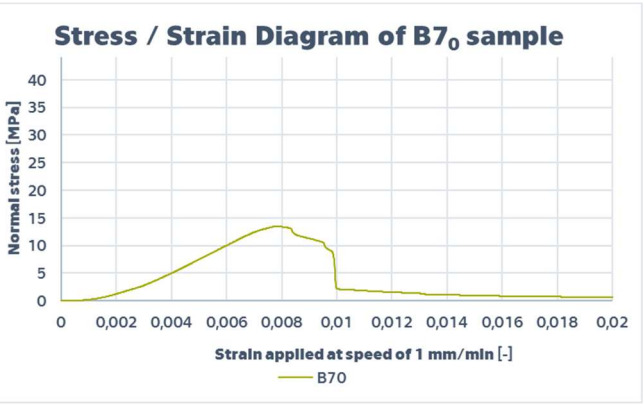

Photo 5–14 $B7_0$ label; Chart 5-5 Stress / Strain diagram $B7_0$

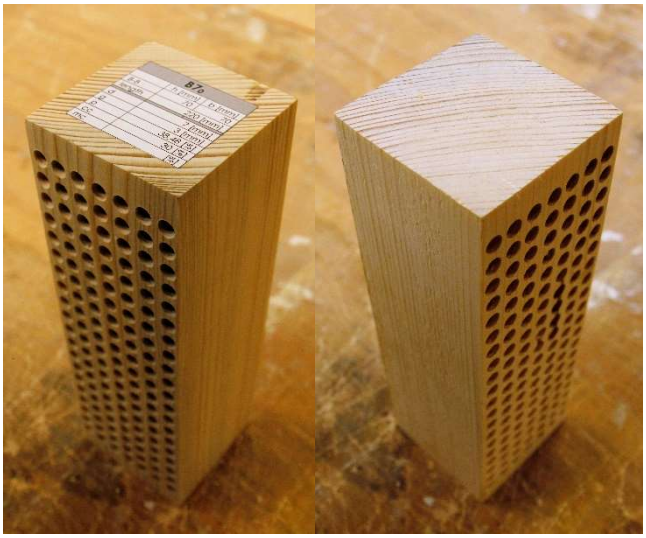

Photo 5–15 $B7_0$ before test

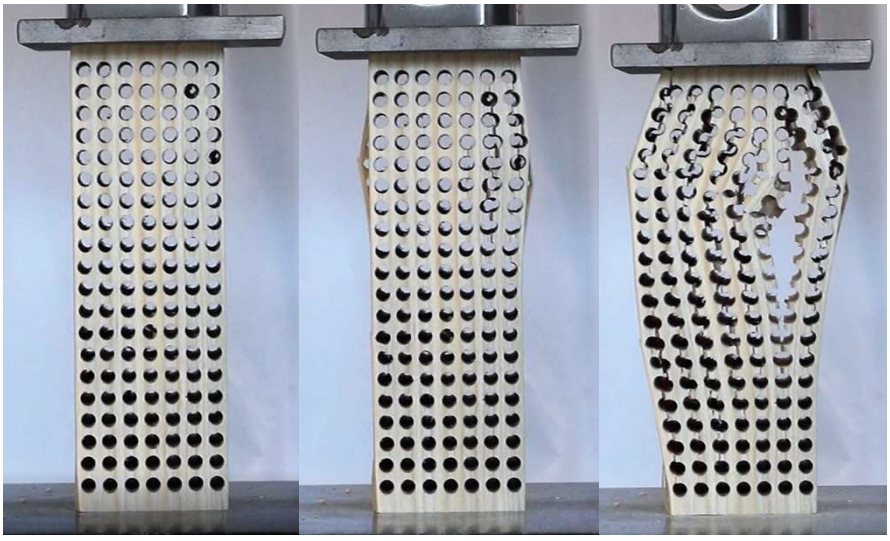

Photo 5–16 $B7_0$ compressive strength test

5.1.6 B34₀A

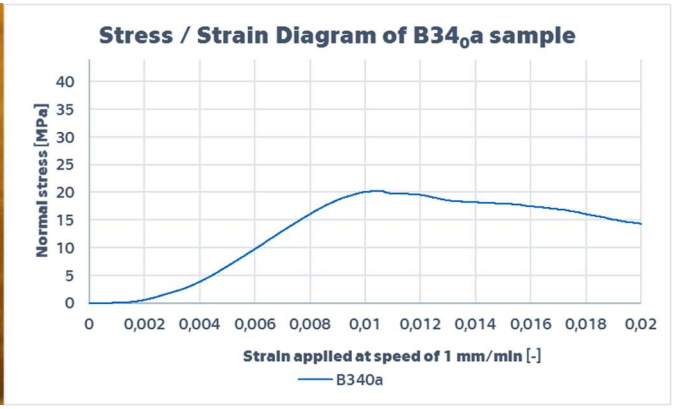

Photo 5–17 B34₀a label; Chart 5-6 Stress / Strain diagram B34₀a

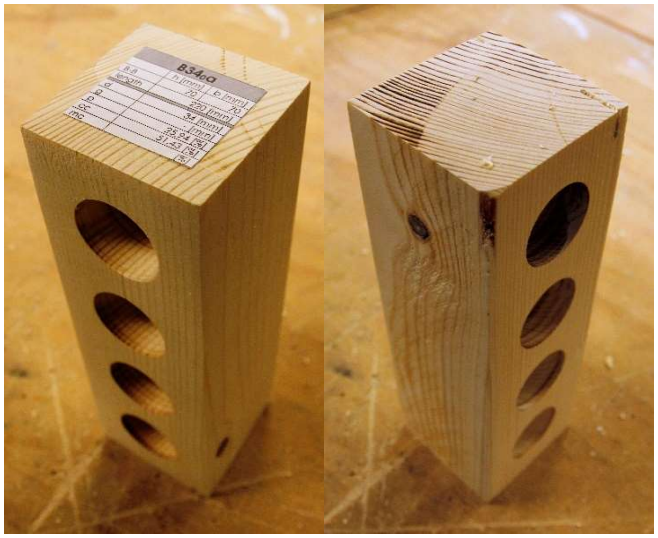

Photo 5–18 B34₀a before test

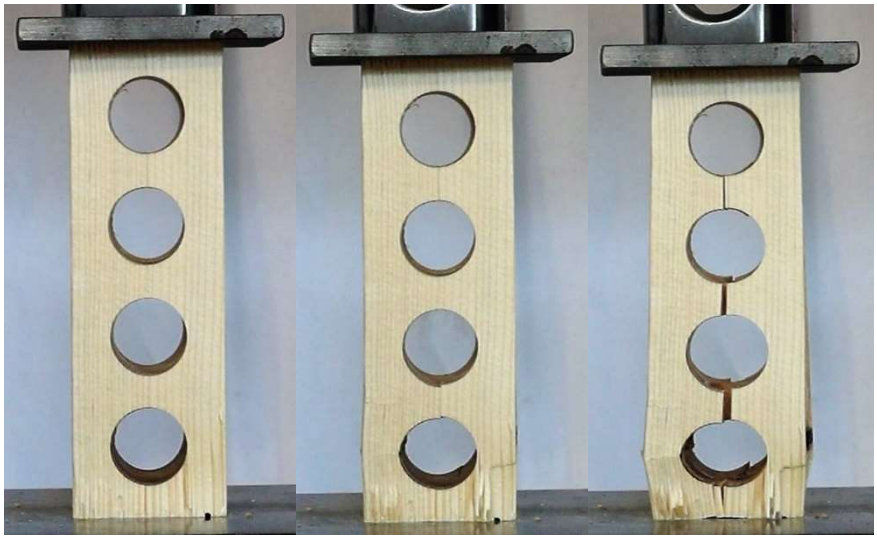

Photo 5–19 B34₀a compressive strength test

5.1.7 B34₀B

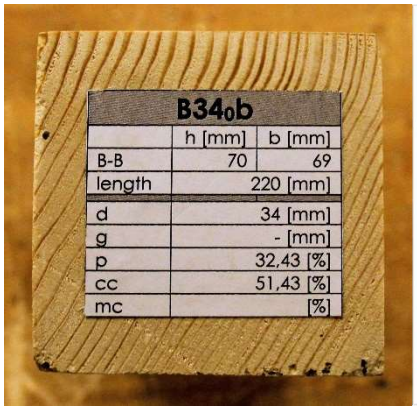

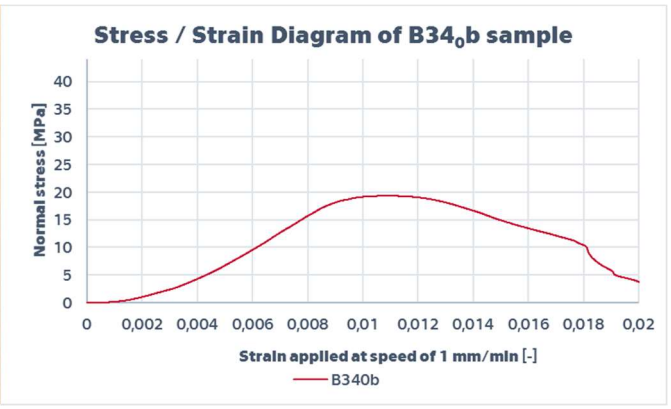

Photo 5–20 B34₀b label; Chart 5-7 Stress / Strain diagram B34₀b

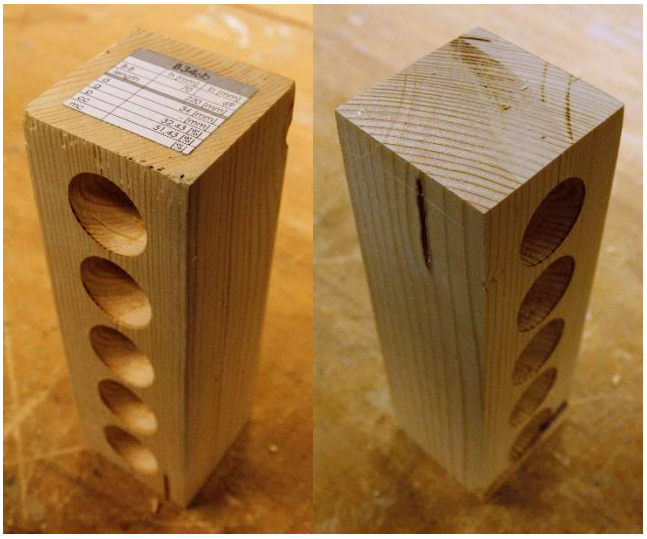

Photo 5–21 B34₀b before test

Photo 5–22 B34₀b compressive strength test

5.2 B COLUMNS

Set of 6 columns with simulated damage in the middle of the length used for examination of the influence of a damaged zone on the load bearing capacity of a column.

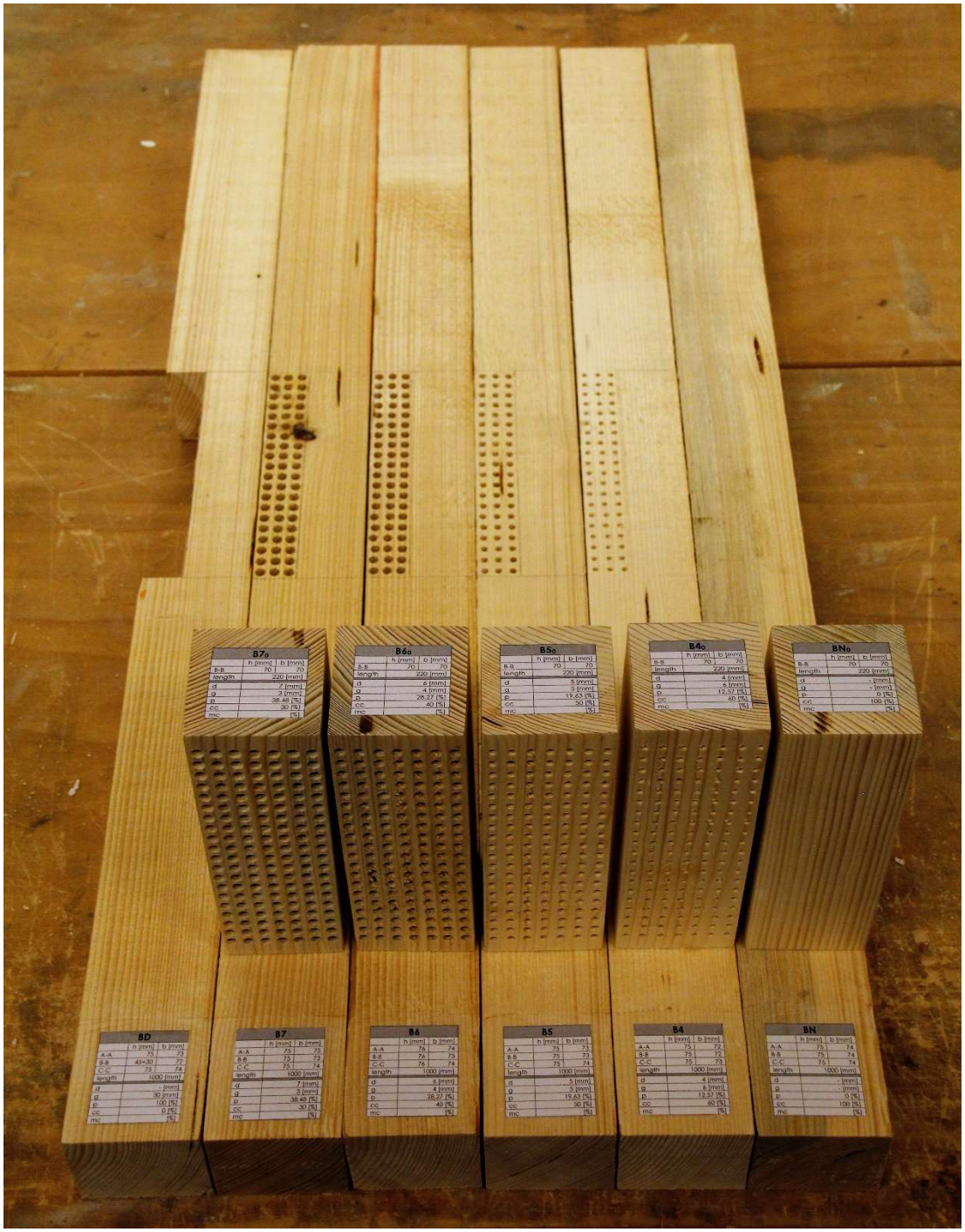

Photo 5–23 B columns

5.2.1 COLUMN BN

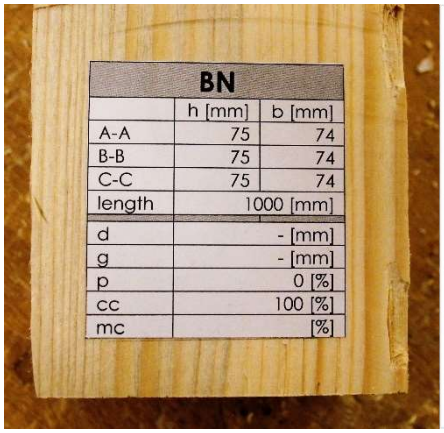

BN		
	h [mm]	b [mm]
A-A	75	74
B-B	75	74
C-C	75	74
length	1000 [mm]	
d	- [mm]	
g	- [mm]	
p	0 [%]	
cc	100 [%]	
mc	[%]	

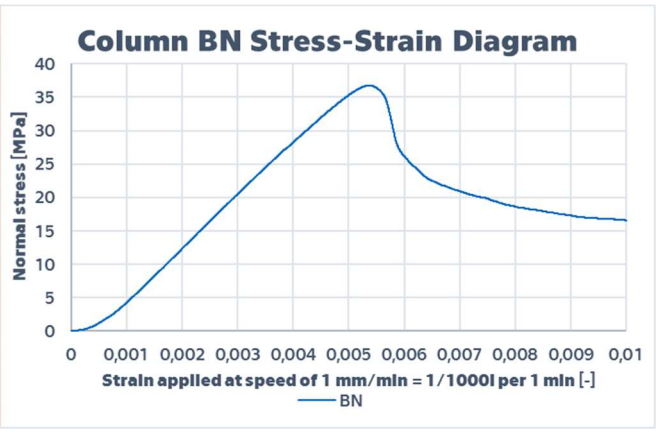

Photo 5–24 BN label; Chart 5-8 Stress / Strain diagram column BN

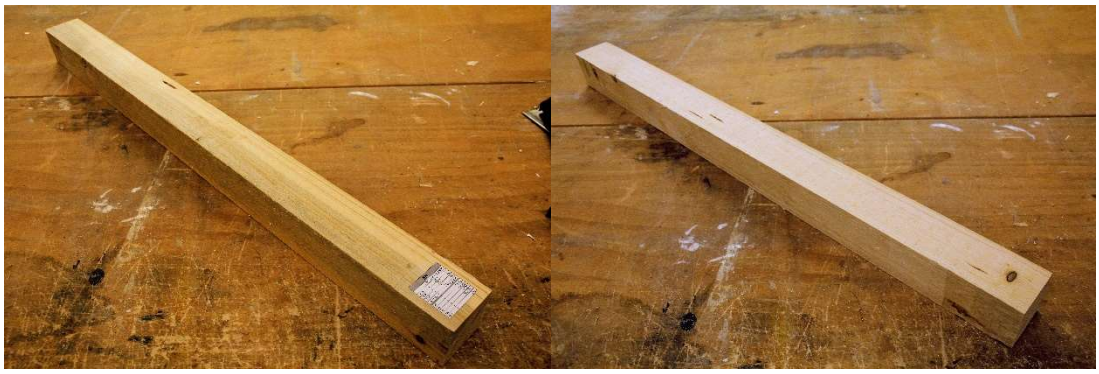

Photo 5–25 Column BN before test

Photo 5–26 Column BN test of load bearing capacity

5.2.2 COLUMN B4

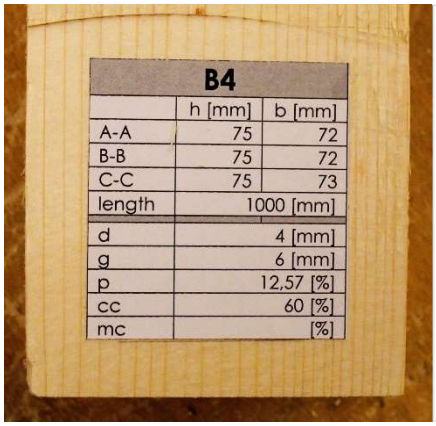

B4		
	h [mm]	b [mm]
A-A	75	72
B-B	75	72
C-C	75	73
length	1000 [mm]	
d	4 [mm]	
g	6 [mm]	
p	12,57 [%]	
cc	60 [%]	
mc	[%]	

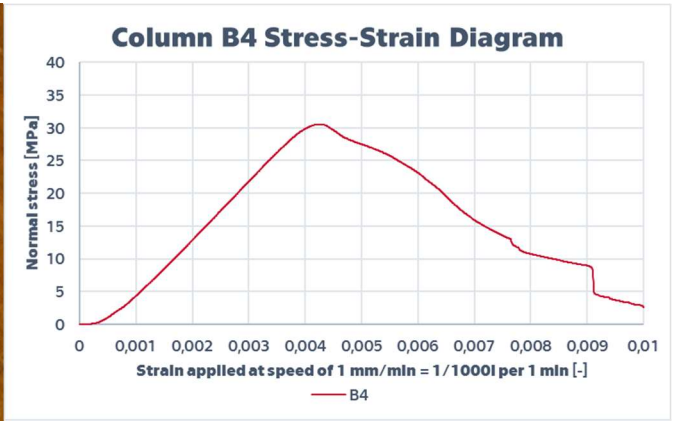

Photo 5–27 B4 label; Chart 5-9 Stress / Strain diagram column B4

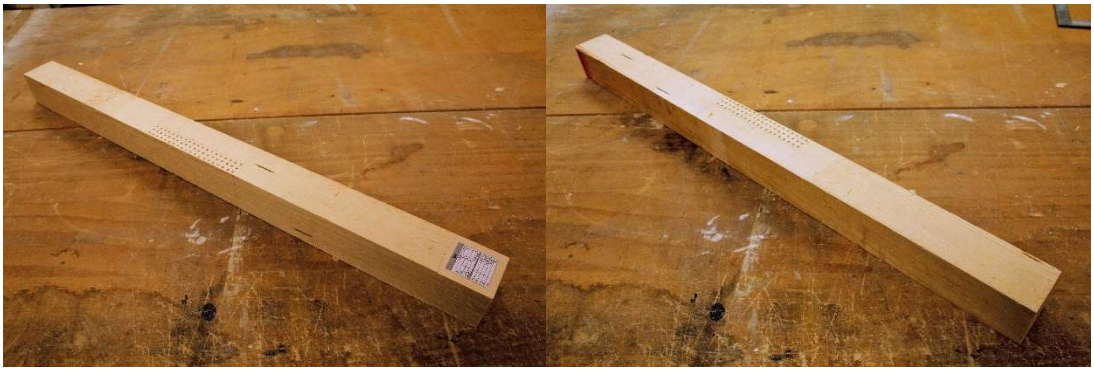

Photo 5–28 Column B4 before test

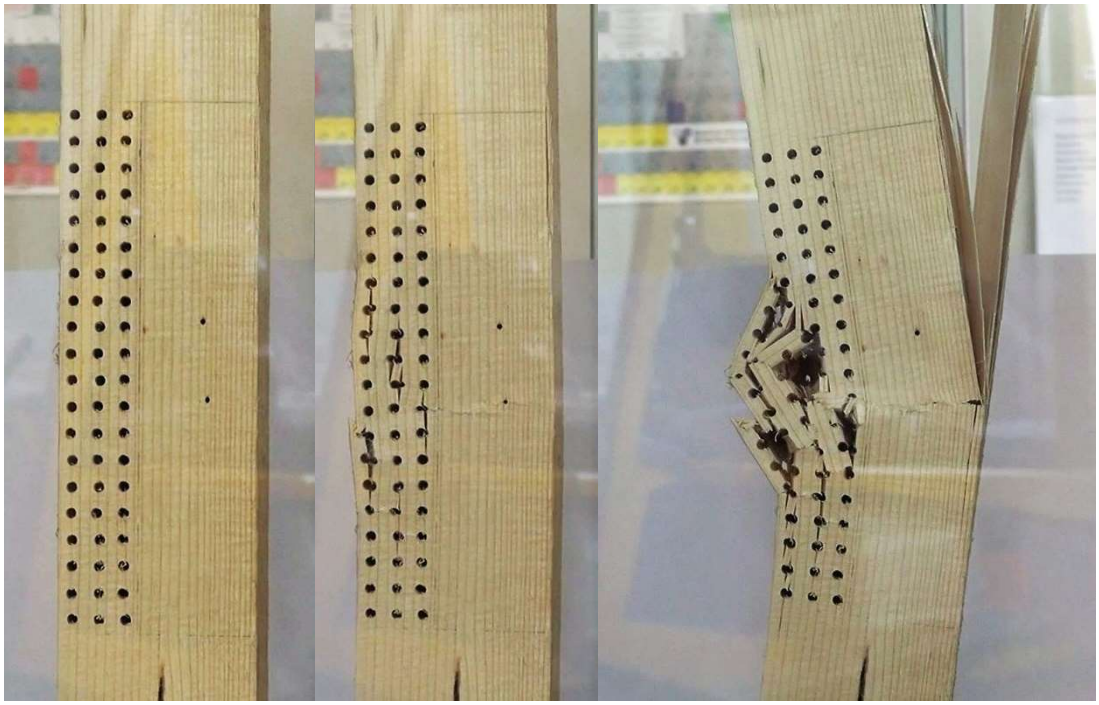

Photo 5–29 Column B4 test of load bearing capacity

5.2.3 COLUMN B5

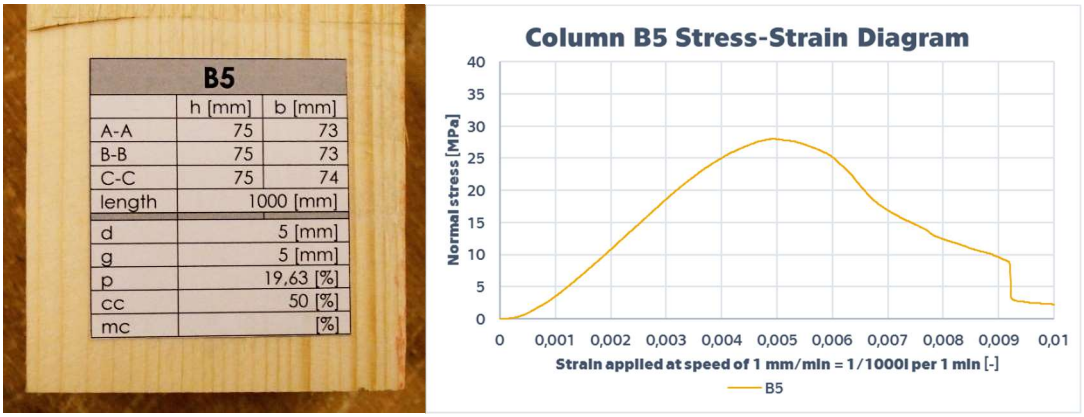

Photo 5–30 B5 label; Chart 5-10 Stress / Strain diagram column B5

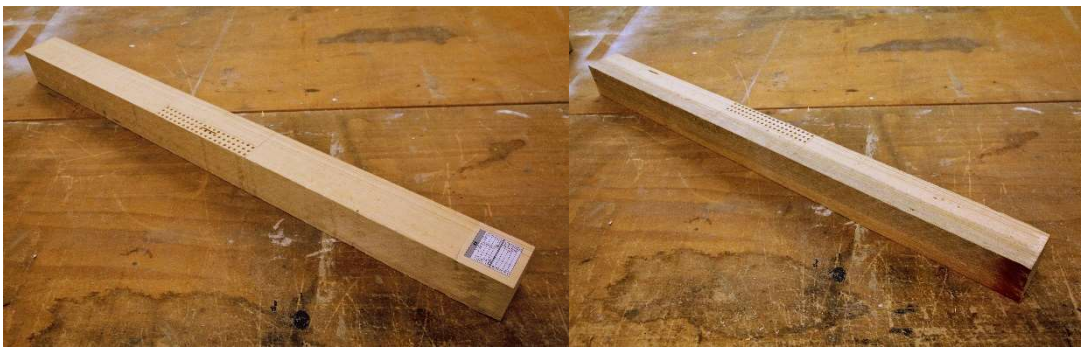

Photo 5–31 Column B5 before test

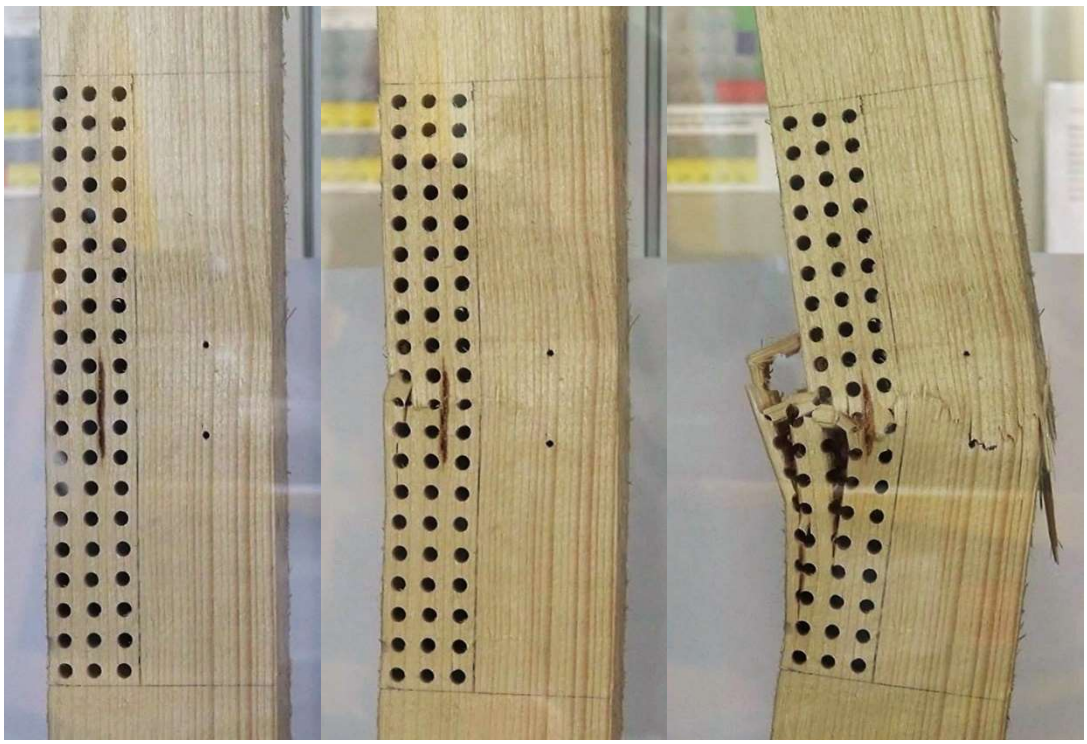

Photo 5–32 Column B5 test of load bearing capacity

5.2.4 COLUMN B6

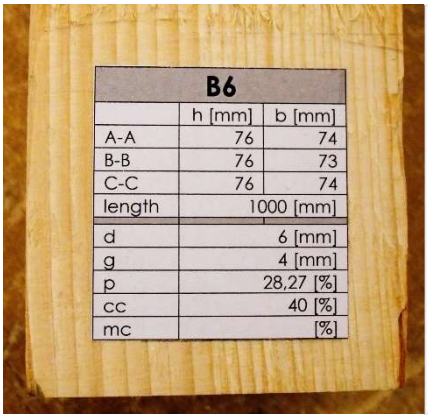

B6		
	h [mm]	b [mm]
A-A	76	74
B-B	76	73
C-C	76	74
length	1000 [mm]	
d	6 [mm]	
g	4 [mm]	
p	28,27 [%]	
cc	40 [%]	
mc	[%]	

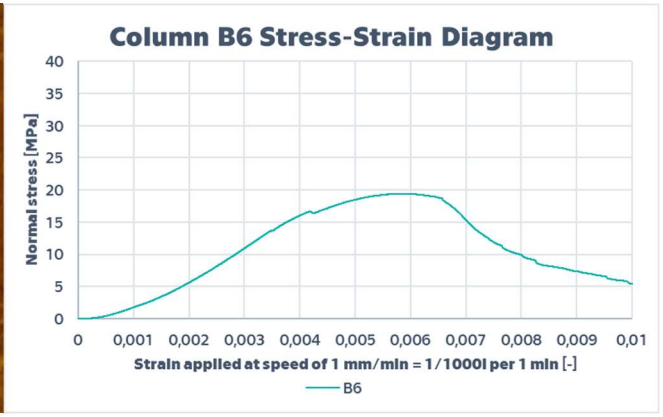

Photo 5–33 B6 label; Chart 5-11 Stress / Strain diagram column B6

Photo 5–34 Column B6 before test

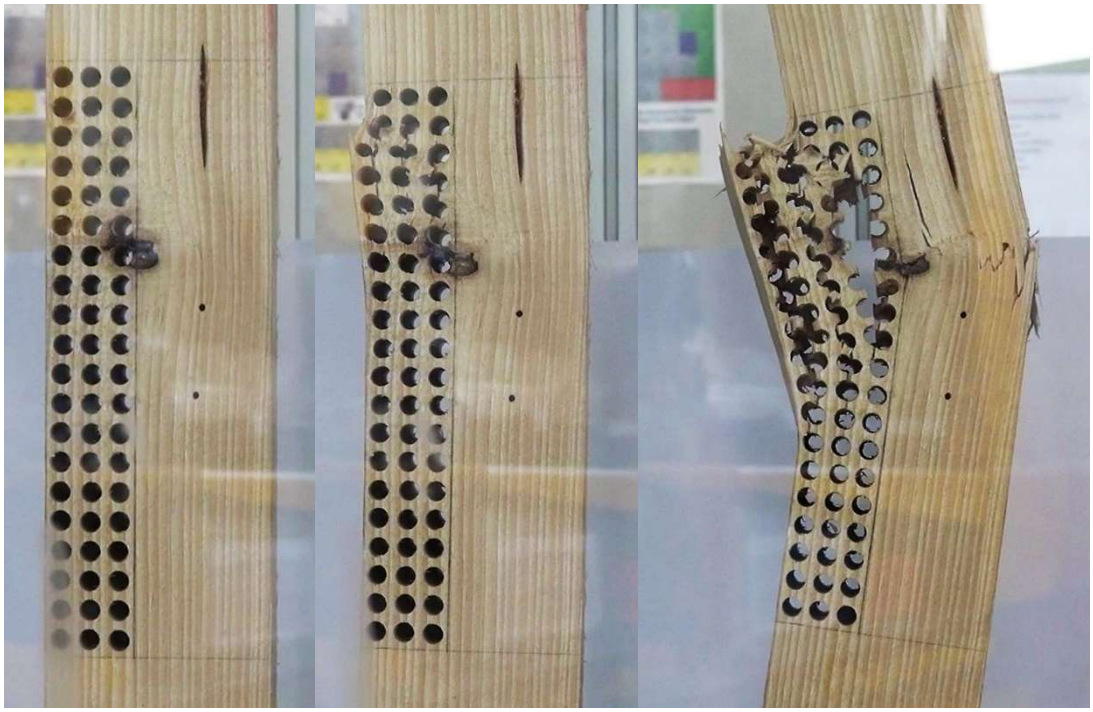

Photo 5–35 Column B6 test of load bearing capacity

5.2.5 COLUMN B7

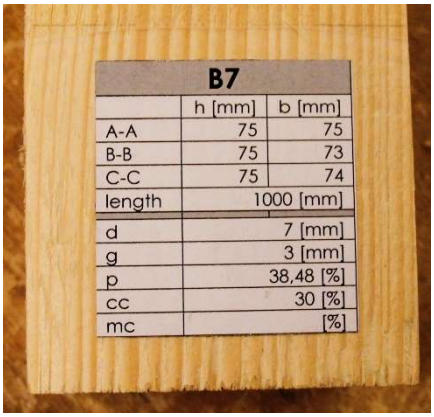

B7		
	h [mm]	b [mm]
A-A	75	75
B-B	75	73
C-C	75	74
length	1000 [mm]	
d	7 [mm]	
g	3 [mm]	
p	38,48 [%]	
cc	30 [%]	
mc	[%]	

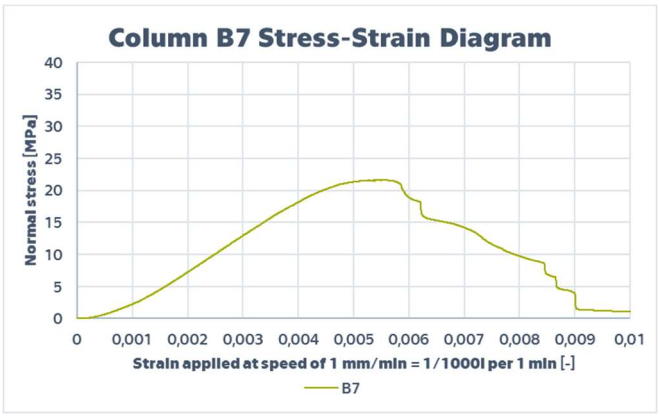

Photo 5–36 B7 label; Chart 5-12 Stress / Strain diagram column B7

Photo 5–37 Column B7 before test

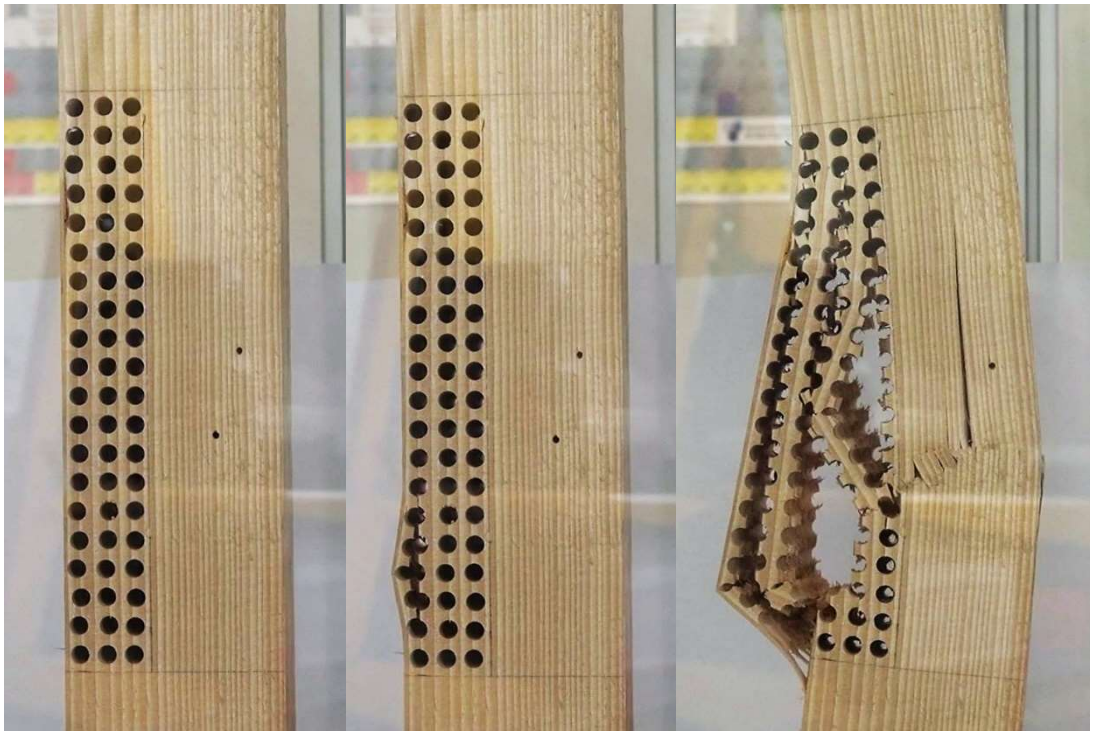

Photo 5–38 Column B7 test of load bearing capacity

5.2.6 COLUMN BD

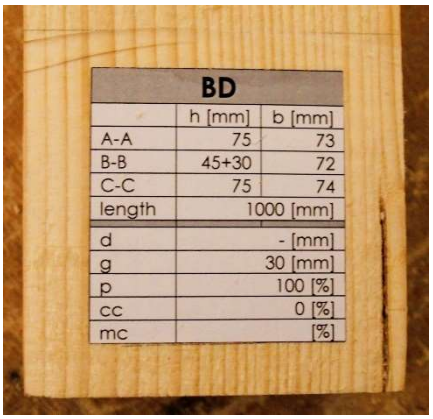

BD		
	h [mm]	b [mm]
A-A	75	73
B-B	45+30	72
C-C	75	74
length	1000 [mm]	
d	- [mm]	
g	30 [mm]	
p	100 [%]	
cc	0 [%]	
mc	[%]	

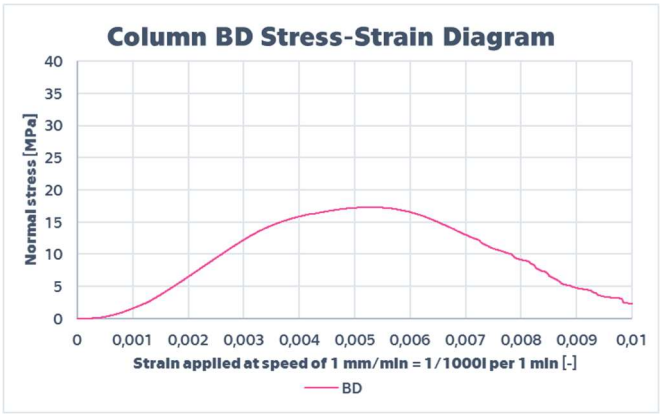

Photo 5–39 BD label; Chart 5-13 Stress / Strain diagram column BD

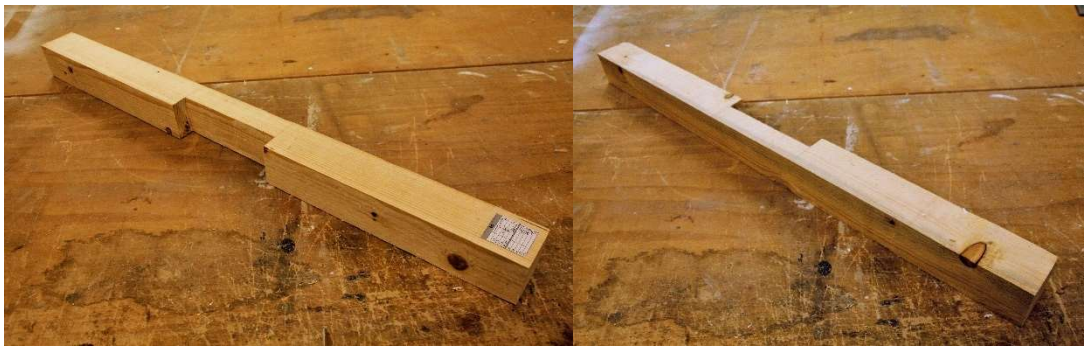

Photo 5–40 Column BD before test

Photo 5–41 Column BD test of load bearing capacity

5.3 COLUMN S

Column S is an old piece of fir wood which is naturally damaged by rot. One task of this thesis was to investigate its load bearing capacity.

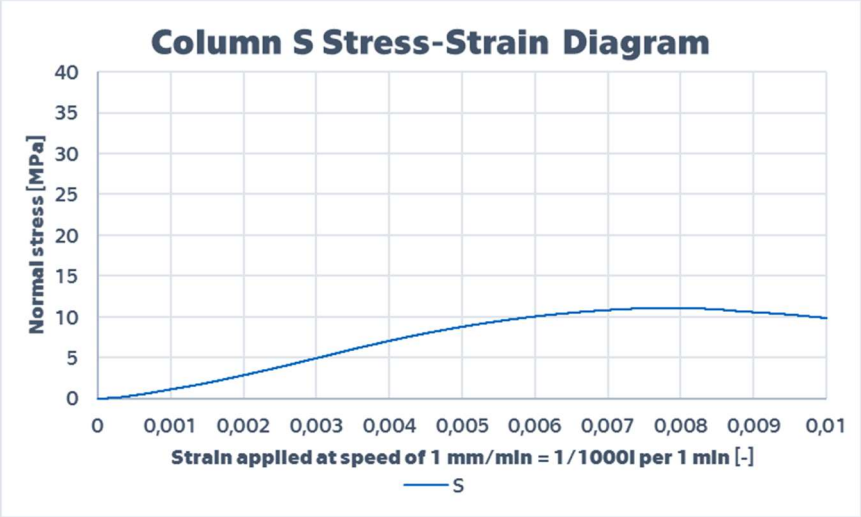

Chart 5-14 Stress / Strain diagram column S

Photo 5–42 Column S after collapse

After the test of load bearing capacity the column S was cut in spots of drillings to see how the cross section looks like in reality. The calculation was done based on diagrams from Resistograph® only. Here is comparison of real cross section and designated distribution of degree of damage based on resistance drilling.

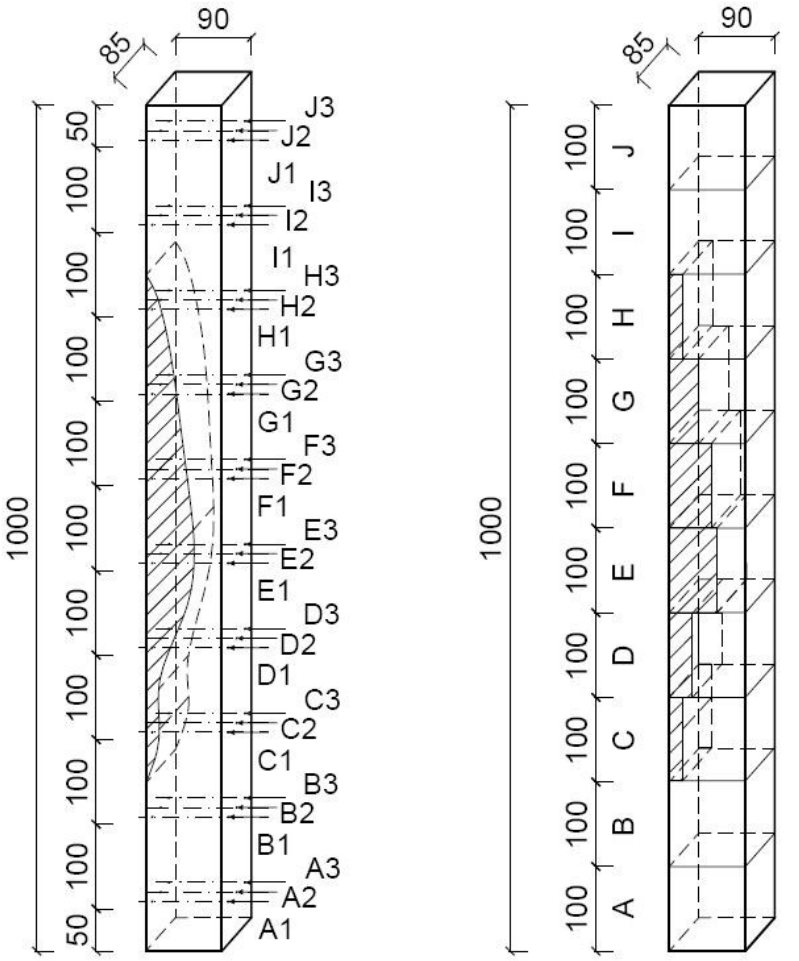

Figure 5-1 Geometry of the column S

Photos were rotaited so that drillins were made from letf side of a cross section which corespond to distribution of degree of damge in tables.

		1	2	3	4	5	6	7	8	9
A	1	0,0	0,0	0,0	0,1	0,1	0,1	0,0	0,0	0,0
	2	0,0	0,0	0,0	0,0	0,0	0,0	0,2	0,2	0,2
	3	0,0	0,0	0,0	0,0	0,0	0,0	0,0	0,0	0,0

Photo 5–43 Cross section A; Figure 5-2 Cross section A

		1	2	3	4	5	6	7	8	9
B	1	0,0	0,0	0,0	0,0	0,0	0,0	0,0	0,0	0,0
	2	0,0	0,0	0,0	0,0	0,0	0,0	0,0	0,2	0,2
	3	0,0	0,0	0,0	0,0	0,0	0,0	0,0	0,0	0,0

Photo 5–44 Cross section B; Figure 5-3 Cross section B

		1	2	3	4	5	6	7	8	9
C	1	0,0	0,0	0,0	0,0	0,0	0,0	0,0	0,0	0,0
	2	0,0	0,0	0,0	0,0	0,0	0,0	0,0	0,0	0,0
	3	0,0	0,0	0,0	0,2	0,2	0,0	0,0	0,0	0,0

Photo 5–45 Cross section C; Figure 5-4 Cross section C

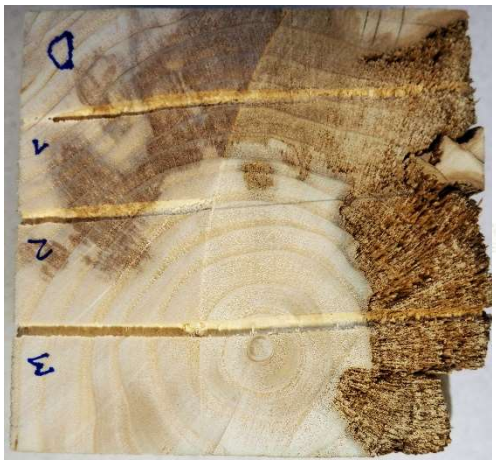

D

	1	2	3	4	5	6	7	8	9
1	0,0	0,0	0,0	0,0	0,0	0,0	0,4	0,4	0,4
2	0,0	0,0	0,0	0,0	0,0	0,0	0,5	0,5	0,5
3	0,0	0,0	0,0	0,0	0,0	0,0	0,5	0,5	0,5

Photo 5–46 Cross section D; Figure 5-5 Cross section D

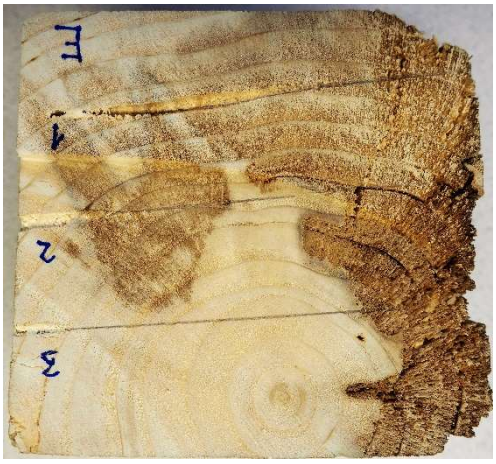

E

	1	2	3	4	5	6	7	8	9
1	0,0	0,0	0,3	0,3	0,3	0,3	0,3	0,6	0,6
2	0,0	0,0	0,1	0,1	0,1	0,1	0,5	0,5	0,5
3	0,0	0,0	0,0	0,0	0,0	0,0	0,5	0,5	0,5

Photo 5–47 Cross section E; Figure 5-6 Cross section E

F

	1	2	3	4	5	6	7	8	9
1	0,0	0,2	0,2	0,2	0,2	0,0	0,0	0,4	0,4
2	0,0	0,0	0,0	0,0	0,0	0,2	0,2	0,4	0,4
3	0,0	0,0	0,3	0,3	0,3	0,0	0,0	0,7	0,7

Photo 5–48 Cross section F; Figure 5-7 Cross section F

G	1	2	3	4	5	6	7	8	9
1	0,0	0,0	0,0	0,3	0,3	0,0	0,0	0,5	0,5
2	0,0	0,0	0,0	0,0	0,3	0,3	0,3	0,5	0,5
3	0,0	0,0	0,0	0,0	0,0	0,0	0,8	0,8	0,8

Photo 5–49 Cross section G; Figure 5-8 Cross section G

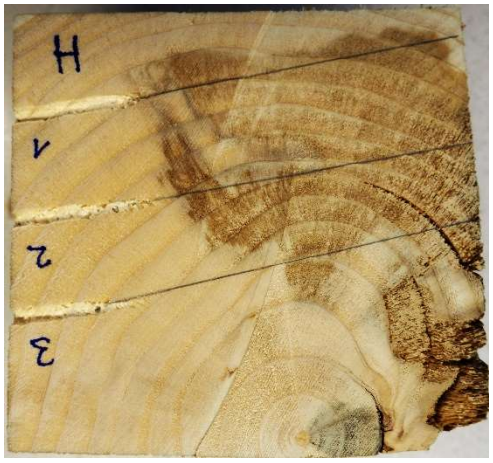

H	1	2	3	4	5	6	7	8	9
1	0,0	0,0	0,1	0,1	0,1	0,0	0,0	0,0	0,0
2	0,0	0,0	0,0	0,0	0,2	0,2	0,2	0,2	0,2
3	0,0	0,0	0,0	0,0	0,0	0,0	0,4	0,4	0,4

Photo 5–50 Cross section H; Figure 5-9 Cross section H

I	1	2	3	4	5	6	7	8	9
1	0,0	0,0	0,0	0,0	0,0	0,0	0,0	0,0	0,2
2	0,0	0,0	0,0	0,0	0,0	0,0	0,0	0,2	0,2
3	0,0	0,0	0,0	0,0	0,0	0,0	0,0	0,0	0,0

Photo 5–51 Cross section I; Figure 5-10 Cross section I

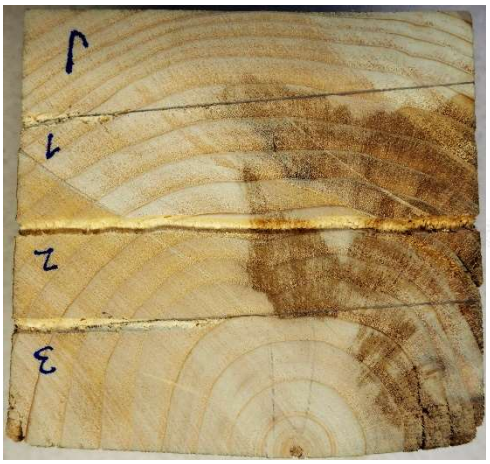

J

	1	2	3	4	5	6	7	8	9
1	0,0	0,0	0,0	0,2	0,2	0,2	0,0	0,0	0,0
2	0,0	0,0	0,0	0,0	0,0	0,0	0,0	0,0	0,2
3	0,0	0,0	0,0	0,0	0,0	0,0	0,0	0,2	0,2

Photo 5–52 Cross section J; Figure 5-11 Cross section J

The reliability of the detection of damaged zones was sufficient for the purpose of the thesis. However, the difference of accordance is noticeable between more radial drillings 3 and almost tangential drillings 1. Results of radial drillings are always more reliable in the case of the Resistograph® and probably in all other cases of micro-resistance drilling devices.

ANNEX 2

CD CONTAINING ALL MEASURED DATA FROM LABORATORY, EXCEL SPREADSHEETS AND DIAGRAMS

The CD is attached on the back cover of the thesis.

Contents:

- Calculations
  - Preliminary calculations (.xlsx)
  - Material properties (.xlsx)
  - Comparison of results (.xlsx)
  - Design load bearing capacity of damaged timber column (.xlsx)
- Laboratory data
  - Compressive strength process
    - Compressive strength test of all B_0 and F_0 samples
  - Columns process
    - Load bearing capacity test of all columns
  - E modulus process
    - Test of modulus of elasticity of all B_0 and F_0 samples
  - Density (.xlsx)
  - E modulus values (.xlsx)
- All diagrams of the column S (.docx)